CAPITAL UNIVERSITY OF SCIENCE AND TECHNOLOGY, ISLAMABAD

A Comprehensive Study on DC Faults in Multi-terminal MMC Based HVDC Power Transmission System

by

Yasir Mehmood

A thesis submitted in partial fulfillment for the degree of Master of Science

in the

Faculty of Engineering
Department of Electrical Engineering

2022

I dedicated this work to my dearest parents

CERTIFICATE OF APPROVAL

A Comprehensive Study on DC Faults in Multi-terminal MMC Based HVDC Power Transmission System

by

Yasir Mehmood

(MEE191005)

THESIS EXAMINING COMMITTEE

S. No.	Examiner	Name	Organization
(a)	External Examiner	Dr. Tahir Nadeem Malik	HITEC Uni., Taxila
(b)	Internal Examiner	Dr. Muhammad Ashraf	CUST, Islamabad
(c)	Supervisor	Dr. Umer Amir Khan	CUST, Islamabad

Dr. Umer Amir Khan
Thesis Supervisor
July,2022

Dr. Noor Muhammad Khan
Head
Dept. of Electrical Engineering
July, 2022

Dr. Imtiaz Ahmad Taj
Dean
Faculty of Engineering
July, 2022

Author's Declaration

I, **Yasir Mehmood** hereby state that my MS thesis titled "**A Comprehensive Study on DC Faults in Multi-terminal MMC Based HVDC Power Transmission System**" is my own work and has not been submitted previously by me for taking any degree from Capital University of Science and Technology, Islamabad or anywhere else in the country/abroad.

At any time if my statement is found to be incorrect even after my graduation, the University has the right to withdraw my MS Degree.

(Yasir Mehmood)

Registration No:MEE191005

Plagiarism Undertaking

I solemnly declare that research work presented in this thesis titled "**A Comprehensive Study on DC Faults in Multi-terminal MMC Based HVDC Power Transmission System**" is solely my research work with no significant contribution from any other person. Small contribution/help wherever taken has been duly acknowledged and that complete thesis has been written by me.

I understand the zero tolerance policy of the HEC and Capital University of Science and Technology towards plagiarism. Therefore, I as an author of the above titled thesis declare that no portion of my thesis has been plagiarized and any material used as reference is properly referred/cited.

I undertake that if I am found guilty of any formal plagiarism in the above titled thesis even after award of MS Degree, the University reserves the right to withdraw/revoke my MS degree and that HEC and the University have the right to publish my name on the HEC/University website on which names of students are placed who submitted plagiarized work.

(Yasir Mehmood)
Registration No:MEE191005

Acknowledgement

After being utmost grateful to Almighty Allah who gave me help and courage to complete my M.S research work, My sincere gratitude goes to my parents for their love, support and patience throughout my master degree studies.

Special thanks due to my supervisor Dr. Umer Amir Khan for his guidance, support and rightful critics and encouragement, kept me in right direction during my entire thesis work to get this demanding task. I am fortunate to work with him which make me able to benefit myself from his knowledge regarding research skills and HVDC transmission.

I would like to extend my gratitude to my colleagues and friends especially Ayaz Ahmed, Muhammad Haseeb, Ahsan Mohi-ud-din for always being their whenever I needed them for help. I would like to pay huge debt of gratitude to my dearest family members My father, Mother, Brother and Sister who always supported me during my thesis work and encouraged me to stay motivated throughout my degree program in order to achieve my goals.

(Yasir Mehmood)

Abstract

As energy demand rises and our conventional or fossil fuel reserves are depleted, as well as due to environmental concerns, the power industry is shifting toward green energy or renewable energy resources. Renewable energy resources are a viable option. So the world is focusing on it. To integrate these resources into our existing AC grid, HVDC systems have become the reliable solution for such interconnections. As the super grid is in its growing stage, it is composed of a large number of converter stations, so the probability of fault occurrence is large, so it is a matter of time to investigate DC faults in the MTDC power transmission system. In the near future, because of the large-scale integration of power resources, severe faults have occurred. A comprehensive study and analysis are required to tackle these upcoming faults. In this research, the behaviour of an MMC-based MTDC system was investigated under DC fault conditions. The first step is to develop a grid-connected 7-level MMC simulation model in the Matlab/Simulink environment. The MTDC comprises three 7-level MMC converters connected in series, star, and ring configurations. On the AC side, all MMC converter stations are connected to a 220 kV AC grid via coupling transformers and phase reactors. On the DC side, the MMC converter stations are connected with pi-type transmission lines that have different lengths. The DC-link has a voltage of 100 kV. After the development of MTDC, DC fault analysis is carried out. The pole to pole and pole to ground faults are being investigated. The pole to pole fault is severe. Due to a pole to pole fault, all voltages, like pole to pole, positive pole, and negative pole voltages, are drastically reduced. Power transmission will be terminated if the positive and negative pole currents increase drastically. Due to the pole to ground fault, the faulted pole voltages drop to zero, the un-faulted pole voltages become twice, and this pole supports the pole to pole voltages, which will be constant and power transmission will not be terminated. The observations acquired from this research help the researchers to get an idea about the peak values of fault currents and voltages and also provide assistance in designing the future MTDC that survives under severe fault conditions.

Contents

List of Figures

List of Tables

Abbreviations

AC	Alternating Current
APOD-PWM	Alternate Phase opposition disposition pulse width modulation
CSC	Current Source Converter
DC	Direct Current
DQ,dq	Direct quadrature
FB	Full bridge
HVDC	High Voltage Direct Current
HVAC	High Voltage Alternating Current
HB	Half bridge
IGBT	Insulated Gate Bipolar Transistor
Km	Kilometer
LS-PWM	Level shifted pulse width modulation
LCC	Line Commutated Converters
MMC	Modular Multilevel Converter
MTDC	Multi-terminal Direct Current
MW	Mega watt
NLM	Nearest Level modulation
POD-PWM	Phase opposition disposition pulse width modulation
PWM	Pulse Width Modulation
PLL	Phase locked loop
PS-PWM	Phase shifted pulse width modulation
PD-PWM	Phase disposition pulse width modulation
PTP	Pole-To-Pole

PTG	Pole-To-Ground
PCC	Point of common coupling
RoW	Right of Way
STATCOM	Static Synchronous Compenstor
SHEM	Selective harmonics elimination modulation
SPWM	Sinusoidal pulse width modulation
SM	Sub Module
SAM	Sampled average modulation
SVM	Space vector modulation
THD	Total Harmonic Distortion
VSC	Voltage Source Converter

Symbols

dv/dt	change in voltage with change in time
N, n	Number of sub-modules
L	Inductance
C	Capacitance
R	Resistance
V_{dc}	DC bus voltages
V_c	Capacitor voltages
V	Volts
di/dt	Change in current to change in time
$T1, T2$	Used for IGBT switches
V_{sm}	Sub-module voltages
$D1, D2$	Diodes
ϕ_{cr}	Phase shift carrier phase angle
α	Alpha
β	Beta
U_{dc}	pole to pole dc voltage
U_p	positive pole dc voltage
U_n	negative pole dc voltage
L_g	Phase reactor inductance
R_g	Phase reactor resistance
i_{dc}	DC side current
i_{upa}, i_u	upper arm current
i_{lowa}, i_l	lower arm current

i_t	converter terminal current
V_t	converter terminal voltage
V_s	AC grid voltage
i_{su}	dc source current
i_{dif}	circulating current
n_k	sub-module insertion index
L_{arm}	arm inductance
R_{arm}	arm resistance
V_{tabc}	three phase output terminal voltage of converter
V_{sabc}	three phase AC grid voltages
P	Active power
Q	Reactive power

Chapter 1

Introduction

1.1 Background

As the world is evolving very fast, the demand for electrical energy to assist development also increases. This requires the electrical system to be enlarged to meet the electrical energy requirement. Starting in 1882, when Edison developed the DC generator, the DC power transmission system went through various development processes [1], [2].

In the past, the DC transmission systems were not adapted for some technical reasons, as the technology was in its grooming state and was not mature.

DC transmission has many drawbacks, as there are no DC/DC transformers. Due to this, DC power is transmitted at very low voltage levels over short distances [2].

For the past century, the AC system has been adapted as a global standard for the transmission of electrical power to businesses for many applications and homes. However, for several decades, HVDC has emerged as a viable alternate or complement to AC power transmission because it can interconnect the asynchronous AC

networks and also have the ability to transmit electrical power over long distances with minimum losses.

For example, HVDC has great importance for an application like offshore wind farms. In the case of wind farms, they are located at a faraway distance from the location at which the power is consumed, so the transmission of electrical power generated from that point is only possible with HVDC.

In the past, the reason for the adaption of AC transmission was the availability of the transformer. With the help of transformers, the level of AC voltage is stepped up for power transmission and stepped down at the customer end, thereby minimising the system losses.

It is easy to interrupt AC as compared to DC because of the unavailability of DC breakers. AC transmission systems have some limitations [2].

There are a number of problems regarding AC transmission systems, such as short-distance power transmission constraints, less power transmission capacity, and voltage drop due to reactance (inductive and capacitive) of the transmission line or cable. This means these reactance have a serious impact on transmission capacity. Less transmission capacity means more losses.

Due to inductive and capacitive reactance, the skin effect causes heat that comes with insulation damage. In an AC transmission system, it is impossible to interconnect two asynchronous AC networks having different frequencies [2].

With innovations in technology, HVDC transmission is now becoming a viable solution for electrical power transmission in our increasingly connected global energy ecosystem. HVDC transmission is used for bulk power transmission.

HVDC efficiency across long distances will be an essential part of the global renewable energy solution, integrating into the existing power infrastructure, ensuring that renewable energy is accessible and affordable [3].

Because of large-scale global developments, the future of HVDC appears bright, using HVDC in renewable energy systems. In the development of HVDC, MMC

converters are widely used. So it is required to study and analyze the DC faults in the MMC-HVDC power transmission system.

1.2 HVDC Power Transmission Systems

High Voltage Direct Current (HVDC) power transmission technology was introduced in 1954 and is used in the undersea cable interconnection project between the islands of Gotland (Sweden).

Electric power transmission systems use the high power electronics based HVDC technology to transfer large amounts of power effectively over a long distance [3].

For HVDC power transmission, underground cables or overhead transmission lines are used. The layout of a two terminal HVDC transmission system is shown in Fig. 1.1.

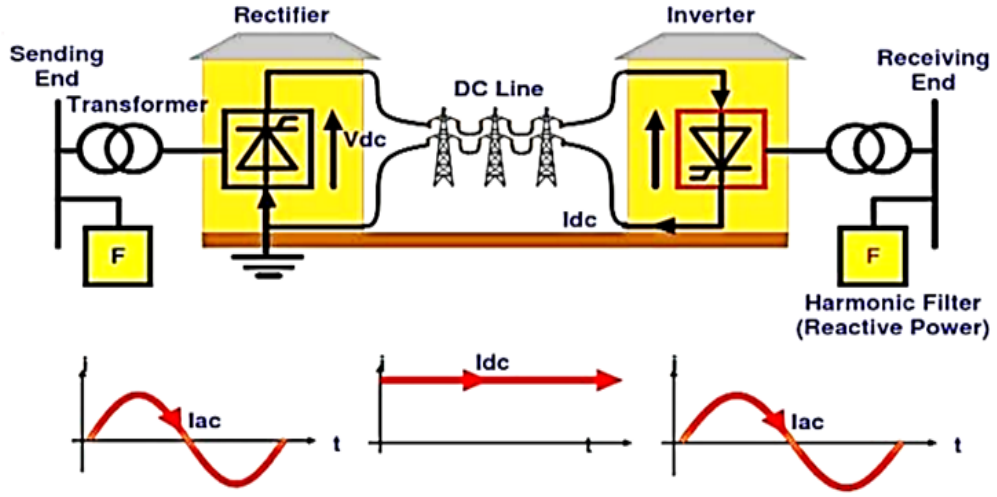

FIGURE 1.1: HVDC Power Transmission System [3]

In 1954 and up to the mid-1970s, in HVDC power transmission systems, mercury arc valves were used as switching devices [4].

In the next couple of years, the Line Commutated Converters (LCC), also known as Current Source Converters (CSC), will be utilized in HVDC transmission systems for the conversion of AC to DC [2].

In the 1990s, with the rapid improvement or advancements made in high-power semiconductor switch technology, especially in the case of Insulated Gate Bipolar Transistors (IGBTs), they had affordable prices and the ability of self-commutation.

Voltage Source Converters (VSC), also known as self commutated converters, have been widely used for HVDC power transmission from that time [2].

The first VSC-HVDC transmission system was installed in 1999 [3]. In comparison to HVAC power transmission systems, it is believed that HVDC systems are a better technical choice for long distance cable connections since the invention of the VSC [4].

With the passage of time, VSC-HVDC also has some constraints and limitations, for example, a limited number of output voltage levels and insufficient scalability for industry needs [5].

Later, Lesnicar and R. Marquardt presented the modular multilevel converter to resolve the aforementioned problems [6].

1.3 Basic Components of VSC Based HVDC System

Basic structure of VSC-HVDC power transmission system is shown in Fig. 1.2. The basic functions and characteristics of the components being used are discussed in this section [7], [8], [9].

1.3.1 Transformer

The transformer is used to make the AC grid voltage level suitable for the rated DC voltage transmission level.

As is clear from the figure, the harmonic filter is situated in between the transformer and the phase reactor, so harmonic current does not have any effect on

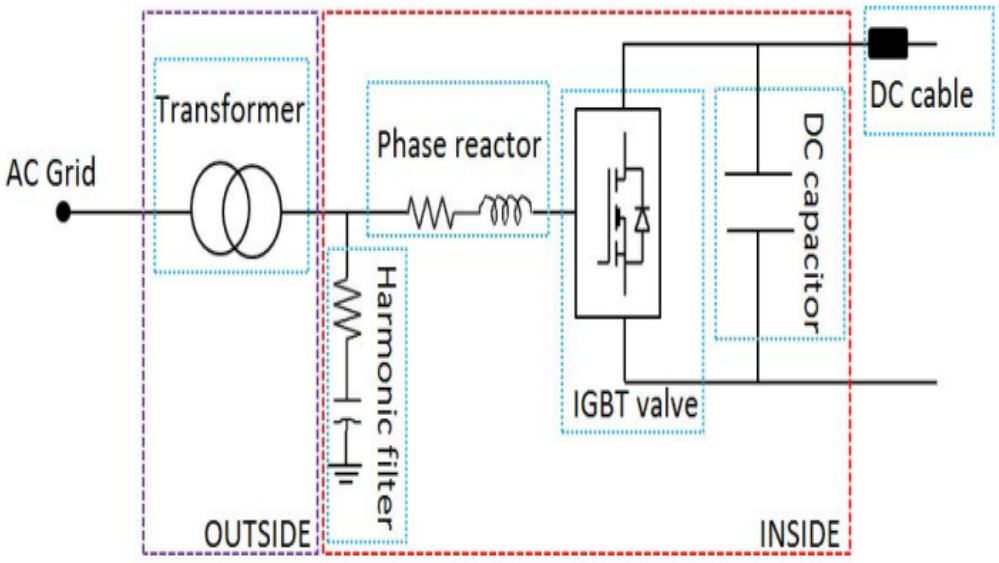

FIGURE 1.2: Basic representation of a VSC-HVDC transmission system [9]

the transformer, so the VSC based HVDC power transmission system can use an ordinary transformer [8].

1.3.2 Harmonic Filter

In VSC based HVDC power transmission systems, harmonics are generated due to the switching of converters. These harmonics are of high frequency and depend upon the converter topology and type of Pulse Width Modulation (PWM) scheme.

The harmonic filters are used to reduce or block high frequency harmonic current that is flowing into the AC system and also make sure that this harmonic current does not affect the transformer performance [7].

1.3.3 Phase Reactor

The phase reactor consists of a large inductor with small resistance. The function of the phase reactor is just like a harmonic filter to reduce the harmonic distortion and make the phase current smooth. The Phase reactor plays an important role in determining converter dynamics on the AC side [9].

1.3.4 Converters

Converters are the essential part of the HVDC power transmission system. The function of converters is to perform conversions between AC and DC. In MMC-based converters, a bridge consists of two arms, known as the upper arm and the lower arm. These arms are composed of several sub-modules containing IGBTs as switching devices, connected in series to create a high-level DC voltage.

Several PWM schemes are used for the switching purposes of these converters to create the desired voltage levels and improve the harmonic distortion of the converters.

1.3.5 Capacitor

The capacitor is used to maintain the DC voltages constant within the desired range by charging and discharging. These DC capacitors also reduce the ripples that are generated by the converters.

1.3.6 DC Cable

In HVDC transmission, the solid dielectric extruded polymer cables have pre-fabricated joints and are used for power transportation. These kinds of cables are lighter in weight and more flexible than the mass-impregnated or gas filled conductors used for HVAC transmission systems, which are expensive and have more weight.

1.4 HVDC and HVAC Transmission System

The HVDC and HVAC systems can be compared in terms of two points of view: installation cost and technology. Fig.1.3 represents the economical comparison between HVDC and HVAC transmission systems [3], [4].

The HVDC transmission system is gaining more importance due to the advancement in renewable energy technology.

The trend of HVDC power transmission system installation is increasing in America, China, and Europe. The main reason behind the increasing demand for HVDC power transmission systems is their lower cost as compared to HVAC for power transportation over long distances.

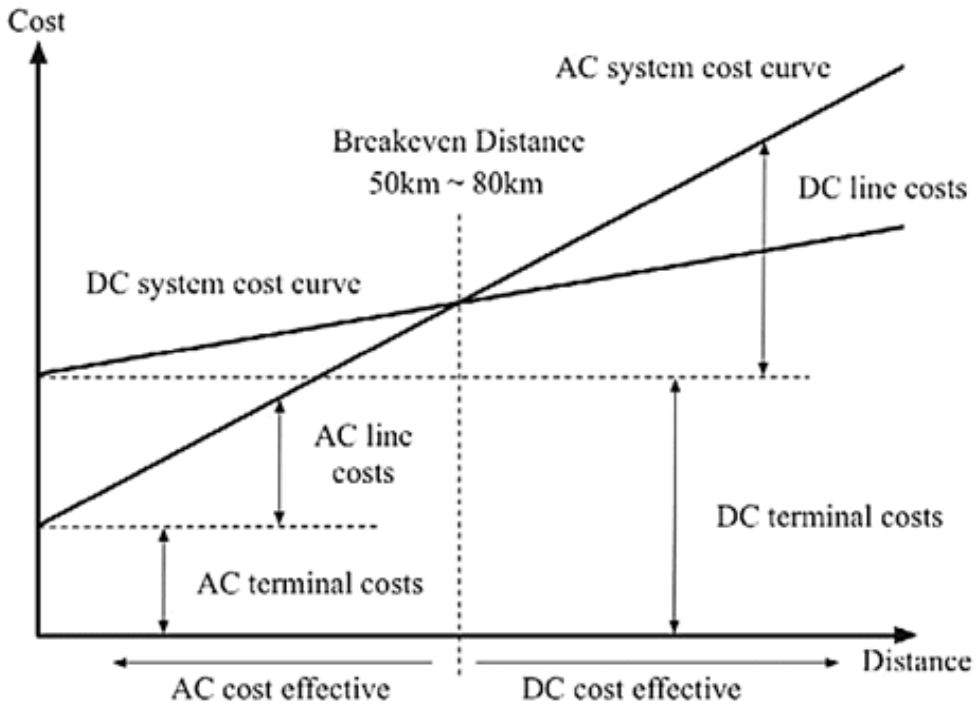

FIGURE 1.3: Comparison between HVDC and HVAC with respect to cost [10]

HVAC technology is considered more suitable than HVDC, mostly for short distances. The reason behind is that, the initial cost of HVDC power transmission system is higher as compared to an HVAC power transmission system because of the requirement for costly components for the conversion of AC to DC, like filters and converters [3].

The HVDC power transmission system is more convenient and suitable for the transmission of power over a large distance. There is no skin effect in DC cable

because of zero frequency, the requirement for reactive power compensation is eliminated. But in the HVAC transmission system, the skin effect exists, so it is required to recoup for the reactive power, as an increase in the distance increases the cost [11].

When it is required to transmit power over a large distance, the installation cost of cables and insulators being used for the power transmission in HVDC is less when compared with the HVAC installation cost.

The loss of transmission cables and the installation costs decrease by about two-thirds [10]. The distance marked as the break-even distance as shown in Fig. 1.3 between the HVAC and HVDC is correlative and may vary depending on the required transmission capacity.

The distance for overhead lines lies between 400 km to 700 km, and 25 km to 50 km for the cable system [10].

HVDC has numerous advantages over HVAC which are listed below [12], [13].

1. No skin effect in the case of an HVDC transmission system, so it can utilize the whole cross-section area of the transmission line conductor [14].

2. There are fewer transmission losses in DC cable, especially for long-distance high voltage applications, because the HVDC operates at zero frequency and, due to this, there exist no capacitive and inductive reactance losses, so power is transmitted with a unity power factor [14].

3. The cost of cable manufacturing for HVDC is lower than for HVAC because manufacturing long-distance and high-voltage cables for HVAC is more difficult and expensive [12].

4. For HVDC systems, it is easy to get or access power from distant or remote resources. For example, offshore wind power farms have lower losses as compared to HVAC, which has more transmission losses [13].

5. Bi-directional power flow [13].

6. HVDC systems have more effective power control.

7. The HVDC power transmission system allows the transmission of power between asynchronous AC systems, meaning the AC systems that are operating at the same or different frequencies.

8. In an HVDC power transmission system, there are no limitations on transmission distance for both underground/submarine cables and overhead transmission lines.

9. Accurate and fast control of power flow means an improvement in power system stability for the HVDC link.

10. At the same size of the conductor, the HVDC transmission system can transmit more power as compared to the HVAC.

11. HVDC does not require a large area for its installation and is also environmentally friendly [15].

1.5 Application of HVDC Transmission System

HVDC transmission systems are widely used in a variety of applications, including those listed below [4], [16],[17] and [18].

1. An important applications of HVDC transmission systems is to interconnect asynchronous AC systems. It is an economical and reliable means of electrical power interconnection between them.

   For this purpose, back to back HVDC systems are utilized, in which power is transmitted between the AC buses at the same location. In the case of a back to back HVDC system, the converter stations, i.e., the inverter and rectifier, are situated at the same station location.

   These converter stations do not have any DC transmission lines between them [4].

2. Large power transmission over a long distance: When the break-even distance (the distance point at which the cost of different transportation systems is the same) increases.

   HVDC is an economical solution for power transportation from remote energy resource, as offshore wind farms and hydroelectric power plants, to different load centers.

   One example of this kind of HVDC power transmission is the Itaipu HVDC power transmission system situated in Brazil [19].

3. Power transmission using submarine and underground cables: The HVDC power transmissions systems are widely used in the submarine and underground cable power transmission.

   These cables are used to transport power into congested or overcrowded areas.

   In such areas, the difficulty is faced in building new generations of plants where it is difficult to acquire permission for the installation of new overhead transmission lines.

   It is easy to get the Right Of Way (ROW) for HVDC underground cable as compared to HVAC transmission line and for the HVDC overhead transmission line [4].

   Similarly, the HVDC submarine cables are utilized to transport power to isolated loads where the power consumption is greater than the power generation.

   One example of such a kind of HVDC application is the Gotland project, situated in Sweden [4].

4. Electric power flow stabilization: HVDC transmission systems provide the fast and accurate control capability.

   They can solve issues like power flow in AC ties (transmission lines that connect one area to another are known as tie lines) can be difficult to control and can cause overloading and stability problems [4].

1.6 Configurations of HVDC System

In power transmission, various HVDC configurations are used. A selection of these configurations is depends upon the location and function of the converter station. Some HVDC system configurations are discussed here in this section.

1.6.1 Mono Polar System

Fig 1.4 shows the mono polar HVDC transmission link. The mono polar HVDC link is the simplest and least expensive configuration for an HVDC transmission link.

In a mono polar HVDC link, a single conductor is used for the transmission of power, and the current return path is an earth, water, or metallic conductor.

Mono polar links are mostly used for submarine cable transmission.

Its installation cost is low, so it is used to interconnect two remote AC systems using an overhead transmission line cable at a distance of 300 km to 3000 km or more [10].

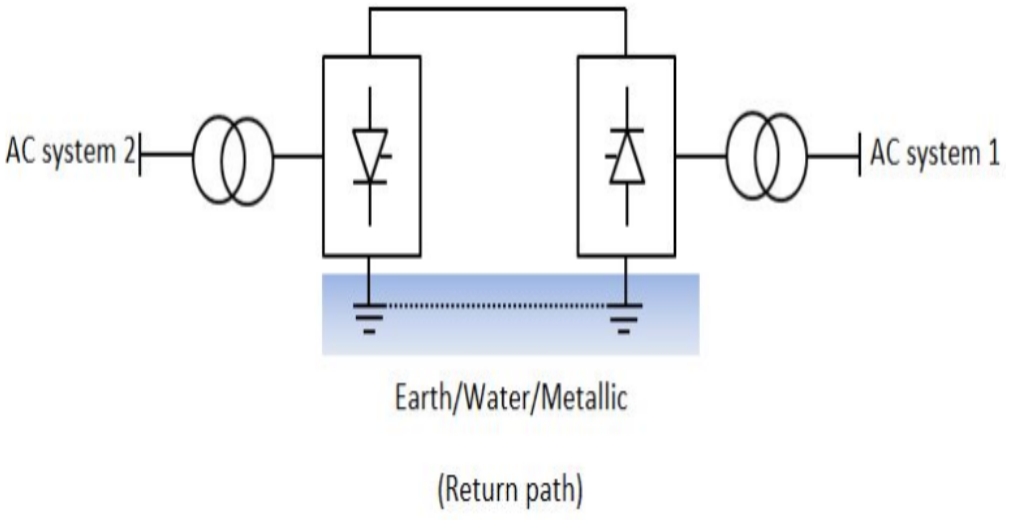

FIGURE 1.4: Mono-polar HVDC link [10]

1.6.2 Bipolar System

Fig 1.5 presents the bipolar HVDC transmission link.

The bipolar HVDC transmission link is widely used for HVDC power transmission systems.

In a bipolar link, the current return path is provided by two earth electrodes or by a metallic conductor.

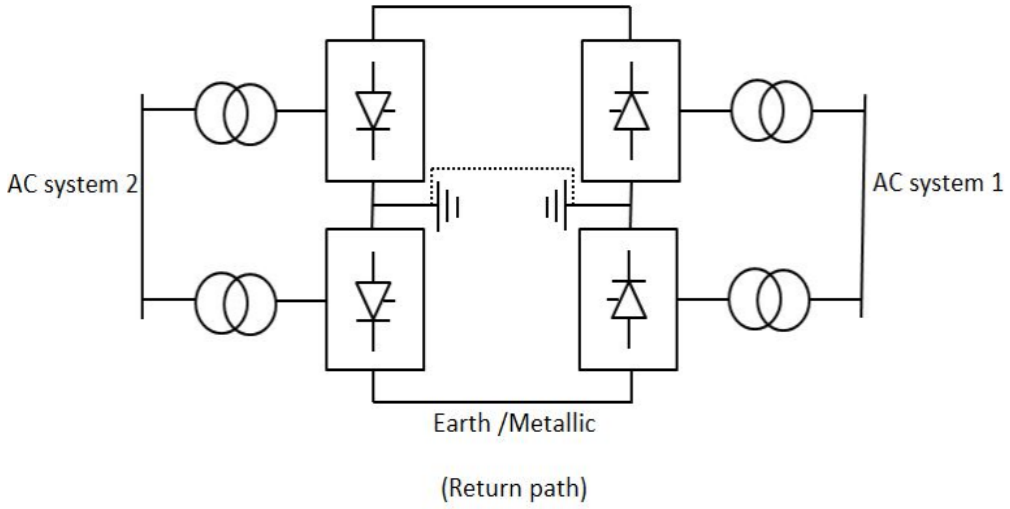

FIGURE 1.5: Bipolar HVDC link [10]

It consists of two poles; one pole is positive and the other pole is negative with respect to the ground. These poles are independent of each other.

A bipolar HVDC system can be operated as two mono polar HVDC systems. In a situation in which one pole is out of order or un-serviceable due to regular maintenance or some fault.

It is possible to transport the power by using the other pole with reduced power transmission capability [20].

1.6.3 Back to Back System

Fig 1.6 shows the back to back HVDC power transmission system.

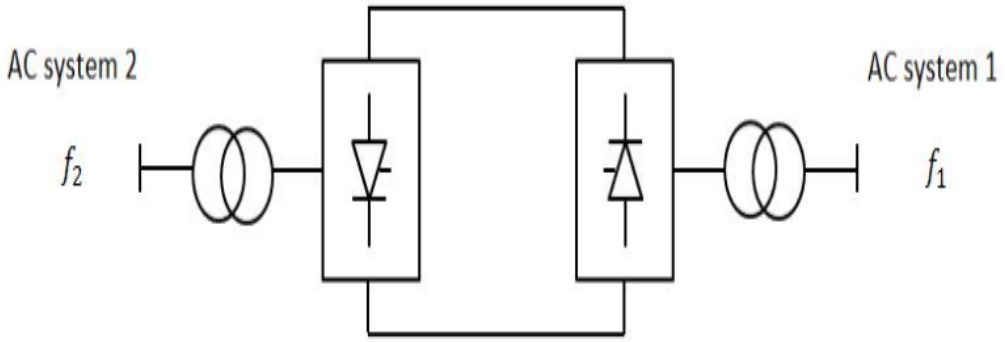

FIGURE 1.6: Back to back HVDC transmission system [10]

The back to back HVDC power transmission system is similar to the bipolar HVDC link without earth return, as is clear from the figure.

The back to back HVDC transmission system is especially utilized for interconnecting asynchronous AC systems having different operating frequencies and different voltage levels. The rectifier station and the inverter station are both located at the same location or in the same building in a back to back HVDC transmission system.

The conductor length between two converters is kept as short as possible. It provides freedom to choose any desired DC voltage level. In general, it is required to decrease the number of semiconductor switching devices used for the sub-modules used in the converter stations, reduces the size of the converter station building. The DC voltage level is fixed at a low level and the DC current level is fixed at a high level [4].

1.6.4 Multi-Terminal HVDC System

The multi-terminal HVDC power transmission system is shown in Fig 1.7. Two or more converter stations can be connected in series or parallel via the multi-terminal HVDC transmission system. Most important features of multi-terminal HVDC transmission systems is the ability to exchange power between multiple suppliers and multiple consumers located in remote places. In multi-terminal

HVDC transmission, one of the converter stations is working as a rectifier and the others are working as inverters [4], [21].

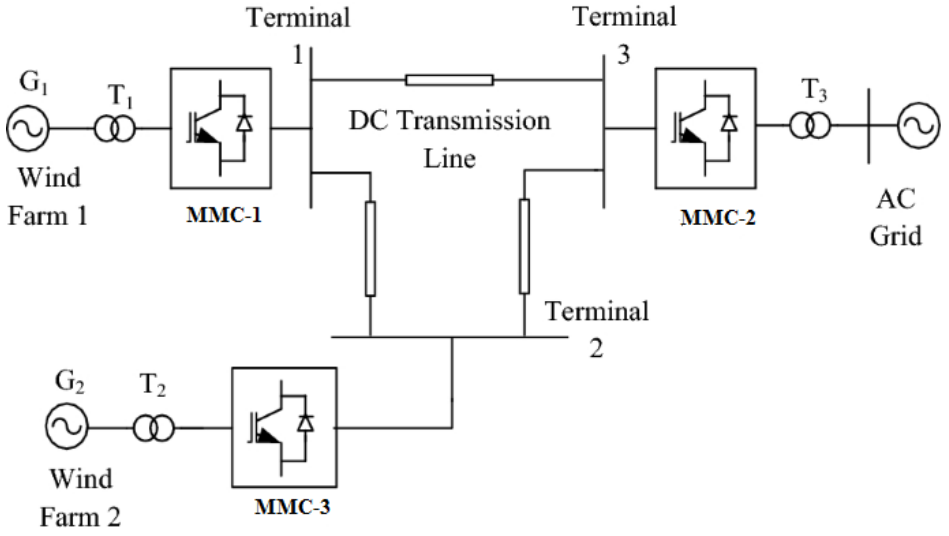

FIGURE 1.7: Multi-terminal HVDC transmission link [21]

1.7 HVDC Converter Technology

Energy conversion from AC to DC and then from DC to AC is the fundamental goal of an HVDC system. The rectifier station, also known as the sending end converter station, and the inverter station, also known as the receiving end converter station.

HVDC power transmission technologies are categorized into two groups based on the type of converter used.

1. Current Source Converter (CSC)
2. Voltage Source Converter (VSC)

1.7.1 Current Source Converter Based HVDC

Fig. 1.8 below shows the Current Source Converter (CSC) based HVDC power transmission system configuration, also called as the classical HVDC transmission

system. For CSC-HVDC transmission systems, thyristors are used as switching devices, and they require the AC line voltage for the commutation process or they commutate at line frequency, so for this reason, the CSC is also called as the Line Commutated Converter (LCC).

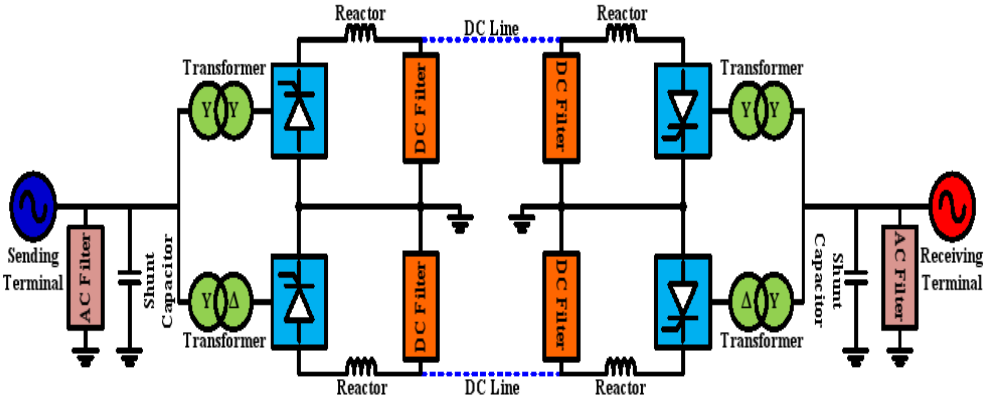

FIGURE 1.8: CSC-HVDC system configurations [16]

It consists of DC filters, AC filters, transformers, phase reactors, converters, shunt capacitors, cables, or DC transmission lines [16]. The LCC-HVDC configuration requires a voltage source such as a wind turbine, or STATCOM station because it cannot control the DC voltage itself [22].

The LCC depends upon the line voltages of the AC system for the conversion process. In LCC the thyristors used as switching devices once turn ON, then they do not have the capability to turn off autonomously, they require the line voltages of an AC system for the commutation process.

In LCC, the current cannot change direction and can be considered as constant current that flows through a large inductor. The LCC acts as a constant current source on the AC side; therefore, it is also called a CSC [22].

At the sending end terminal, the converter performs AC to DC conversion (rectifier) and at the receiving end terminal, the converter performs DC to AC conversion (inverter). In Fig. 1.8 four converters are shown; each converter consists of a six pulse converter bridge. This converter bridge is the fundamental converter unit

of the CSC-HVDC system. Two converter bridges are connected in a series configuration to form a twelve-pulse converter bridge to reduce the harmonic distortion produced by the converter in an AC system [16], [23].

The power that is transported by the HVDC transmission line is controlled by controlling the magnitude and polarity of DC voltages. The DC current remains unidirectional in such a way that one converter station controls the voltage and the other converter station controls the DC current. The transformers are utilized to make the AC voltage level appropriate for the converter stations. The converter stations produce harmonic content in the current that is reduced using AC filters [12], [16]. The shunt capacitors and AC filters are used for the compensation of reactive power that is consumed by the converter stations. Converter stations produce ripples in the DC voltage that are reduced by using DC filters, and ripples in DC current are reduced by using the smoothing reactors [12], [16].

Thyristors used in the CSC-HVDC transmission system have a high power rating, so they are mostly used in practice and are considered the only choice for power transmission over large distances, but they have some drawbacks, and extra effort is required to get the required performance. Some of these are given below:

1. Thyristors used in CSC cannot be turned off automatically [8], [24].
2. Thyristors used in CSC can either commutate with respect to line frequency or by forced commutation [14].
3. Reactive power is required for the commutation of switching devices [24].
4. A synchronous voltage source requires providing reactive power for the commutation of thyristors [25].
5. In LCC, the bulky and expensive filters are required to remove the low-frequency harmonic components present in the output voltage of the converter, and the filters also provide the reactive power required for the commutation of thyristors [25], [26].
6. CSC always operated in delay power factor mode [24], [25], [26].

7. CSC cannot control the active and the reactive power independently because it has poor reactive power control ability [24], [27].

8. CSC cannot work with isolated systems, so for this reason, they have no black start capability [24], [27].

9. In CSC, if it is required to change the power flow direction, the DC voltage polarity also needs to change, which is costly [28].

1.7.2 Voltage Source Converter Based HVDC

In voltage source converter based HVDC power transmission systems, Insulated Gate Bipolar Transistors (IGBTs) are used as switching devices instead of thyristors.

IGBTs have the ability to self commutation or turn off autonomously rather than thyristors in a CSC that requires the line voltage of an AC system for the commutation process, so this allows the utilization of high frequency carrier Pulse Width Modulation (PWM) schemes for the control of the switching devices.

Fig. 1.9 shows two terminal VSC based HVDC system configurations that consist of AC filters, transformers, reactors, converters, DC capacitors and DC line [16].

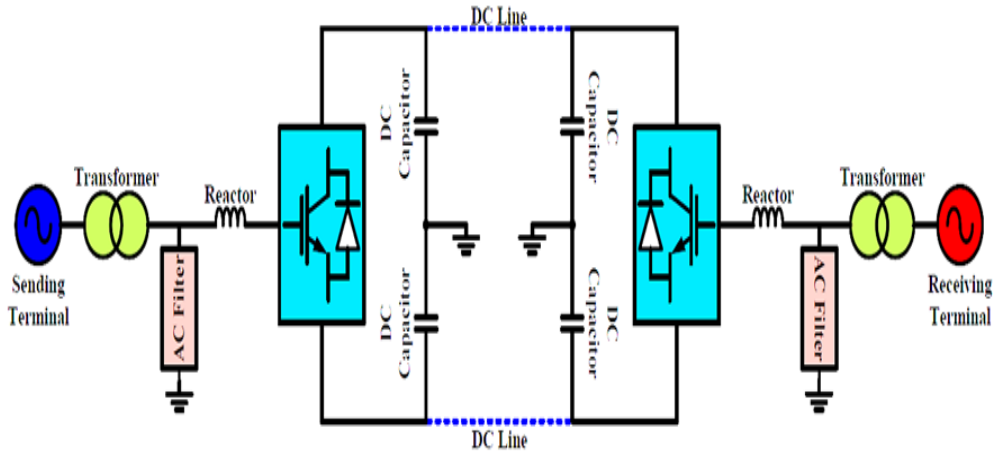

FIGURE 1.9: VSC-Based HVDC system configurations [16]

The difference in operation between the current source converter, also called the LCC HVDC power transmission system, and the VSC HVDC power transmission system is the higher controllability of the VSC. HVDC power transmission system, due to higher controllability, the VSC HVDC system has many advantages over the CSC HVDC system. Some of these are given below [8], [24], [28] [29], [30], [26].

1. In VSC HVDC, IGBTs with self-commutation capability are used [8], [28].
2. In the VSC HVDC transmission system, high-frequency PWM is used that reduces the low-frequency harmonics.
3. VSC-HVDC does not require large, expensive filters.
4. Unlike CSC HVDC, VSC HVDC does not require reactive power for the commutation of switching devices [24], [26].
5. In VSC HVDC power transmission system, the active power and the reactive power can be independently controlled by controlling the PWM signal of the converter station.
6. In VSC HVDC power transmission system, the power flow direction can be changed or reversed without changing the direction or polarity of DC link voltages. By simply reversing the polarity of the current, the power flow direction can be changed or reversed [28].
7. Passive networks can be connected with the VSC-HVDC system.
8. Because VSC HVDC can work with isolated systems, it can perform black starts [30].
9. In CSC or line commutated converters, the commutation process is dependent on the line voltages, but in VSC-HVDC, commutation failure due to AC system disturbance can be avoided because the commutation process is independent of the line voltages.

10. In the VSC HVDC system, the communication between the rectifier and the inverter station does not require [29].

VSC HVDC systems are used as an alternative to classical HVDC (LCC) systems, but they also have some drawbacks. VSC HVDC systems have more switching losses due to high frequency PWM operation, and their cost is higher compared to LCC HVDC systems. The current and voltage ratings of the converter are lower [31], [32], [33].

On the other hand, the VSC HVDC systems are more suitable for interconnecting the remote power resources to the AC grid because they can provide reactive power support and black start capability.

Due to internal capacitors, the VSC has more energy storage capacity as compared to the LCC HVDC system [34]. Despite the LCC having higher current and voltage ratings and fewer losses, they require additional components like AC harmonic filters and STATCOM that increase the cost and complexity as compared to voltage source converter (VSC) based HVDC systems [32].

One of the most advanced voltage source converter technologies that has been developed recently is called Modular Multilevel Converters (MMC). This thesis research topic is based on a multi-terminal MMC based HVDC power transmission system.

MMC has many advantages as compared to conventional voltage source converter based HVDC systems. These will be discussed in detail in upcoming sections.

1.8 Thesis Objectives

The objective of this research thesis is to conduct a comprehensive study of DC faults and their analysis in multi-terminal modular multi-level converters based on HVDC power transmission systems. In Matlab/Simulink, there are various simulation models for HVDC power transmission systems, but they are based on

two-level voltage source converter technology. As there is no MMC simulation model in the Power Simscape library, as a first step, a 7-level MMC model in Matlab/Simulink was developed successfully, with the view of developing MMC-based MTDC power transmission.

The main objective of this thesis is to perform DC fault analysis in a multi-terminal MMC HVDC power transmission system, so for this purpose, three HVDC power transmission topologies were used.

The first one is the series topology, which is composed of three MMC converter stations. One of them serves as a rectifier to convert AC into DC, also called a sending end converter station. The remaining two converters, known as receiving end converter stations, function as inverters to convert DC to AC. The sending end converter station is linked to the receiving end converter stations on the DC side by a 100 km pi-type transmission line. The AC side of all converter stations is connected to the AC grid via phase reactors, coupling transformers, various loads, and transmission lines to make the simulation and analysis more realistic and practical. The second receiving end converter station is connected to the DC bus of the first receiving end converter station via a pi-type transmission line.

The second topology that is being used for the development of HVDC power transmission is the star topology. In star topology, all the converter stations are connected at the common node. In star topology, the tapping is carried out at the node for connecting the receiving end converters. On a three-terminal MMC-HVDC power transmission system, three 7-level MMC converter stations are used; each is connected to the AC grid individually on the AC side, and on the DC side, these converter stations are connected via a pi-type transmission line of 200 km, 300 km, or 500 km. One of these three converter stations is working as a rectifier, and the remaining two converter stations are working as inverters.

The third topology that is being used for the development of HVDC power transmission is the ring topology. In a ring topology, three 7-level MMC converter stations are used, and all converter stations are connected via a pi-type transmission line of a length of 100 km in a ring.

Following the development of the aforementioned MMC HVDC power transmission systems, DC faults, including pole to pole and pole to ground faults, are generated at specific points. The impacts of these generated faults on the currents and voltages on the AC and DC side are examined, for example, faults at the converter terminal on the DC side, faults at the transmission line, or faults that are generated at the node.

The objective of this DC fault analysis is to get information about the impact of a fault on the overall system operation and performance. Once we can acquire information about the variations in current and voltage due to faults, we can get information about the current peaks. This knowledge helps us in the designing of protection devices and helps us in taking the necessary safety measures to bear the minimum damage due to these faults.

This DC fault analysis also helps us in the protection coordination for the MMC converter stations. For example, if, due to some fault, some of the MMC sub-modules stop working or become damaged, these sub-modules are quickly bypassed or replaced with new ones that are in working condition to provide the transmission of power uninterrupted. This increases the power transmission reliability.

1.9 Thesis Outline

This thesis is composed of the following chapters:

Chapter 1

Chapter 1 gives a brief introduction to HVDC technology, the history of HVDC, a comparison of HVDC and HVAC, HVDC configuration, the types of converter technology, and discusses the advantages and disadvantages of HVDC converter technology, etc.

Chapter 2

Chapter 2 presents the literature review regarding the multi-level concept. An introduction to the modular multi-level converter's basic operation is discussed. A comparison between voltage source converters (VSC) and current source converters (CSC) is provided. The topologies used for MMC, the basic operation of MMC topologies, characteristics of MMC, and modulation techniques used for MMC are discussed. Also, a brief introduction of a modular multi-level converter (MMC) based multi-terminal HVDC power transmission system is discussed. First of all, we discuss a 2-terminal modular multi-level converter (MMC) HVDC power transmission system. Then we discuss the three terminal MMC HVDC transmission systems, and finally, we discuss their basic operation.

In this chapter, the basic topologies that are being used for the multi-terminal HVDC transmission system are described briefly. This chapter also gives a brief introduction to DC faults in MTDC transmission lines. The structure and working principles of the MMC HVDC power transmission system are discussed. The DC side fault mechanism of the pole to pole and pole to ground is discussed; Research papers regarding DC fault characteristics and fault current analysis are presented. And at the end, the gap analysis and problem statement are provided.

Chapter 3

In Chapter 3, the MATLAB/Simulink model of the 7-level modular multi-level converter is discussed. After this, the control methods for the MMC are described in detail along with the MATLAB/Simulink model.

Chapter 4

Chapter 4 gives the simulation results regarding DC fault analysis in the multi-terminal modular multi-level converter (MMC) based MTDC power transmission systems. In Matlab/Simulink, DC fault characteristics are analyzed in MTDC power transmission systems by using fundamental MTDC topologies like series, star, and ring topology and, in the end, concluding.

Chapter 5

Chapter 5 concludes the whole thesis work and gives information about the research work that is expected in the future.

Chapter 2

Literature Review

2.1 Introduction

The Voltage Source Converter (VSC) based High Voltage Direct Current (HVDC) technology was used for the first time in a commercial project in 1999 on the island of Gotland [35]. In this project, the two-level VSC-based technology is used with a voltage rating of ±800 kV and a power rating of 50 MW. Since then, the power rating, the DC voltages, and the distance of the VSC-HVDC power transportation have been improving continuously.

Till the end of the year 2017, more than 30 VSC based HVDC power transmission projects are operational worldwide [35]. One of the most advanced voltage source converter technologies that have been developed recently is called modular multilevel converters. This thesis research topic is based on an MMC based HVDC power transmission system. MMC has many advantages as compared to conventional VSC based HVDC power transmission systems. When compared to a line commutated converter , the VSC based HVDC power transmission system has no commutation failure, the DC voltage remains constant when current polarity is changed or reversed, and independent control of active and reactive power [29], [8]. The multi-terminal HVDC system consists of multiple sending and receiving terminals that can transport distributive energy to various distant loads.

MMC based HVDC power transmission systems are now commonly used in HVDC projects [6]. For example, the first commercial Trans Bay Cable project (TBC) and many other projects all utilize the Half Bridge (HB) MMC based HVDC power transmission systems. The DC pole to pole faults and pole to ground DC faults have a serious impact on the normal operations of the MMC based HVDC power transmission system [36]. So it is necessary to have a better understanding of the modular multilevel converter.

2.2 Introduction of Modular Multi-level Converter

The MMC is a type of VSC that converts the AC voltages into DC voltages.

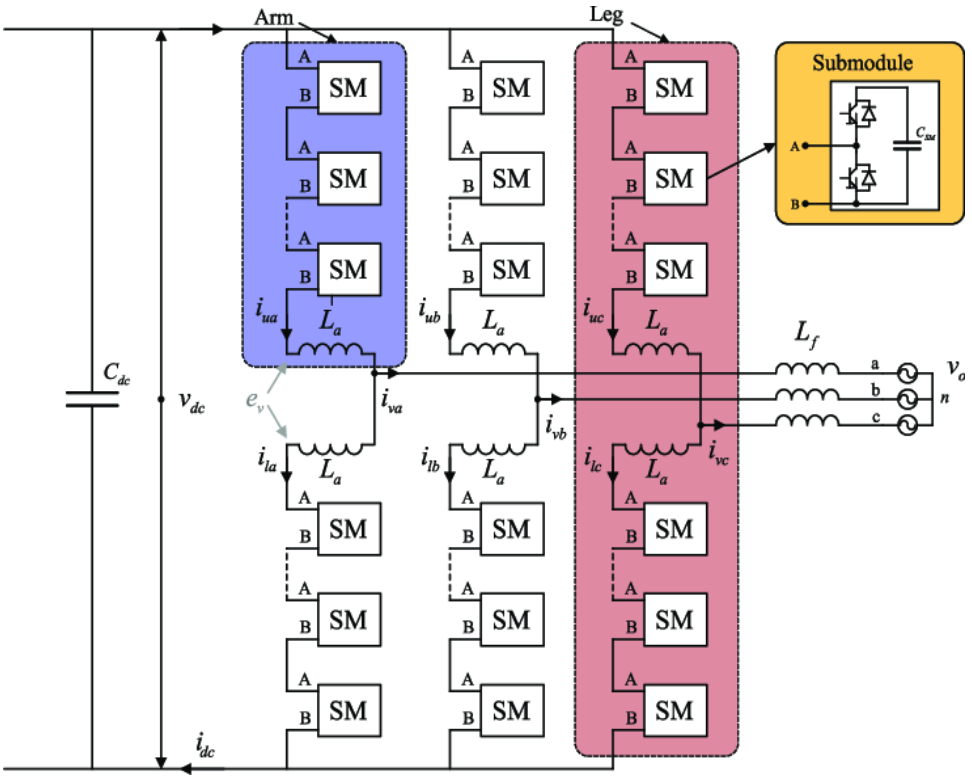

FIGURE 2.1: Modular Multilevel Converter Basic Structure [37]

The word "multi-level converter" means the converter has more than two or at least three levels in its output voltage waveform [37]. In Fig. 2.2 a two-level conventional voltage source converter is shown, having two output levels, as shown in Fig. 2.3.

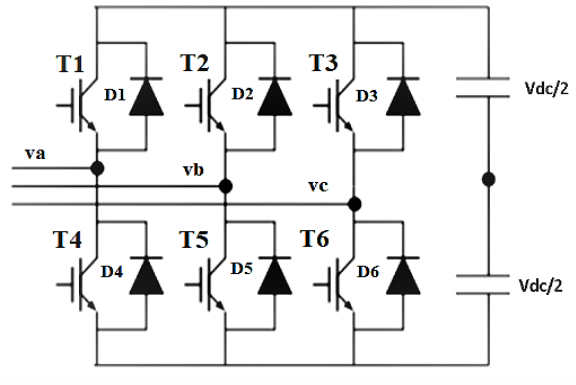

FIGURE 2.2: Two-levels VSC [37]

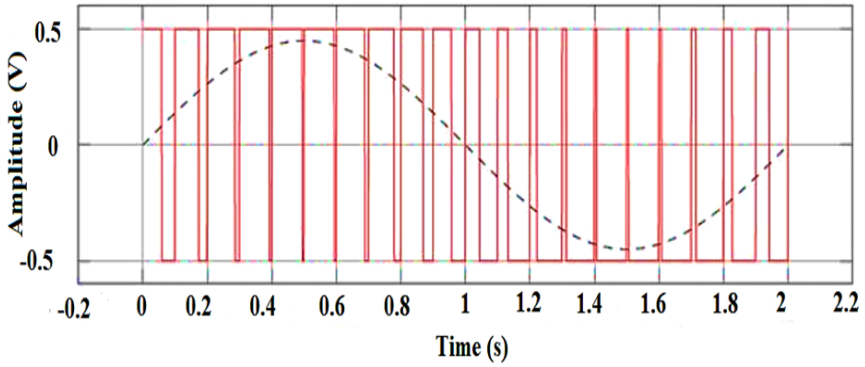

FIGURE 2.3: Voltage waveform that is generated by two-levels VSC [24]

The concept of multilevel is elaborated or described in such a manner that if the output voltage waveform of a converter has a greater number of steps, then the content of harmonic distortion decreases. As a result, the requirements of the AC harmonic filters are eliminated to some extent. The stress on switching devices decreases due to dv/dt (rate of change of voltage) across each switching device being reduced [38].

Fig. 2.3 and Fig. 2.4 shows that the quality of the voltage waveform of MMC is better than the voltage waveform of two-level VSC. The waveform of MMC has more steps or levels as compared to the VSC waveform. The two-level VSC generates the PWM waveform, which contains more Total Harmonic Distortion (THD) as compared to MMC. The waveform generated by MMC is closer to a sinusoidal waveform. In MMC, the requirements for bulky and expensive filters are reduced [24].

Marquardt first introduced the modular multilevel concept in 2003. Siemens' first

commercial project of MMC-HVDC was launched in 2010 [39]. The MMC topology

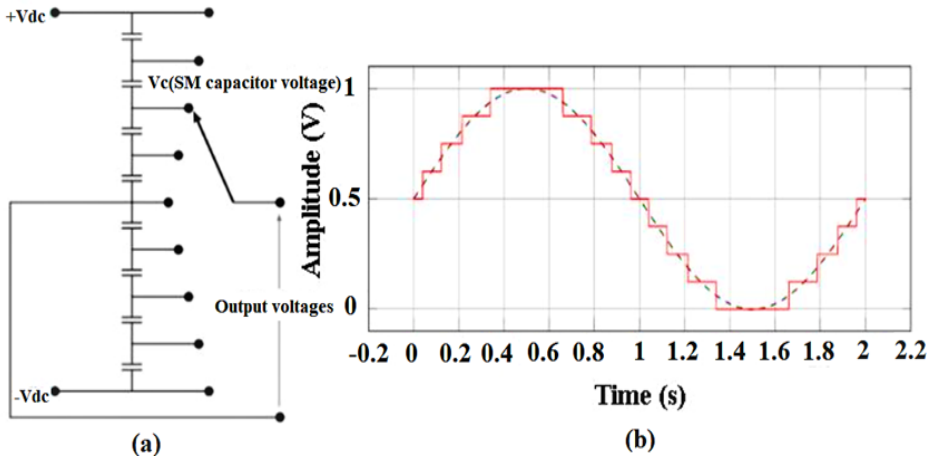

FIGURE 2.4: (a) Principle of operation of multi-level converter (b) MMC output waveform [24]

is widely used in HVDC applications due to its characteristics of modularity. This means MMC's are built with identical Sub-Modules (SM), so it is easy to add or remove any faulty sub-module when required. Another characteristic of MMC is its scalability. This means any voltage level is achieved by using a larger number of sub-module. When levels or steps in the output voltage waveform increase, then the THD reduces, so the output voltage quality increases, and the requirements for bulky and expensive harmonic filters reduce. MMC allows for lower switching frequencies, which results in lower switching losses [24].

2.3 MMC Basic Operation

The basic operation of MMC is discussed in this section. Fig. 2.5 shows the basic structure of MMC. MMC is composed of three phase legs, and in each phase leg, two arms exist, called the upper arm and lower arm. In each phase leg arm N or n (number of sub-module) sub-modules also called a cell, often hundreds of SM are connected in series to get hundreds of kilo volts [39], each arm also has a series arm reactance indicated by L that is essential in order the limit the current called circulating current produced by the voltage difference in arms [40]. The arm reactor also reduces the fault currents when a short circuit occurs during dc

faults. The output voltage of each phase leg arm is the sum of the voltages of

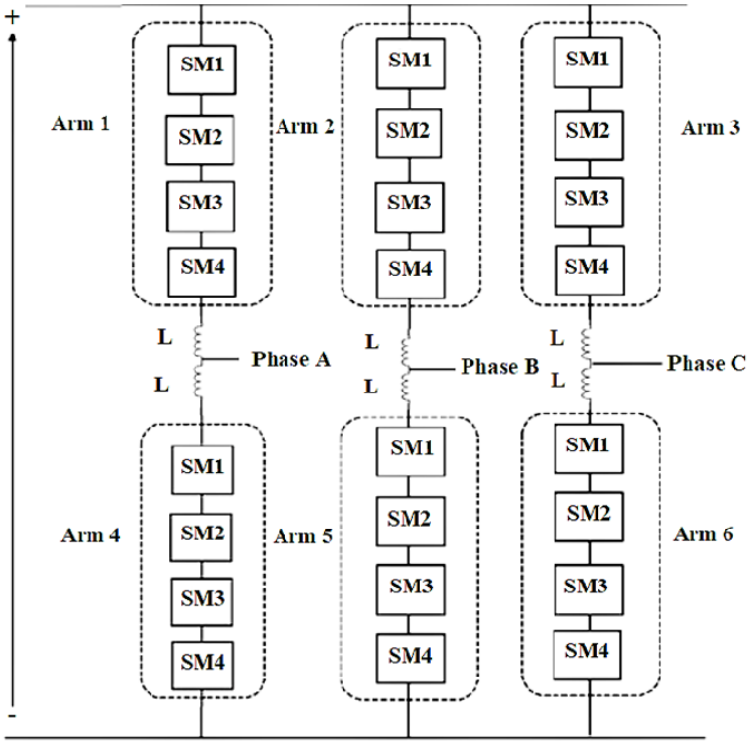

FIGURE 2.5: Basic structure of 3-Phase 5-level MMC [39]

each sub-module connected in series. An MMC that has a large number of sub-modules connected in series can provide an output voltage waveform quite similar to a sinusoidal waveform due to the large number of levels of voltage that can be produced by the converter. That has fewer harmonic components in the output voltage, so there is less requirement for bulky and expensive filter [41].

In MMC, the voltage across each sub-module capacitor is given by the following equation.

$$V_c = \frac{V_{dc}}{n} \tag{2.1}$$

The basic structure of 5-level MMC is presented in Fig. 2.5. The figure clearly shows that 5-level MMC consists of three 3 phase legs, two arms in each phase leg, and N (numbers of sub-module) sub-modules connected in series in each phase leg arm. The Half Bridge (HB) or Full Bridge (FB) topology is used for sub-modules. N+1 refers to the number of output voltage levels for MMC. In a case study

of 5-level MMC, there will be N = 4 sub-modules in an arm, four sub-modules connected in series in an arm, and a total of eight sub-modules in a phase leg, and N+1 (4+1=5) levels in the output voltages. The states for the MMC operation are stated in a table given below [24].

TABLE 2.1: States for MMC Operation

States	n_{up}	n_{low}	V_{oa}
1	4	0	$\frac{-V_{dc}}{2} + 0\frac{V_{dc}}{4}$
2	3	1	$\frac{-V_{dc}}{2} + 1\frac{V_{dc}}{4}$
3	2	2	$\frac{-V_{dc}}{2} + 2\frac{V_{dc}}{4}$
4	1	3	$\frac{-V_{dc}}{2} + 3\frac{V_{dc}}{4}$
5	0	4	$\frac{-V_{dc}}{2} + 4\frac{V_{dc}}{4}$

When all the above states presented in the above table are executed, a 5-level voltage waveform will be generated, as shown in Fig. 2.6.

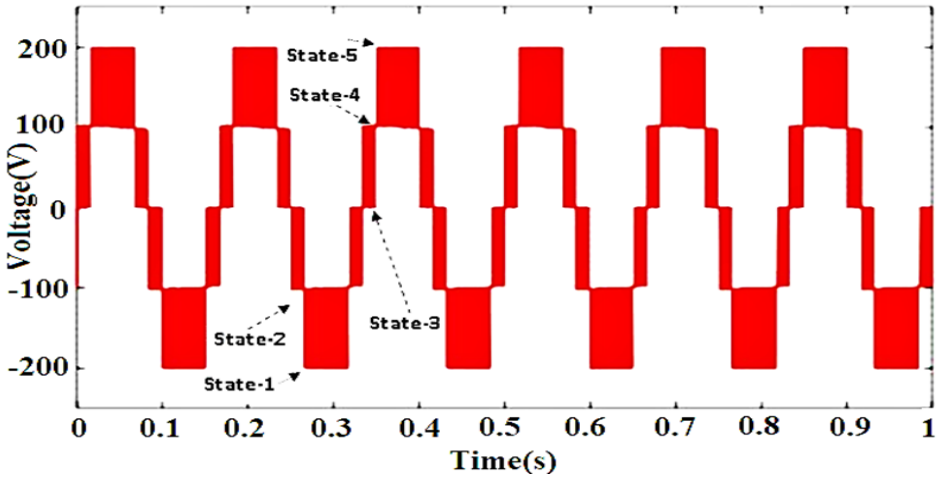

FIGURE 2.6: Levels for 5-level MMC output voltages

For the 5-Level MMC, there are five states presented in table 2.1. Several PWM techniques are being utilized for the execution of these states to achieve the required converter phase voltage V represented in table 2.1. V has 5-levels depending upon the on off condition of sub-modules. In table 2.1, the terms n_{up} and n_{low} represent the number of sub-modules in the upper phase leg arm and lower phase leg arms of MMC.

2.4 States of MMC

The value of Vdc presented in table 2.1 is 400 V.

1. In state 1, four sub-modules in the upper phase leg arm will be in ON state and no sub-module in the lower phase leg arm will be in ON state.

$$\frac{-V_{dc}}{2} + 0\frac{V_{dc}}{4} = \frac{-V_{dc}}{2} = -200\ V \tag{2.2}$$

2. In state 2, three sub-modules in the upper phase leg arm will be in ON state, and one sub-module in the lower phase leg arm will be in ON state.

$$\frac{-V_{dc}}{2} + 1\frac{V_{dc}}{4} = \frac{-V_{dc}}{4} = -100\ V \tag{2.3}$$

3. In state 3, two sub-modules in the upper phase leg arm will be in ON state, and two sub-modules in the lower phase leg arm will be in ON state.

$$\frac{-V_{dc}}{2} + 2\frac{V_{dc}}{4} = 0\frac{-V_{dc}}{4} = 0\ V \tag{2.4}$$

4. In state 4, one sub-module in the upper phase leg arm will be in ON state, and three sub-modules in the lower phase leg arm will be in ON state.

$$\frac{-V_{dc}}{2} + 3\frac{V_{dc}}{4} = \frac{V_{dc}}{4} = 100\ V \tag{2.5}$$

5. In state 5, no sub-module in the upper phase leg arm will be in ON state, and four sub-modules in the lower phase leg arm will be in ON state.

$$\frac{-V_{dc}}{2} + 4\frac{V_{dc}}{4} = \frac{V_{dc}}{2} = 200\ V \tag{2.6}$$

2.5 Comparison Between VSC and MMC

Historically, the thyristor controlled LCC was used for HVDC power transmission systems [42]. They have various limitations, such as the semiconductor devices used in the system do not have self commutation capability, and external voltages are required for the commutation process [43].

Later on, as converter technology advanced, the Voltage Source Converter (VSC) was used for the HVDC power transmission system [44]. They consist of insulated gate bipolar transistors. They can self commutate. The VSC has several limitations. Some of these are given below [42].

1. Power losses in semiconductor devices due to PWM.
2. Great stress on semiconductor devices due to the very high rate of change (dv/dt) of voltage across switching devices.
3. High harmonic distortion in the output waveform so requires expensive filters.
4. They cannot limit their fault currents.

To cater to these limitations, multi-level VSC's have been developed, but they also have several disadvantages. For example, they cannot meet the industrial power level requirements because they have limited voltage levels in the output voltage waveform.

So they have total harmonic distortion in the output voltage waveform. For the first time, Lesnicar and R.Marquardt presented the concept of a MMC to improve all of the given problems in multi-level VSC [6].

1. They can limit the DC side fault currents, so they are considered suitable for multi-terminal HVDC power transmission systems.

2. In MMC, the high di/dt (rate of change of current) in switching devices is avoided because the arm current flows continuously.

3. MMC has more steps or levels in the output voltage waveform, so the output voltage waveform looks closer to a sinusoidal waveform, having less harmonic distortion, and as a result, the requirement for a bulky and expensive filter is reduced [24].

4. MMC allows lower switching frequency, hence lower switching losses [24].

5. In MMC, many sub-modules are connected in series, so the total voltage bearing capacity is divided between the sub-modules of each phase leg arm.

2.6 Sub-Module Topology for MMC

Many topologies are used for sub-modules, as shown in Fig. 2.7.

The two basic topologies that are mostly used for the sub-modules are the Half Bridge (HB) and Full Bridge (FB) topologies, shown in Fig. 2.7 (a) and (b). The half bridge topology has the limitation that it can only generate a two-level output that is positive and has zero voltage. The full bridge topology can generate positive, zero, and negative voltages.

One drawback of the full bridge topology is that it requires a higher number of electronic components as compared to the half bridge topology.

To resolve this problem, the unidirectional sub-module topology shown in fig (c) is used, but its utilization is limited due to the current direction [45].

Some more topologies are used for sub-module. These are multi-level NPC's, as shown in Fig. (d), and multi-level flying capacitors as shown in Fig. (e), but their configuration is complex.

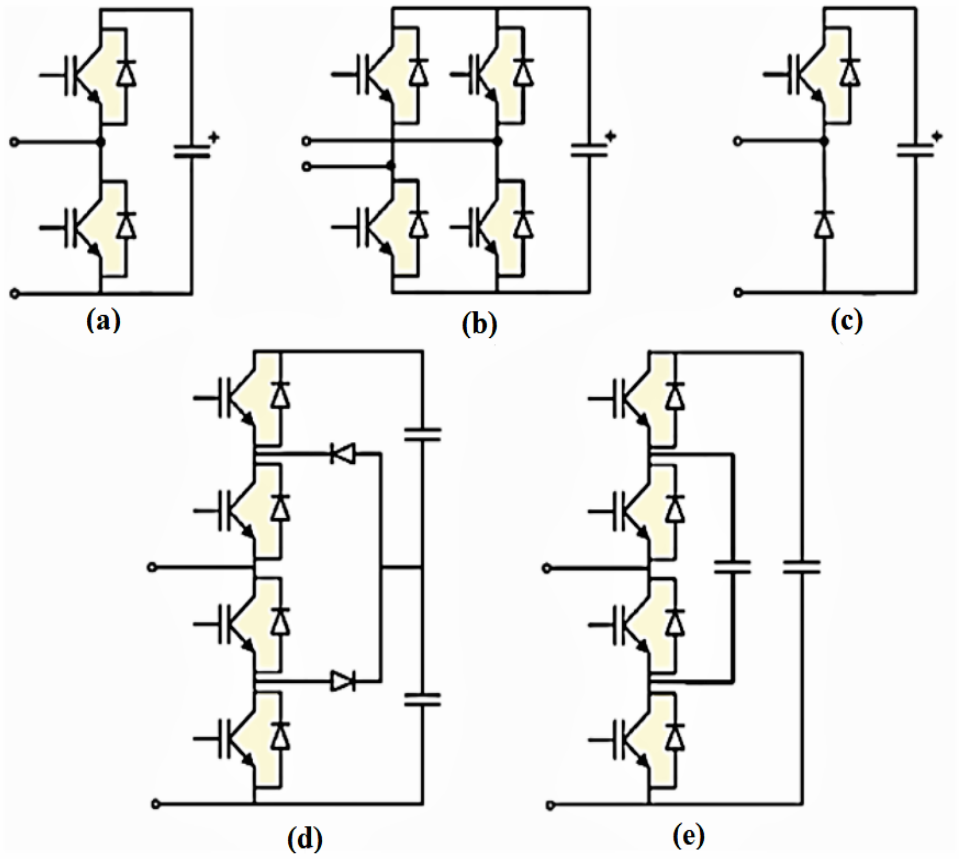

FIGURE 2.7: Sub module topologies (a) Half Bridge (b) Full Bridge (c) Unidirectional (d) Multi-level NPC's (e) Multi-level flying capacitors [45]

The half bridge and full bridge topologies are mostly used for the MMC, so these topologies are discussed in detail in the next section.

2.6.1 Operation of Half Bridge Topology

In Fig. 2.8 the half bridge topology is presented. A single half bridge sub-module consists of two IGBTs and two anti-parallel diodes connected across each IGBT and a capacitor.

The sub-module capacitor is either connected or bypassed by controlling the ON and OFF conditions of T1 and T2. Each half bridge sub-module functions as an independent 2-level voltage converter, producing an output voltage of $V_s m$ or 0 V.

The sub-module is in ON state when T1 is ON and T2 is OFF in the case of insulated gate bipolar transistors used as a switching device in MMC. When the

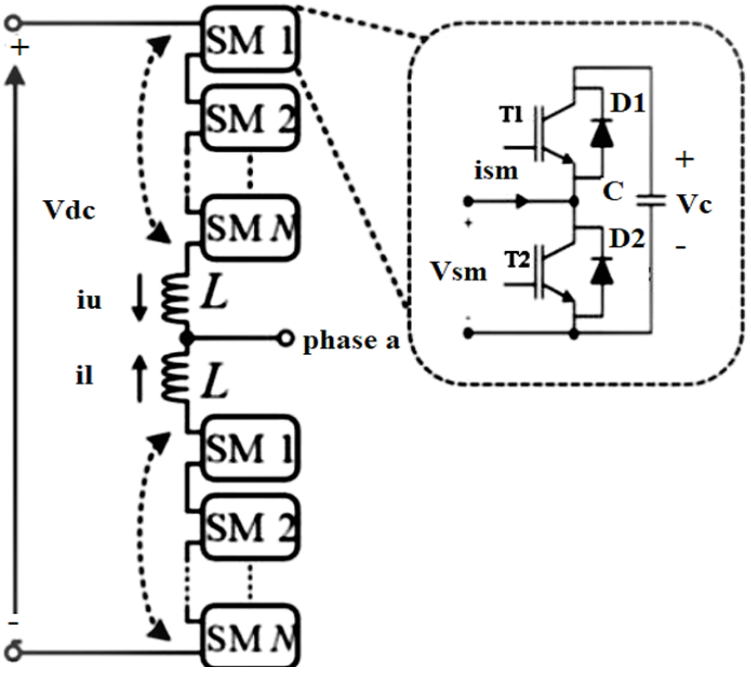

FIGURE 2.8: Half bridge topology of sub-module used in MMC [46]

capacitor is connected or inserted into the circuit in ON state, the output voltage (V_sm) equals the capacitor voltage (V_c).

When T1 is OFF and T2 is ON, the sub-module is in OFF state, and the capacitor is bypassed, resulting in a 0 V output voltage (V_sm). When the sub-module is in ON state, the current flows through the capacitor.

If the direction of current is toward the capacitor shown in Fig. 2.9 (a), then we say that the direction of current is positive and the capacitor charges.

If the direction of current is in the opposite direction to that of the capacitor shown in Fig. 2.9 (b), then we say that the direction of current is negative and the capacitor discharges. The short circuit condition occurs when the IGBTs T1 and T2 cannot turn ON simultaneously [24].

Fig. 2.9 represents the operation of a sub-module. The above figure shows that when diode D1 conducts in Fig. 2.9 (a), then it is shown that the current is in a positive direction, or toward the capacitor, so the capacitor charges.

In Fig. 2.9 (d), when diode D2 conducts, the current is in a negative direction or going away from the capacitor, so the capacitor discharges [46].

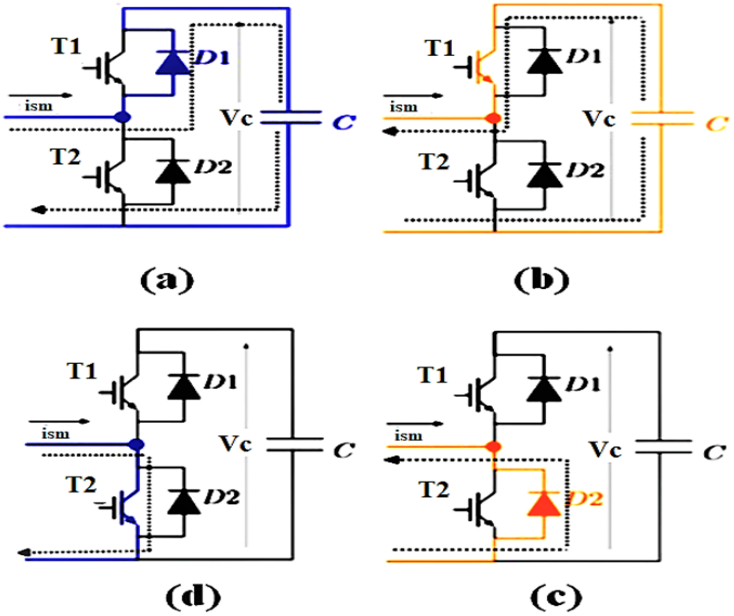

FIGURE 2.9: Sub-module operation according to the direction of current (a) direction of current is positive, capacitor charges (b) direction of current is negative and the capacitor discharges (c) when diode D2 conducts, the current is in a negative direction (d) T2 is ON, the sub-module is in OFF state [24]

2.6.2 Operation of Full Bridge Topology

In Fig. 2.10 the full bridge topology is presented.

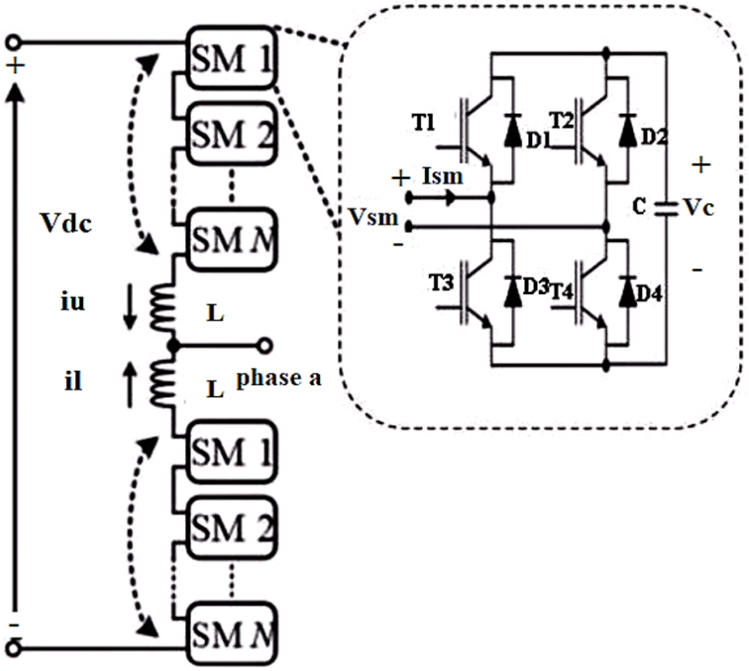

FIGURE 2.10: Full bridge topology of sub-module used in MMC [46]

In Fig. 2.10 the full bridge topology is presented. A single full bridge sub-module consists of four IGBTs and four anti-parallel diodes connected across each IGBT and a capacitor. Above figure shows that when the IGBT, T1, and T2 are in the ON state, the output voltage of the sub-module (V_sm) equals the sub-module capacitor voltages ($V_sm = +V_c$). When T1 and T3 are in the ON state, or when T4 and T2 are in the ON state, the output voltage of the sub-module (V_sm) is zero ($V\,sm = 0$). When T3 and T4 are in the ON state, the output voltage of the sub-module (V_sm) equals the sub-module capacitor voltage (V_c) but has the opposite polarity ($V_sm = -V_c$). When the direction of current is positive or towards the capacitor, the capacitor will charge, and when the direction of current is negative or the current flows away from the capacitor, the capacitor will discharge.

2.7 Characteristic of Modular Multilevel Converters

MMC topology is a state of the art voltage source converter topology due to its ability of high design flexibility and scalability to achieve high voltage ratings easily [47]. It is an economical solution for high power quality; efficiency is high due to fewer harmonic losses, and due to multilevel, there is less requirement for bulky and expensive harmonic filters, even negligible in some cases. Some characteristics of modular multilevel converters are as follows [48], [49], [50].

1. One of the important characteristics of MMC is Modularity which means identical sub-modules [47].

2. Scalability, by increasing the number of sub-modules, any voltage level can be achieved [47].

3. MMC has a high number of levels or steps in the output voltage waveform, less Total Harmonic Distortion (THD), and low power losses [50].

4. Due to less harmonic distortion, filter requirements are less [50].

5. Balancing of capacitor voltage is not required [50].

Due to all these characteristics, the MMC is extensively utilized in HVDC power transmission systems.

2.8 Grid Tied MMC System

In this section, the control strategies for MMC are discussed. The control strategies of MMC involved the DQ transformation, phase locked loop designing, and modelling of grid-connected MMC in a DQ reference frame.

The control system's block diagram for the grid-connected MMC is presented in Fig. 2.11. The control structure model consists of an MMC converter station. V_{dc} is the DC bus voltage applied to MMC.

The converter output voltages are represented by V_t. The phase reactor is connected to the MMC's output, where L represents the phase reactor's inductance and R represents the phase reactor's equivalent resistance. The P and Q represent the active power and the reactive power, respectively. The converter is connected to the AC grid through the PCC. PCC is the point at which the converter is connected to the AC grid.

The mathematical expression of the above control model is given in the below equation (2.7).

$$L\frac{d}{dt}i_{abc} = -Ri_{abc} + V_{abc} - V_{sabc} \tag{2.7}$$

In equation (2.7), the i_{abc} represents the three-phase output current of MMC. V_{abc} represents the three-phase AC output terminal voltages of MMC and V_{sabc} represents the three-phase grid voltages in the ABC reference frame.

L indicates the inductance of the phase reactor, and R indicates the equivalent resistance offered by the phase reactor.

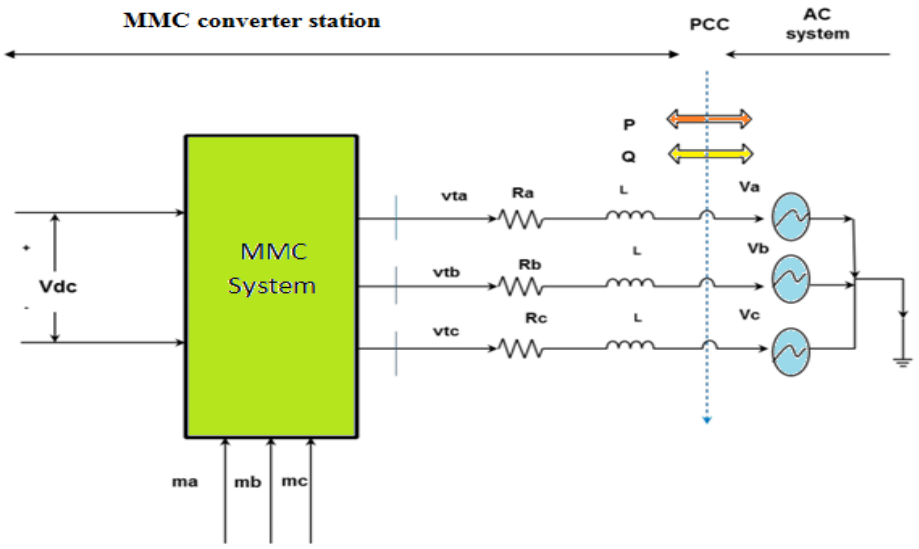

FIGURE 2.11: Control model of grid connected MMC [51]

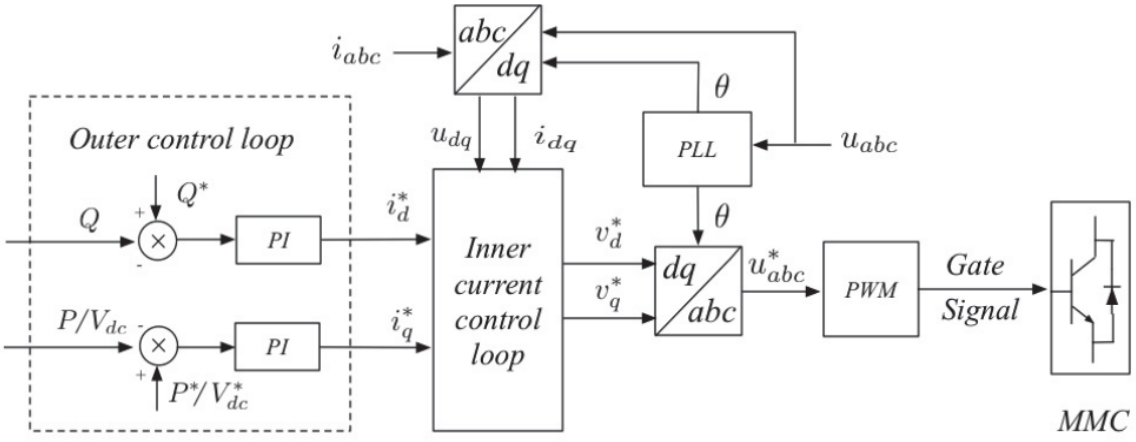

FIGURE 2.12: Control diagram of MMC including inner and outer current control loop [51]

Fig. 2.12 shows the general control diagram of MMC and generally consists of two types of control loops called the outer control loop and the inner control loop.

According to Fig. 2.12, the inner control loops take the reference currents i^* in the form of Direct-Quadrature (DQ) reference frame, which is described in detail in the upcoming section, so it takes the current values and produces the reference voltages in DQ reference frame, which are the control signals for the MMC.

In the inner control loop, the input current controls the output voltages, so the inner control loop is called the current-controlled loop.

The control for the outer loop is also presented in Fig. 2.12, the outer control loop takes reference powers active P or reactive Q, DC voltages V_{dc} as input, and produces the reference currents for the inner current control loop.

The inner current controller is the most important part of the control loop. The inner current controller requires the Phase Locked Loop (PLL) to generate the frequency and phase angle information of the AC grid voltages measured at the PCC. When phase angle information is obtained with the help of PLL, then two strategies are adopted for the control of MMC.

1. Direct Control Method
2. Vector Control Method

The direct control method directly controls the amplitude m and phase angle (*theta*) of the MMC output voltage based on the AC voltages of the grid measured at the PCC [52].

The vector control method that is mostly adopted for MMC control is called the *dq* vector control. This method was developed for electrical machines and electrical drive applications, but it has not been widely adopted for the control of MMC converters [52].

This research work employs the *dq* vector control method to generate the control voltages via an inner current control loop for the MMC converter.

For the analysis or control purposes, the execution of three-phase current and voltages is very complex, and the development of their control structure is not simple [53].

For the implementation of DQ vector control, the three-phase currents and voltages waveforms are transformed from the natural or the stationary reference frame into the rotating DQ reference frame, where the vector quantities are converted into two constant DC vectors called D and Q vectors. This transformation is called the DQ0 or DQ transformation [54].

2.9 Control Strategy for MMC in Dq0 Reference Frame

The modeling of the three phase modular multi-level converter in DQ reference frame is presented in Fig. 2.13.

The 3-phase current and voltages are transformed into a rotating DQ reference frame for better control system analysis and system simplicity because it has only two dc values that are easy to handle in the complex control process.

The mathematical equation given in (2.7) for the given model of the MMC shown in Fig. 2.11 is transformed into a DQ mathematical model, the equations of which are shown in equations (2.8), (2.9), and (2.10) to simplify the control system.

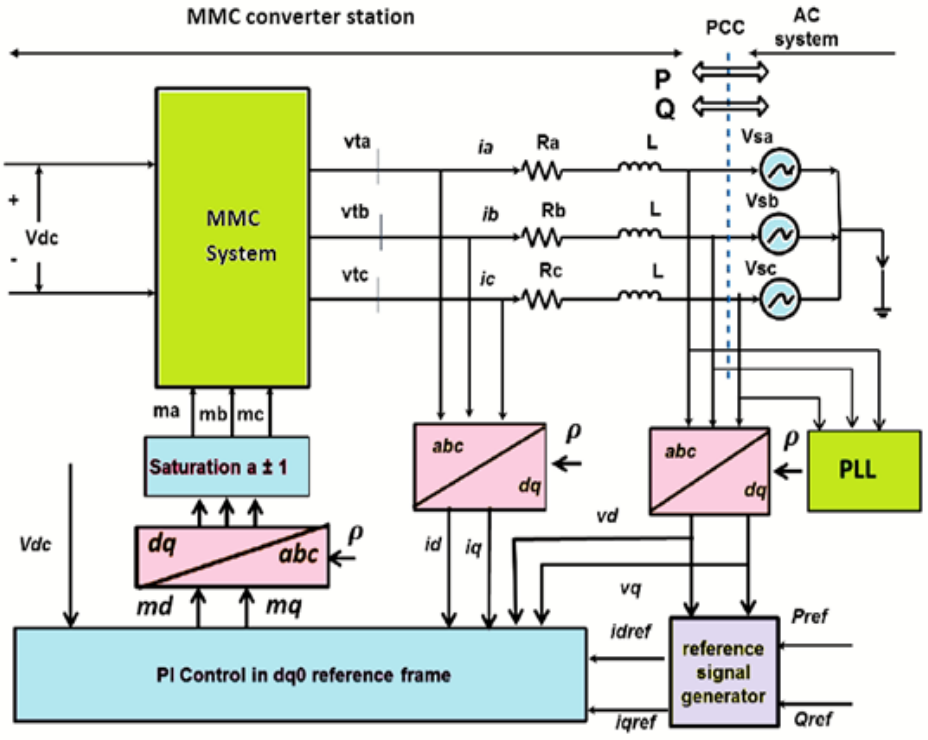

FIGURE 2.13: Schematic diagram of current-mode control for the active power and the reactive power control of MMC in *dq* reference frame [51]

$$L\frac{d}{dt}i_d = L\omega(t)i_q - Ri_d + V_{td} - V_{sd} \tag{2.8}$$

$$L\frac{d}{dt}i_q = L\omega(t)i_d - Ri_q + V_{tq} - V_{sq} \tag{2.9}$$

$$\frac{d\rho}{dt} = \omega(t) \tag{2.10}$$

The DQ model of MMC control is presented in Fig. 2.13. It is composed of an MMC system and phase reactors at the output of the MMC system to reduce the harmonic components from the output voltage waveform of MMC, working as a harmonic filter.

The MMC is coupled to the AC grid through the PCC. The v_t represents the MMC converter output terminal voltages, the v_s represents the grid voltages, the i_d and i_q represent the converter dq currents, the v_d and v_q represent the grid DQ voltages, and the rho represents the grid phase angle. P_{ref} and Q_{ref} are the active and reactive reference power values, respectively. i_{dref} and i_{qref} are the reference DQ current values generated by the reference signal generator. An abc to dq converter block is used to convert the MMC output current and AC grid voltages to a dq reference frame.

The PLL block is utilized for synchronization purposes. The PLL is utilized to generate the phase angle information and the frequency of the AC grid voltages measured at the PCC.

The reference signal generator gets the reference active and reactive power values as an input and generates the dq reference currents i_{dref} and i_{qref} for the inner current control loop to generate the control voltages m_d and m_q for the modular multi-level converter station.

In Fig. 2.11, the control model of the grid-connected MMC is presented. The MMC exchanges the active power and the reactive power components with the AC grid at the PCC.

The d-axis components are used to control the active power while the q-axis components are used to control the reactive power.

In Fig. 2.11, The dc side of the MMC is connected to a dc voltage source, and the goal of this control system is to control the instantaneous active power and reactive power, denoted as P and Q, that the MMC converter exchanges with the AC system.

Two methods are adapted to control the active power and the reactive power in the MMC system.

1. The voltage mode control
2. The current mode control

The schematic diagram of voltage-mode control for the active power and the reactive power control of MMC is presented in Fig. 2.14. This control method is commonly used in high voltage converter applications, such as FACTS systems [55], [56].

The active and reactive powers P and Q of a voltage controlled MMC system are controlled by controlling the amplitude and phase angle of the AC side output terminal voltage of the MMC converter measured at the PCC [57]. If the amplitude and phase angle of the MMC output terminal voltages, denoted by V_tabc, are closer to the amplitude and phase angle of the AC grid voltages, V_sabc, the active and reactive powers, P and Q, are almost decoupled, allowing two independent controllers or compensators to control active and reactive power separately. The structure of the voltage mode control is quite simple and composed of a small number of control loops [51].

The disadvantages of the voltage mode control are that, in this control mode, the output terminal voltages of the MMC converter are controlled but there is no control loop for the output terminal current of the MMC converter.

Due to a lack of current control, the MMC converter is not protected against over currents. Large variations in the current occur if power values are changed or if faults occur in the AC system, so they have a severe impact on MMC converters, or even damage the MMC converter components [51].

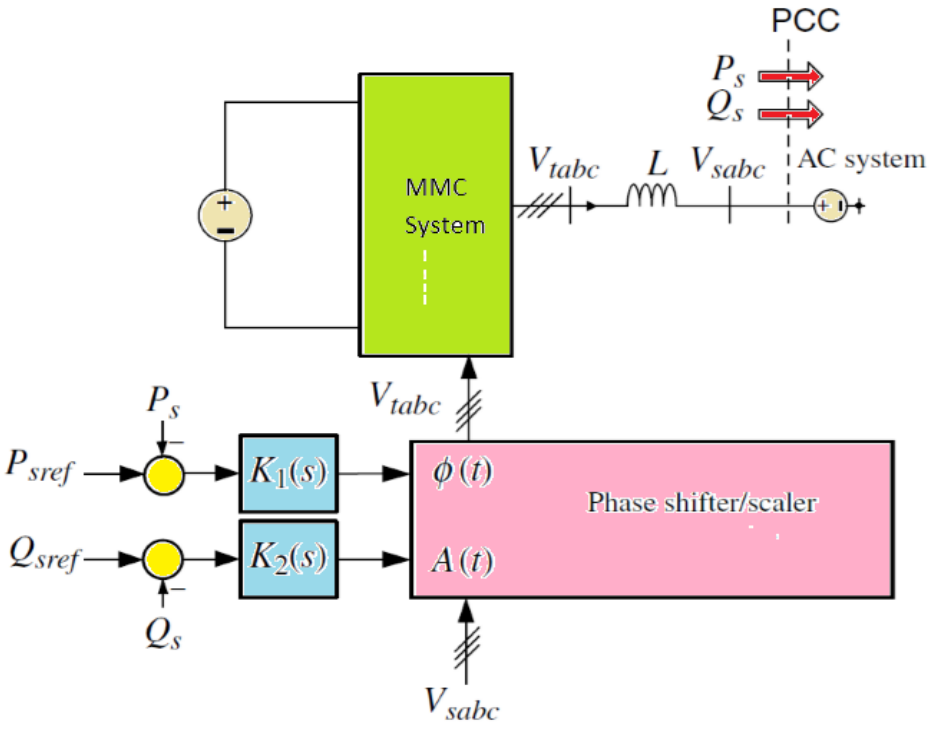

FIGURE 2.14: Schematic diagram of voltage mode control used for the active power and the reactive power control of MMC [51]

The second method to control the active power and the reactive power in MMC converters is the current-mode control shown in the schematic diagram in Fig. 2.13.

In this control approach, the line current of MMC, denoted by i_{abc} is regulated by a specific control scheme, through the MMC AC side output terminal voltages. After regulating the MMC line current i_abc, the amplitude and phase angle of the MMC line current i_abc with respect to PCC voltages control both the active and reactive power for current regulation.

The MMC is protected from the over current in this power control scheme. Another advantage of the current mode control is its robustness against the variation of parameters of MMC and the AC system, superior performance, and precise control [58].

Fig. 2.13 presents the schematic diagram of the current-mode controller to control the active power and the reactive power. This controller is executed in dq reference

frame. The active and reactive powers are controlled by the dq components of the line current i_abc, denoted as i_d and i_q, respectively. It is clear from Fig. 2.13 that all feed forward and feedback signals are transformed into dq rotating reference frame and then applied to the compensator block or controller. The compensator block produces the control signals for MMC in dq reference frame. In the last stage, the control signals are again transformed from dq rotating reference frame to the stationary abc reference frame and applied to the MMC.

The schematic diagram of the current-mode controller for the active and reactive power is shown in Fig. 2.13. ρ is the phase angle between the three-phase abc natural or stationary reference frame and the rotating dq reference frame, and ω is the angular speed at which the rotating dq reference frame rotates [59].

The $P_s(t)$(active power) and $Q_s(t)$(reactive power) delivered to the AC system at the PCC can be expressed mathematically as follows:

$$P_s(t) = \frac{2}{3}(V_{sd}(t)i_d(t)) + (V_{sq}(t)i_q(t)) \tag{2.11}$$

$$Q_s(t) = \frac{2}{3}(-V_{sd}(t)i_q(t)) + (V_{sq}(t)i_d(t)) \tag{2.12}$$

In equations (2.11) and (2.12), the V_{sd} and V_{sq} are the AC system DQ frame voltages, i_d and i_q are the MMC converter line currents.

The coupling states of converter line currents in the dq reference frame, i_d and i_q, as shown in equations (2.11) and (2.12), indicate that grid-connected MMC systems are strongly coupled systems. Because of these coupling currents, it is not possible to control the active and reactive power independently until the q component of the AC grid voltage becomes zero, or $V_sq(t) = 0$. The $V_{sq}(t)$ term is common in both equations so if it becomes zero by adapting some method [59].

The equations (2.11) and (2.12) will become as follows:

$$P_s(t) = \frac{2}{3}(V_{sd}(t)i_d(t)) \tag{2.13}$$

$$Q_s(t) = \frac{2}{3}(-V_{sd}(t)i_q(t)) \tag{2.14}$$

From the equation (2.13) and (2.14) it is clear that when $V_{sq}(t) = 0$, then it allows the independent control of the $P_s(t)$(active power) and $Q_s(t)$(reactive power) using the dq current component of MMC converter line current that is i_d and i_q respectively when the q component of AC grid voltages V_{sq} forces to zero $V_{sq} = 0$ [59], [51]. In Fig. 2.13, the reference active power P_{sref} and reference reactive powers Q_{sref} are applied to reference signal generator. The reference active power and the reactive powers can be obtained by the following equations.

$$P_{sref} = \frac{2}{3}[V_{sd}i_{dref}] \tag{2.15}$$

$$Q_{sref} = \frac{2}{3}[-V_{sd}i_{qref}] \tag{2.16}$$

According to our analysis, the q components of AC grid voltages must be equal to zero to control the active and reactive power independently, i.e., $V_{sq} = 0$ for synchronization of the MMC converter with the AC grid. Synchronization means when the q component of AC grid voltages becomes zero, then the converter current will be in phase with the AC grid voltages and its outcome is that the flow of power either from the converter to the grid or from the grid to the converter becomes reliable [51].

When the MMC converter and AC grid are synchronized, then the active and reactive powers are independently controlled at the PCC.

The condition for their synchronization is that the q components of AC grid voltages must be equal to zero. This condition is achieved by using the PLL.

2.10 Multi-Terminal Direct Current Power Transmission System

MTDC power transmission systems have the ability to take power from multiple offshore and onshore power resources and transport it to the multiple consumers situated at different locations by using existing DC bus systems [60]. It enhances supply and grid security, provides power balance between various offshore renewable resources, and has greater power transportation capability than two terminal point to point HVDC power transmission systems [61]. The DC side faults severally affect the overall performance of MTDC power transmission systems. This section discusses the fundamental structure of MTDC transmission systems, their configurations, topologies, and benefits of MTDC transmission systems.

For example, before going into the discussion of the MTDC transmission system, first discuss the MMC-based Point to Point HVDC power transmission system, presented in Fig. 2.15, utilized for the interconnection of two asynchronous AC systems. For example, it connects an onshore AC grid with an offshore wind farm [39].

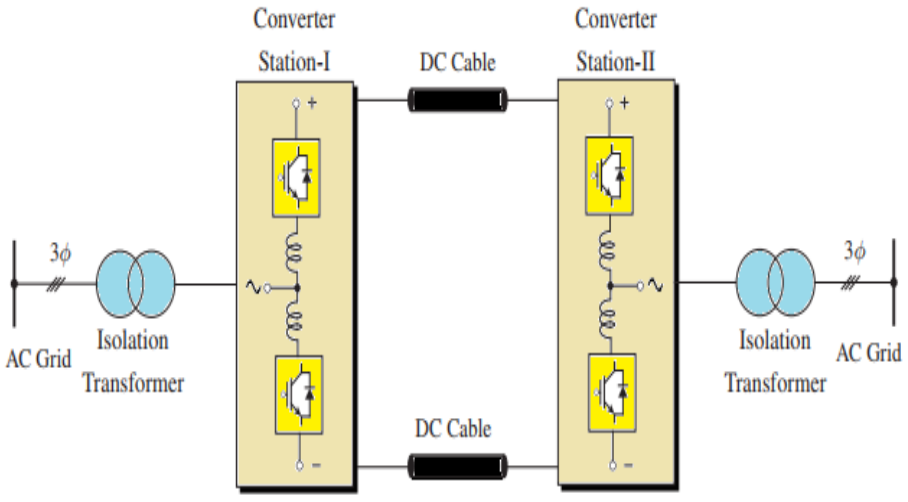

FIGURE 2.15: Point to point MMC HVDC transmission system [39]

In Fig. 2.15 for converter station-I and converter station-II, modular multi-level converts are utilized. Isolation transformers are utilized for the interconnection

of the AC sides of the converter station-I and the converter station-II with the AC grids. The DC sides of the converter station-I and converter station-II are interconnected through a several-kilometer long DC cable.

The MMC has the capability of providing better or good quality output current and voltage waveforms that reduce the requirements of harmonics filters on the AC and DC sides [39].

Recently, four major types of MMC-based HVDC technologies are being used in commercial projects worldwide. These are as follows [62]:

1. HVDC Plus
2. HVDC Light Gen.4
3. HVDC Flexible
4. HVDC MaxSine

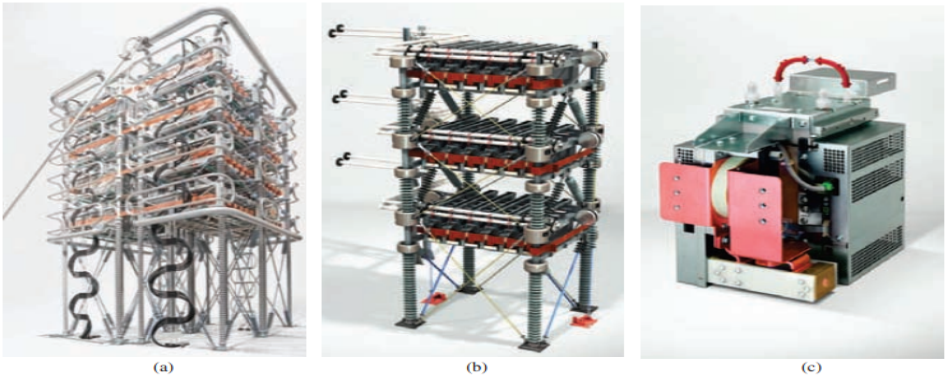

FIGURE 2.16: HVDC plus technology: (a) converter leg (b) converter arm (c) sub-module [39]

The point-to-point HVDC power transmission system has some constraints and limitations. It does not support the exchange of power among three or more distant locations. To overcome these limitations of point to point HVDC power transmission systems, the concept of multi-terminal HVDC power transmission systems is presented in [63], [64].

The MTDC power transmission system can provide an improved exchange of power between multiple distant locations, so decreasing the operational cost for long-distance remote power transmission [63].

The basic configuration of an MMC based MTDC power transmission system is presented in Fig. 2.17.

The MMC-based MTDC power transmission system interconnects more than two HVDC power transmission systems to make an HVDC grid that has better efficiency and controllability [39]. MMC converters are implemented in Converter Stations I, II, and III. The converter's AC sides are connected to the AC grid by using isolation transformers, and the DC sides of converters are connected using the several hundred kilometer DC cable. The P (active power) and the Q (reactive power) flows in between asynchronous AC systems are controlled by these power converter stations.

The MTDC power transmission systems are vulnerable to DC side faults. The primary goal of this thesis is to conduct a thorough investigation into DC fault analysis in MMC based MTDC power transmission systems. For this reason, the MTDC power transmission systems are discussed here in detail.

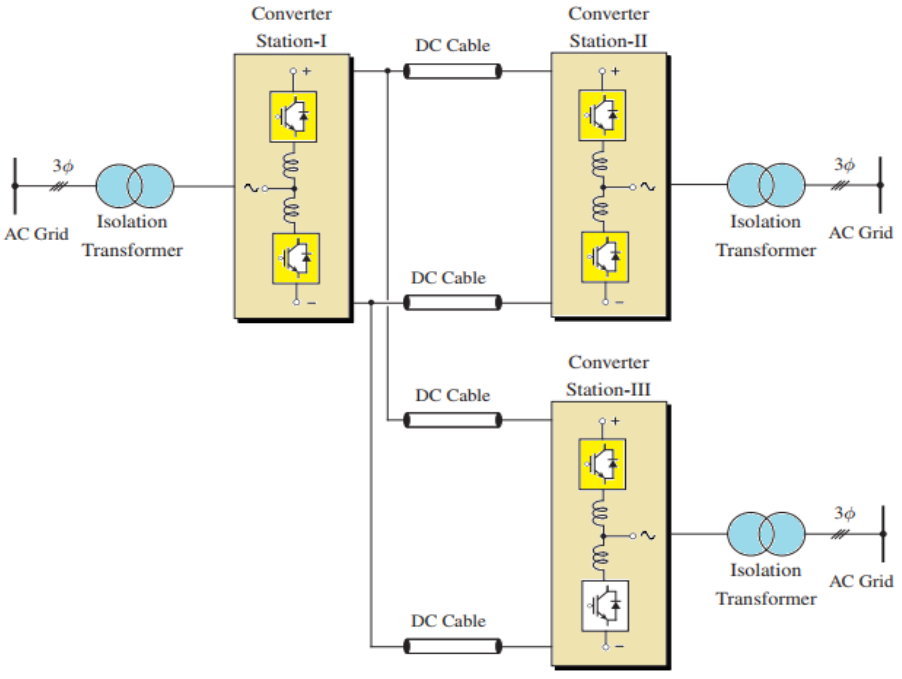

FIGURE 2.17: MTDC power transmission system [39]

2.11 Types of MTDC Topologies

MTDC has the following fundamental topologies:

1. Series Topology
2. Star Topology
3. Ring Topology

2.11.1 Series Topology

A series topology that is used for MTDC power transmission systems is presented in Fig. 2.18

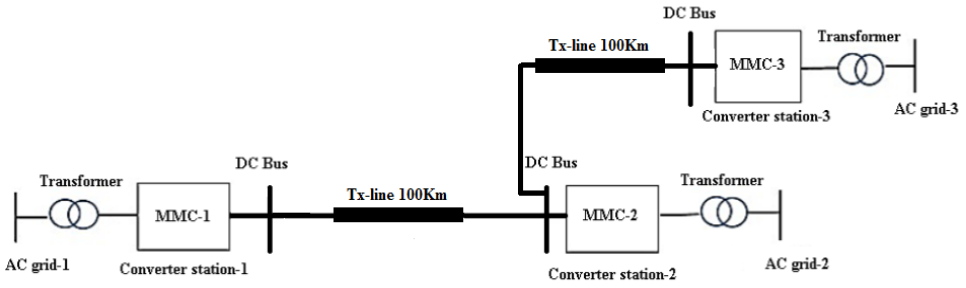

FIGURE 2.18: Series topology used for MTDC power transmission system

The series topology consists of three converter stations; one serves as a rectifier and the other two serve as inverters. The converter stations 1 and 2 are connected by the HVDC transmission line to transmit power over a long distance. Converter station 3 is connected to the DC bus of converter station 2 via an HVDC transmission line. This topology does not require any DC breakers or communication systems for its operation. In this case, the converter station and the transmission line both have the same power rating [22].

The cost and losses in the transmission system will be lower in this topology. When a fault arises or takes place in the transmission line or a fault comes in the converter station, the power transmission will be lost [65].

2.11.2 Ring Topology

Ring topology is presented Fig. 2.19

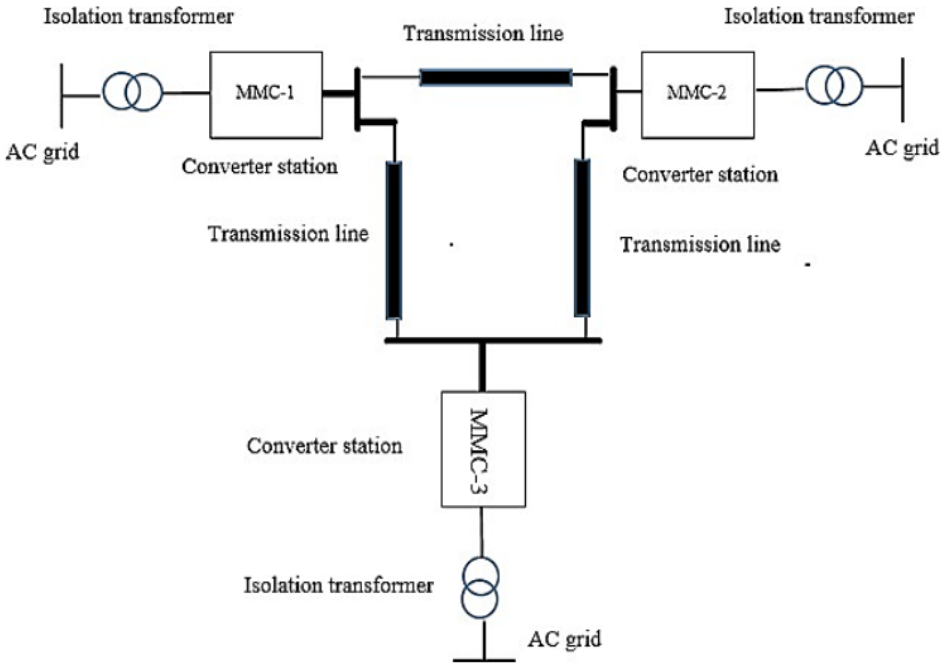

FIGURE 2.19: Ring Topology used for MTDC power transmission system

In this topology, all offshore wind farms and converter stations are connected in series by a DC cable or link, forming a ring.

The ring topology is used for voltage source converters as well as for line commutated converters based HVDC systems [66].

The ring topology either operates in an open loop or in a closed loop mode. The ring topology is operated in a closed loop during normal operation. This topology requires the DC breakers and communication system for their operation. When a DC line is interrupted due to some fault or a fault occurs in the converter station, the DC breakers situated at both ends of the transmission line will suddenly open up at the same time and disconnect the faulty line or the faulty converter. The rest of the system is now operating in the open loop configuration, which also makes sure that we are not losing any wind farm output. This provides a system with better redundancy. This configuration has some limitations. This topology requires that the transmission lines that are used for power transportation have

as much power rating as possible and must have the capability to transport the maximum output power of the offshore wind farm. This configuration also required a fast communication system for the coordination between the DC circuit breakers to detect the fault and disconnect the faulty line or faulty converter [67].

2.11.3 Star Topology

Star topology for MTDC power transmission system is shown in Fig. 2.20 In the

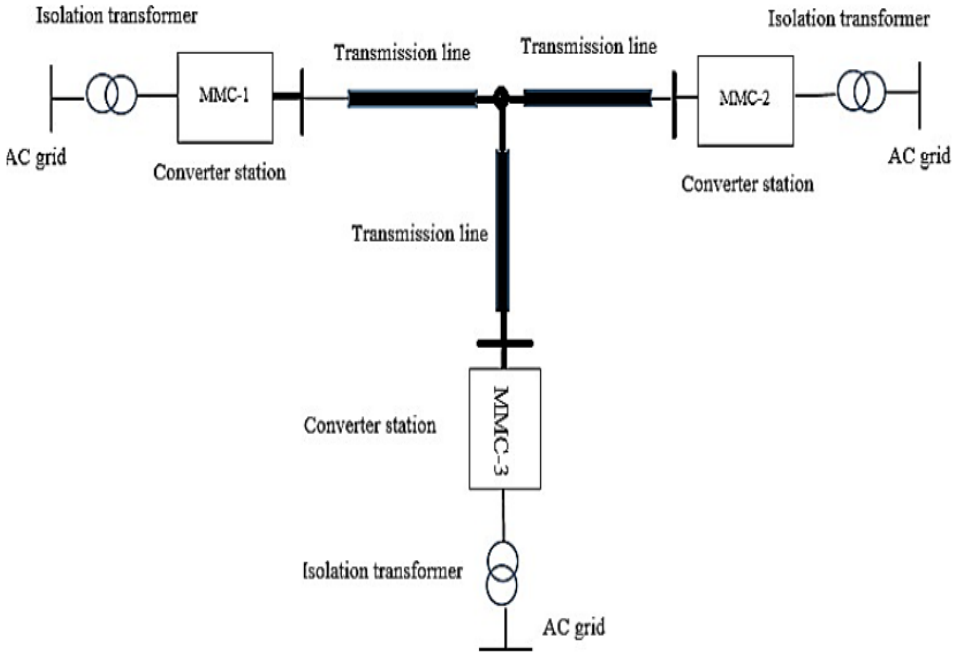

FIGURE 2.20: Star Topology used for MTDC power transmission system

star topology of the MTDC power transmission system, all the offshore wind farms and all onshore converter stations are linked or connected to a central node.

In the star topology, the power ratings of transmission line, converter stations, and offshore wind farms are equal. The major disadvantage of star topology is that if a fault comes at the central node location, then the whole power transmission system will collapse and lose all the connected wind farms. The entire system will be shut down. Due to these limitations, star topology is not feasible for the MTDC power transmission system [65].

2.12 Advantages of MTDC Power Transmission System

Some advantages of MTDC power transmission systems are presented in [61].

1. Improves the supply and grid security: In a point-to-point HVDC transmission system, if any converter station or DC link is interrupted or becomes out of order, then the power transmission is badly affected, and the whole system is interrupted. No power can be transported between the onshore grid and the offshore wind farm. The MTDC system interconnects multiple power resources. If some of them are interrupted due to some fault, in this case, they support the transmission system.

2. Improves the power balance between renewable energy resources: The MTDC power transmission systems can provide a power balance between different distant renewable energy resources for example: The wind speed varies depending on location, so the power generated by these distant offshore wind farms varies as well. The MTDC system has the ability to interconnect these wind farms located at different locations and evenly distribute the power that is taken from all distant power sources to the onshore grid. Observations show that as the distance between the offshore wind farm and the multi-terminal HVDC transmission system is increased, it allows a greater number of offshore wind farms to be linked to the MTDC transmission system, and the output power will be more constant.

3. Reduce the crowding or congestion in the existing system: Just similar to taking the example of buildings, roads, and highways that interlink different cities to relieve the traffic flow, the MTDC power transmission systems have the same characteristic of transportation of power to various distant areas from multiple renewable energy resources with an existing bus system [60].

4. The MTDC power transmission system improves the transient stability of the inter-linked AC systems if proper control strategies are used.

2.13 Case study-1: DC Side Faults in HVDC Power Transmission Systems

MMC have been widely used in HVDC power transmission system projects recently because of their modular structure, scalability, low harmonic distortion, high output voltage quality, and low switching frequency losses. Because it has a unique kind of topology as compared to VSC based HVDC transmission systems and it has unique fault and protection strategies that also have many advantages over conventional VSC topology and have been extensively used in MTDC transmission systems, it is desirable to study and analyze the DC fault characteristics of MMC based MTDC power transmission systems to take necessary actions for their protection against faults.

In this research thesis, the fault mechanisms of DC side pole to pole fault and pole to ground faults in MMC based MTDC power transmission systems are studied, investigated, and simulated in the MATLAB/Simulink environment. This given research paper presents the DC fault characteristics for point-to-point HVDC power transmission systems, but this research thesis provides the investigation of DC fault characteristics for MTDC using series star and ring topology, and the results acquired from this thesis are also verified according to the presented paper when comparing the outcome waveforms for AC and DC fault currents and voltages.

2.13.1 Structure and Working Principle of MMC Based HVDC Power Transmission Systems

The MMC based MTDC power transmission system consists of three parts: an AC power grid; MMC have the capability to function in both the rectifier and the inverter mode; and a transmission line situated among converter stations.

Two terminal MMC based HVDC power transmission system is presented in Fig. 2.21. The converter station utilized here has the capability of converting from rectifier station to inverter station and from inverter station to rectifier station

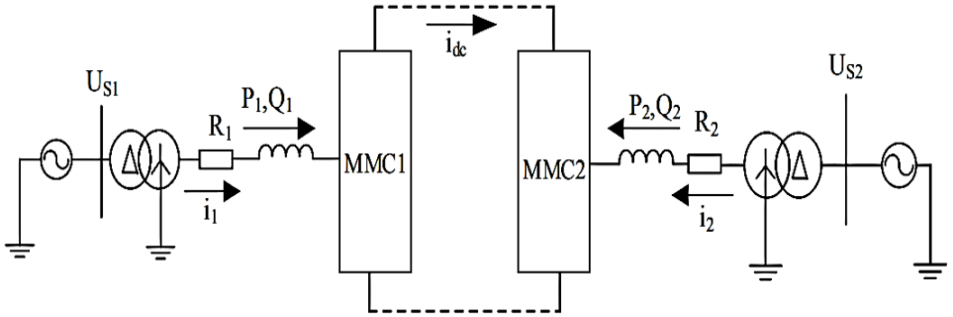

FIGURE 2.21: Two terminal MMC based HVDC power transmission system [68]

when power is reversed. The most critical parts of the HVDC transmission system are the MMC based converter stations, which are made up of a modular structure of series-connected sub-modules with a half bridge topology.

2.14 DC Side Fault Mechanism

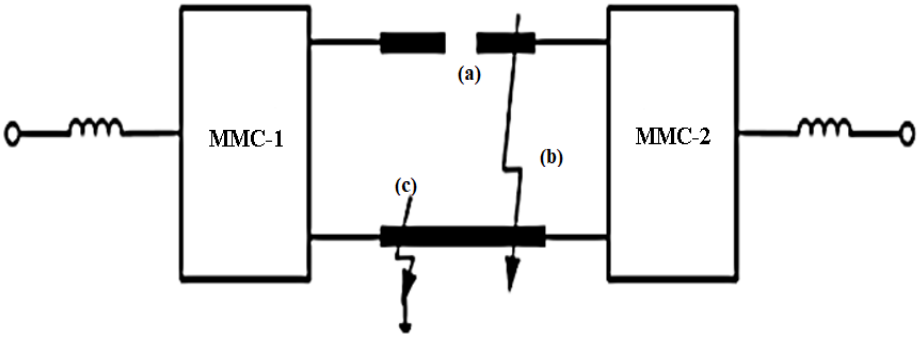

FIGURE 2.22: DC side fault structure (a) DC transmission break fault (b) pole to pole fault (c) pole to ground fault [68]

As it is defined in the above section, the MMC based HVDC power transmission system is based on three main parts: the converter station, the AC power grid, and the DC transmission line [69].

The performance and reliability of the entire power transmission system are severely impacted if a fault develops in any of these identified HVDC transmission system components. Depending on the needs, such as cable transmission (underground or submarine) and overhead transmission lines, the DC transmission mode is chosen.

In comparison to overhead transmission lines, cable power transmission has various advantages, including lower fault occurrence, a less environmental impact, and the ability to supply power to remote locations.

So, in recent projects, the HVDC has utilized cable power transmission and adopted the bipolar power transmission mode.

Positive and negative pole to ground faults, also known as single pole to ground faults, DC transmission break faults, and pole to pole faults, also known as bipolar short circuit faults, occur on the DC sides, and their structures are shown in Fig. 2.22 [69].

2.14.1 Single Pole to Ground Fault

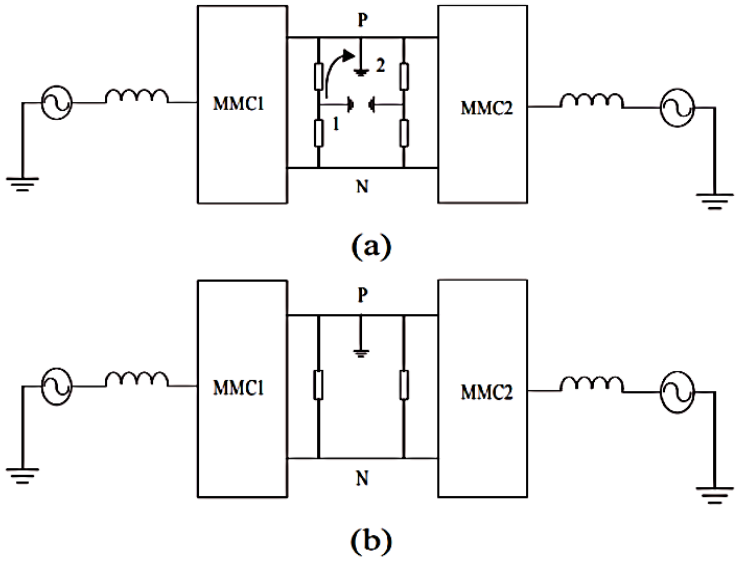

FIGURE 2.23: Positive pole to ground fault (a) Positive pole to ground fault occurs, the clamping resistor of pole (P) is shorted to the ground (b) The equivalent structure after the fault, the potential reference point changes from 1 to 2 [68]

A single pole to ground fault is caused by single pole cable breakage and connects to the ground terminal or cable insulation damage and is connected to the ground caused by an external force. When a pole is connected to the ground, a large short circuit current flows.

To limit this large amount of short circuit current, two clamping resistors of high values are connected between the positive and negative poles of the DC transmission line to provide a potential reference point for the DC transmission line and clamp the DC voltages [70].

Figure 2.23 shows the configuration of the positive pole to ground fault. When a positive pole to ground fault occurs, the clamping resistor of P (pole) is shorted to the ground as expressed in Fig. 2.23 (a).

The equivalent structure of the MMC based HVDC power transmission system after the fault is presented in Fig. 2.23 (b). The reference point changes from 1 to 2. When this happens, the DC side will transform or change from bipolar power transmission mode to uni-polar power transmission mode [71].

When a pole to ground fault occurs, the positive pole voltage U_p amplitude becomes 0 V, the negative pole clamp resistor can support the entire dc side voltages U_dc, doubling the voltage across the negative pole clamp resistor. Positive and negative pole voltages are unchanged at both pole ends. These are shown in Fig. 2.24.

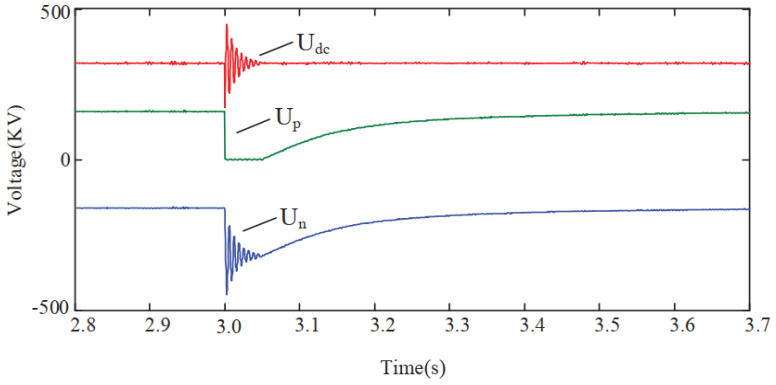

FIGURE 2.24: DC Voltages during positive pole to ground fault [68]

Because a clamping resistor is present in an MMC based MTDC power transmission system, during a pole to ground fault, the DC voltage remains constant and the power transmission is unaffected [68].

Due to the pole to ground fault, the DC side currents increase drastically, as shown in Fig. 2.25

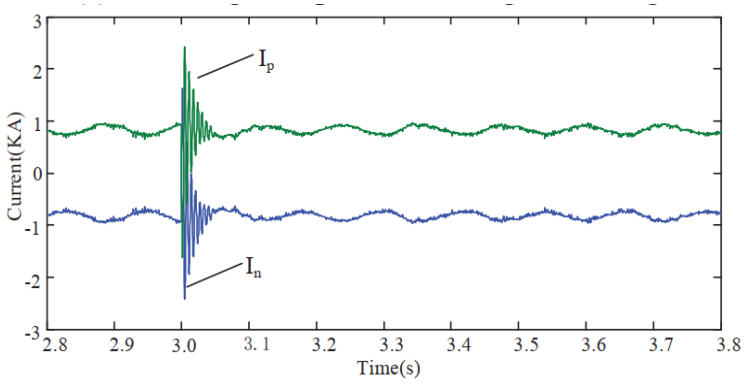

FIGURE 2.25: DC currents during positive pole to ground fault [68]

Due to the pole to ground fault, the bridge arm currents are also affected, as shown in Fig. 2.26

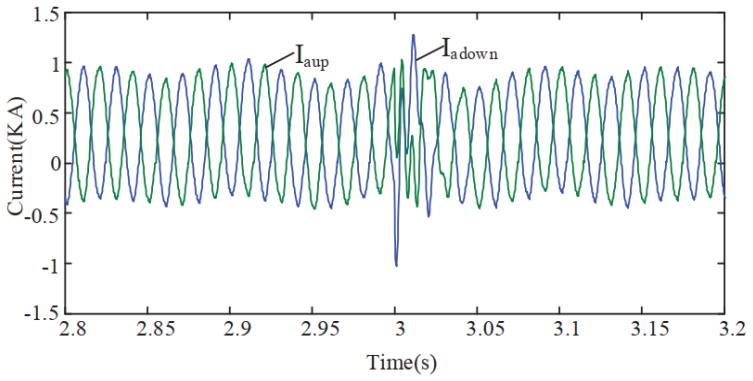

FIGURE 2.26: Bridge arm during positive pole to ground fault [68]

Due to the pole to ground fault, the reference point of the AC side voltages of the MMC converter changes to single pole voltages because of the sudden change in positive pole voltages to 0 V shown in Fig. 2.27. During a pole to ground fault, the MMC converter AC side current is unaffected, as shown in Fig. 2.28.

2.14.2 Pole to Pole Fault

The most severe fault on the DC side is the pole to pole fault. The pole to pole fault is a permanent fault caused by insulation damage [72].

It is shown in Fig. 2.29 that the positive pole and the negative poles of the MMC are short circuited to each other. The sub-module capacitors in both side converter

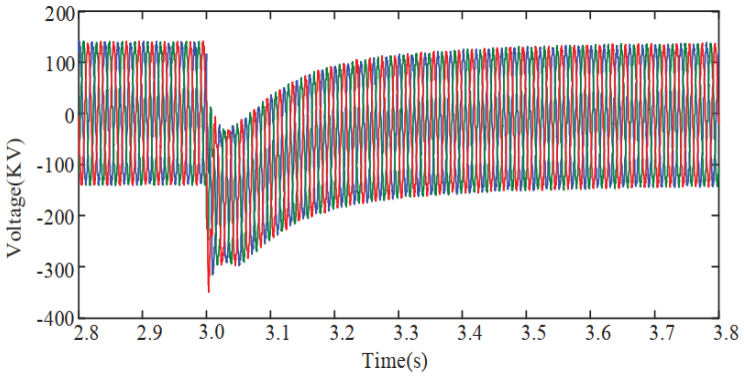

FIGURE 2.27: MMC AC side voltages during positive pole to ground fault [68]

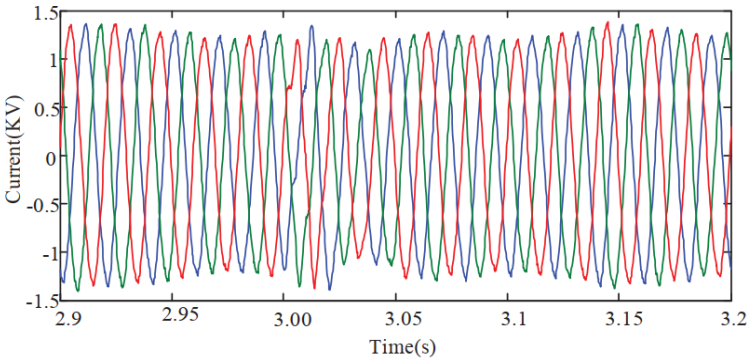

FIGURE 2.28: MMC AC side current during positive pole to ground fault [68]

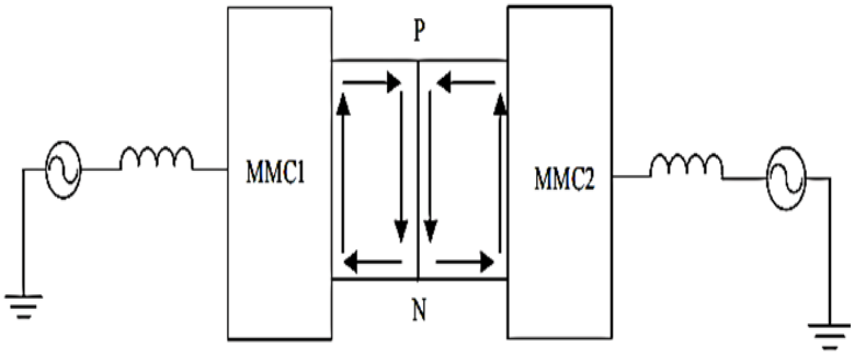

FIGURE 2.29: Schematic diagram of the pole to pole fault in MMC based MTDC power transmission system [68]

stations are rapidly discharged through the point at which the fault occurs, which is shown in Fig. 2.30.

Pole to pole voltages, positive pole voltages, and negative pole voltages all drop to 0 V when a pole to pole short circuit fault occurs, as shown in Fig. 2.31, and DC currents rise rapidly, as shown in Fig. 2.32.

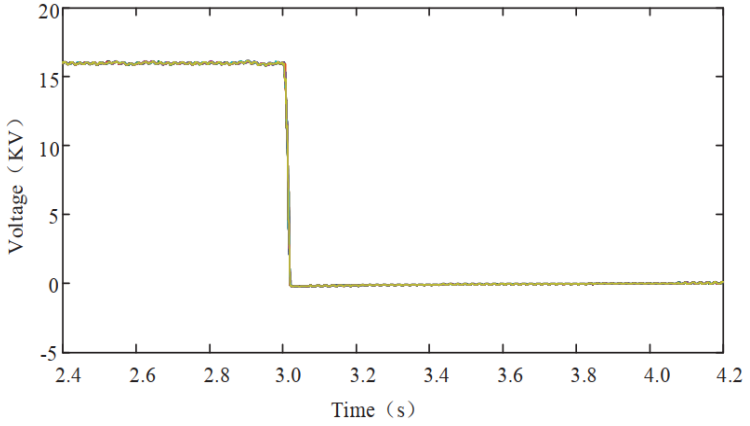

FIGURE 2.30: MMC sub-module capacitor voltages due to pole to pole fault [68]

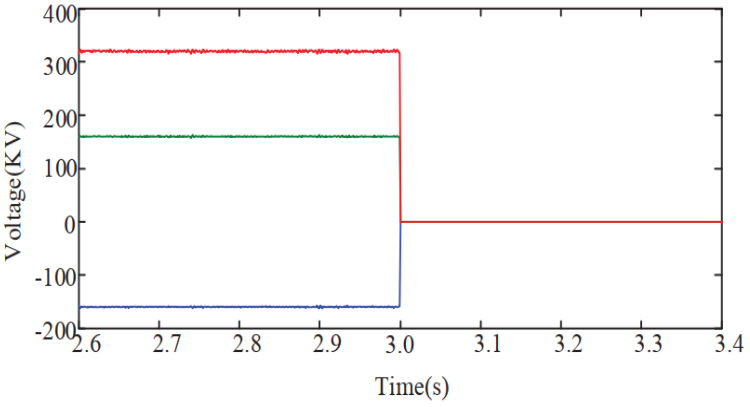

FIGURE 2.31: DC voltages due to pole to pole fault [68]

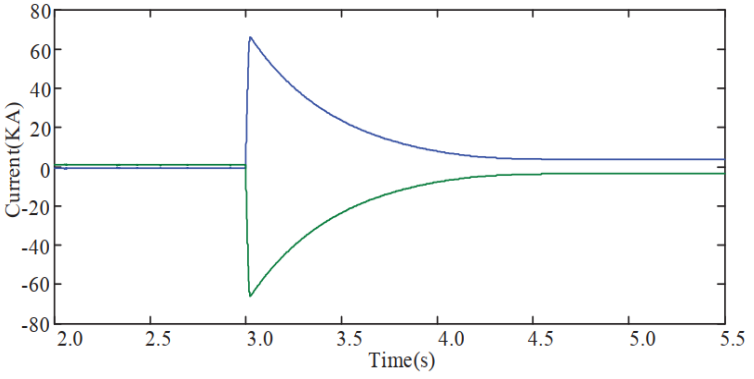

FIGURE 2.32: DC currents due to pole to pole fault [68]

Due to pole to pole fault, MMC AC side voltages decrease, and AC side current increases rapidly, as shown in Fig. 2.33 and Fig. 2.34.

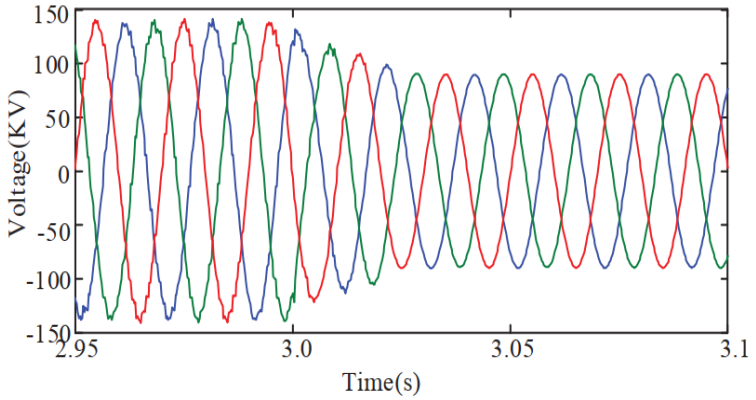

FIGURE 2.33: MMC converter AC side voltages due to pole to pole fault [68]

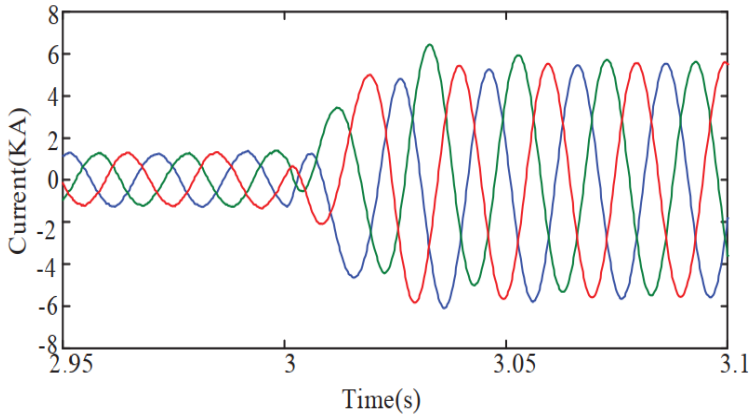

FIGURE 2.34: MMC converter1 AC side current due to pole to pole fault [68]

2.15 Case study-2: Analysis of Fault Current in an MMC Based HVDC System under the DC Pole to Pole Fault

The primary goal of this research is to investigate the DC fault characteristics and to analyse the mathematical model of the DC fault current for the MMC based HVDC power transmission system.

In this case study, an improved analytical approach for calculating the DC fault current for MMC-based HVDC systems is presented.

The fault current that is calculated from the proposed model is then compared with the acquired simulation results.

2.15.1 System Model for MMC HVDC System

In Fig. 2.35, the MMC structure of a single terminal HVDC topology is shown. It is composed of three phase legs, or bridges, and two arms referred to as the upper arm and lower arm in each phase.

There are twenty sub-modules in each arm of a phase leg. Sub-modules use a half-bridge topology.

The sub-module consists of two IGBTs denoted as $T1$ and $T2$, two anti-parallel diodes denoted as $D1$ and $D2$ and a capacitor C_0.

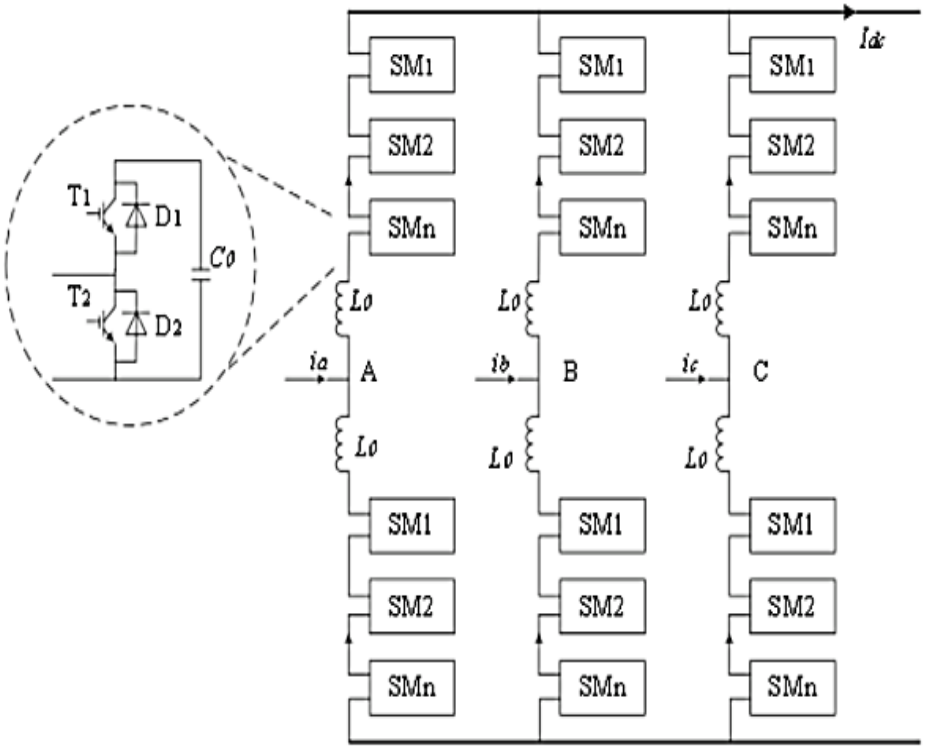

FIGURE 2.35: MMC Structure of single terminal HVDC topology [73]

The arm inductor L_0 in each arm suppresses the circulating current.

A 21-level MMC based HVDC model was developed in PS-CAD to analyse the MMC characteristics, as shown in Fig. 2.36.

FIGURE 2.36: MMC HVDC model [73]

2.15.2 Investigation of Pole to Pole Short Circuit Characteristics in MMC DC link

2.15.2.1 Analysis of Over Current Before Blocking

Due to a pole to pole fault, the converter stations inject a short circuit current through the sub-module diode D_2, which behaves exactly like a three-phase short circuit current.

As a result, the sub-module's capacitor $C0$ discharges through the upper IGBT of the sub-module. The bridge current of the MMC is the combination of two arm currents in which the capacitor discharge current is the main component.

After a while, both converter stations are blocked, and the capacitor ceases to discharge, but the current is still injected by the AC grid via the diode D_2. Fig. 2.37, shows the path of AC current injection from the AC grid.

Fig. 2.37 shows the fault current path during the pole to pole fault.

Power transmission between two converter stations is interrupted when a pole to pole fault occurs.

In the MMC converter, the sub-module capacitors of the converter stations on both sides are discharged via IGBT T1. The capacitor discharge loop is expressed in Fig. 2.37

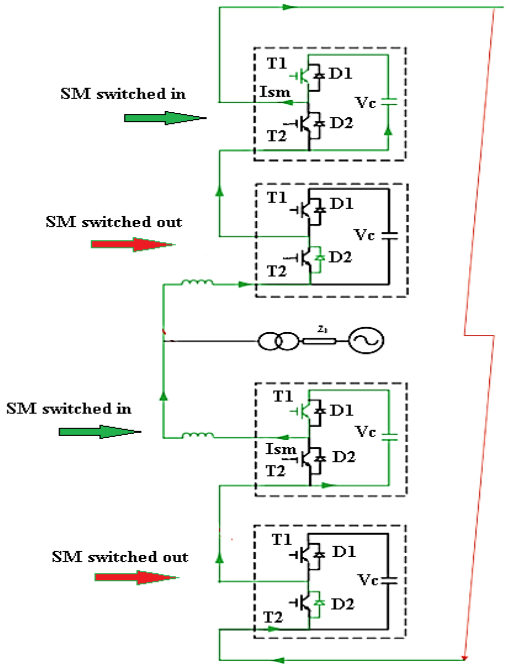

FIGURE 2.37: Fault current path in case of pole to pole fault [73]

In this case, the AC system injects a short circuit current through each sub-module's diode D2 and into the short circuit point. Consequently, the bridge or phase leg current rises to a high value in a very short time [68].

2.15.2.2 Calculation of over-current before blocking

The MMC converter stations will be blocked in a few milliseconds due to a pole to pole short circuit. Before the blocking stage, the sub-module's capacitor discharges, causing an over current to occur.

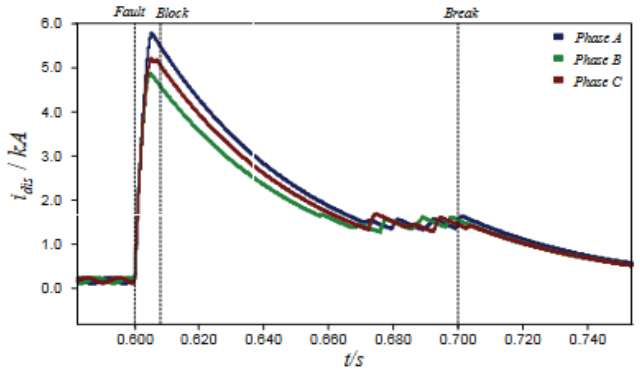

FIGURE 2.38: Discharge current of the sub-module capacitors [73]

The waveforms of the discharge current i_{dis} are shown in Fig. 2.38. For the over current calculations, let us take a single phase leg or bridge, for example. The sub-module capacitor $C0$ discharges before the sub-module being blocked, and the equivalent discharge circuit is seen in Fig. 2.39 and Fig. 2.40.

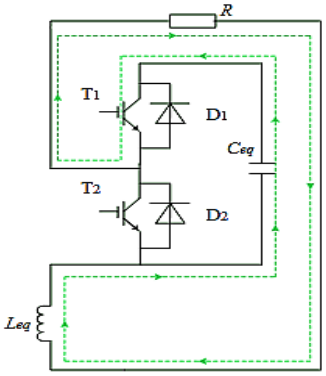

FIGURE 2.39: Path for the discharge current [73]

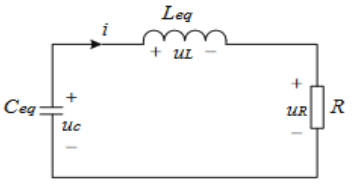

FIGURE 2.40: Equivalent circuit for the current calculation [73]

In Fig. 2.40, u_c is the sub-module capacitor voltages. C_{eq} is the sub-modules equivalent capacitance , L_{eq} is the equivalent arm inductance and R is the path resistance. We can quickly acquire the voltage and current calculation formulas by referring to Fig. 2.39 and Fig. 2.40 [73].

$$u_c = A_1.e^{p_1.t} + A_1.e^{p_2.t} \tag{2.17}$$

In the above equation, A_1 is a constant defining some amplitude. p_1 and p_2 are the roots of quadratic equation.

$$p_1 = \frac{R}{2L_{eq}} + \sqrt{(\frac{R}{2L_{eq}})^2 - (\frac{1}{L_{eq}.C_{eq}})} \tag{2.18}$$

$$p_2 = -\frac{R}{2L_{eq}} - \sqrt{(\frac{R}{2L_{eq}})^2 - (\frac{1}{L_{eq}.C_{eq}})} \tag{2.19}$$

Initial state is :

$$u_c(0_+) = u_c(0_-) = U_{dc} \tag{2.20}$$

In the above equation, the U_{dc} is the DC link voltages.

$$i(0_+) = i(0_-) = -C_{eq}\frac{d.u_c}{dt} = I_o \tag{2.21}$$

In the above equation, the I_o is the initial current when the sub-module capacitor discharges.

Equivalent capacitor voltages can be obtained from the following equation:

$$u_c = e^{-\frac{t}{\tau}}\left[\frac{U_{dc}.\omega_0}{\omega}.\sin(\omega.t+\phi) - \frac{I_0}{\omega.C_{eq}}.\sin(\omega.t)\right] \tag{2.22}$$

Where

$$\tau = \frac{R}{2L_{eq}}, \omega_0 = \sqrt{\frac{1}{L_{eq}C_{eq}}}, \omega = \sqrt{\frac{1}{L_{eq}C_{eq}} - (\frac{R}{2L_{eq}})^2}, \phi = \arctan(\omega\tau) \tag{2.23}$$

In the above equation, τ is the damping factor, ω_0 is the resonance frequency, ω is the ringing frequency and ϕ is the phase angle.

In general, the resistance R $\lll\lll 2\sqrt{\frac{L_{eq}}{C_{eq}}}$,is greater than the current:

$$i = e^{\frac{t}{\tau}}.\left[U_{dc}\sqrt{\frac{C_{eq}}{L_{eq}}}\sin(\omega.t) + I_0\cos(\omega.t)\right] \tag{2.24}$$

From equation 2.25, we can extract the capacitor discharge time t_m, when the value of the discharge current reaches its peak value.

$$t_m = \frac{1}{\omega_0} \arctan .(\frac{U_{dc}}{I_0}\sqrt{\frac{C_{eq}}{L_{eq}}}) \tag{2.25}$$

the discharge current peak value I_m:

$$I_m = e^{\frac{-t_m}{\tau}}.(U_{dc}\sqrt{\frac{C_{eq}}{L_{eq}}} + \frac{I_0^2\omega_0 L_{eq}}{U_{dc}})\sqrt{\frac{U_{dc}^2}{I_0^2\omega_0^2 L_{eq}^2 + U_{dc}^2}} \tag{2.26}$$

For the verification of the above analysis, the simulations are performed in PSCAD and a pole to pole short circuit fault is generated at the output terminal of the MMC converter station shown in Fig. 2.41 and simulation parameters are given in the table below.

TABLE 2.2: MMC-HVDC Simulation parameters

Description	**Symbol**
Arm inductance (L0)	15 mH
Sub-module capacitor (C0)	5 mF
DC voltage (Udc)	40 kV
Num. of sub-modules in an arm (N)	20
AC line to line voltages (Vac)	10 kV
Rated power (P)	40 MW

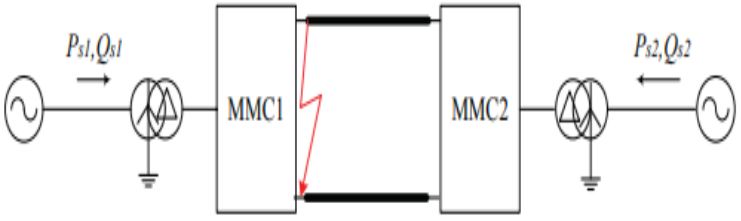

FIGURE 2.41: MMC HVDC simulation topology [73]

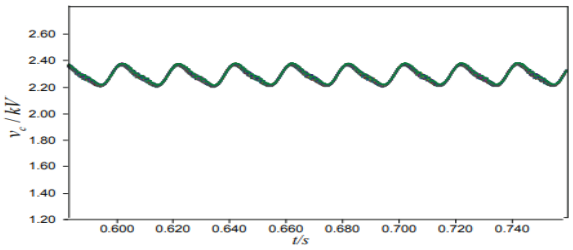

FIGURE 2.42: Sub-module capacitor voltages before fault [73]

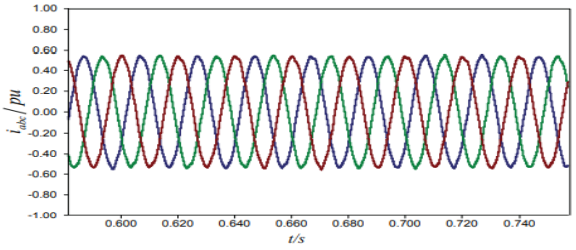

FIGURE 2.43: AC grid current [73]

Fig. 2.42 and Fig. 2.43 shows the sub-module capacitor voltage and AC grid current

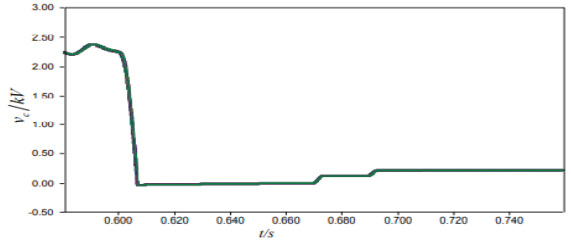

FIGURE 2.44: Sub-module capacitor voltages after fault [73]

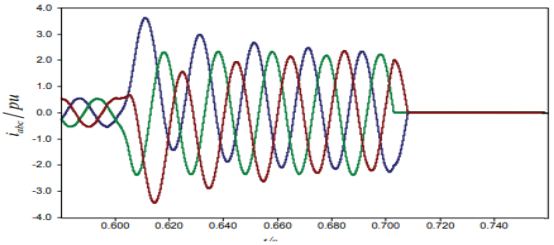

FIGURE 2.45: AC grid current after fault [73]

Fig. 2.44 and Fig. 2.45 shows their values after the fault occurrence at 0.6s. From Fig. 2.44 it is observed that the sub module capacitor voltages rapidly drop to zero, and from Fig. 2.45 the AC grid current also rises after a fault.

2.16 Gap Analysis

Recent years have seen a variety of research projects on MTDC power transmission systems' DC side faults.

In [68], the author presents the study of DC faults for the point to point MMC HVDC topology. It is also called two terminal MTDC, in which power is transmitted only between two converter stations. Pole to pole and pole to ground faults in the middle of the transmission line between converter stations are explored in this paper. This research is restricted to describing DC faults in point to point HVDC power transmission systems. When a fault occurs in the middle of the transmission line, just one point in relation to DC faults is covered. In [73], the author presents the fault current analysis for the MMC HVDC system under the DC pole to pole fault conditions. The capacitor discharge current, fault current path prior to blocking condition, and sub-module capacitor voltages are all covered in this paper. This research is restricted to describing DC faults only for the internal MMC structure. In [74], the author discusses the DC fault for MTDC using ring topology. In this study, the MTDC is composed of four MMC converter stations forming a ring, and pole to pole and pole to ground faults occur at the MMC converter terminal. This research is restricted to describing DC faults only for the ring topology. In [75], the author presents the DC fault current analysis for MMC based HVDC systems. In this study, the effects of pole to pole and pole to ground fault on the internal structure of MMC are discussed. This study elaborates on the MMC's blocking and unblocking states due to DC faults. It also provides the reason for the voltage oscillations during the pole to ground fault. The consequences of DC faults on the AC and DC sides of the MMC are not discussed in this paper. In [76] and [77], the authors discuss the DC fault in the MTDC star topology. In [78], DC faults are analyzed in a meshed HVDC super grid. Both of the aforementioned research publications focus primarily on a single MTDC topology, and DC faults are discussed only at a single point.

These research articles explore the MTDC topologies and their structure. In these research papers, the DC side faults and how they affect the system's behavior are

not thoroughly discussed. Moreover, no one has examined the characteristics of these faults when they occur in MTDC. The types of DC faults are discussed . Various topologies are employed for MTDC, and for these topologies, a detailed investigation into DC faults is not presented. So it is a fundamental requirement to analyze the DC side fault characteristics in these topologies to obtain knowledge of peak values of fault currents and voltages for fault detection and protection coordination between the converters. As a consequence, make the arrangements to quickly address these faults as soon as possible for power transmission reliability and stability.

2.17 Problem Statement

Keeping in view the challenges discussed in gap analysis, the pole to pole and pole to ground faults are considered when the fault occurs at the output terminal of the sending end converter station. Nobody has described what happens to the behaviour of the multi-terminal HVDC system when these faults occur at the node terminal or at the transmission line. This research focuses on analyzing how fundamental MTDC topologies like series, star, and ring topologies are affected by DC side faults. In this thesis, we conduct research in which faults are generated at the sending end terminal, on the transmission line, and at the node terminal. A three terminal MMC HVDC based power transmission systems simulation models are developed for stated topologies in the Matlab/Simulink environment. The bulk power transmission and high power generation are handled by MTDC. It can deliver power to several terminals or it can extract power from several terminals, so severe faults come. In the context of faults, the pole to pole and pole to ground faults have been investigated.

A pole to pole fault is a severe MTDC fault in which a light striking or an object falling across the positive and negative poles of a transmission line causes the positive and negative poles to short circuit one another. When a positive pole or a negative pole is short circuited to the ground terminal, a pole to ground fault

occurs. These faults compromise the stability and safety of the MTDC networks as well as the overall system operation. The impact of pole to pole and pole to ground faults on AC side and DC side currents and voltages is also observed in this thesis. This research provides the peak fault current values as well as an estimate of the voltage fluctuations under both fault conditions.

Chapter 3

Development of Grid Tide Modular Multilevel Converter

In this chapter, first of all, the MATLAB/Simulink model of a 7-level MMC is discussed. After this, the control methods of MMC are described in detail.

3.1 Introduction

At earlier stages, the HVDC power transmission systems were employed by using Line Commutated Converts (LCC). LCC are also called Current Source Converters (CSC). Thyristors are used as a switching device.

The disadvantage of a LCC is that, it requires the AC line voltage for the commutation process or it commutates on line frequency, so for this reason, the CSC is also known as the LCC. In LCC, the thyristor switches can be turned on by a control action, but the thyristor switches can not be turned off by any control action.

They require the line voltages of the AC system for the commutation process. In LCC, the current cannot change direction and can be considered as a constant

current that flows through a large inductor. It acts as a current source on the AC side, therefore it is also called a current source converter (CSC) [22].

After that, a new HVDC technology, Voltage Source Converter (VSC), was developed. It uses advanced semiconductor devices instead of thyristors, like Insulated Gate Bipolar Transistors (IGBT). IGBTs have the ability to self-commutate or turn off autonomously rather than thyristors in a current source converter that requires the line voltage of the AC system for the commutation process, so this allows the utilization of high-frequency carrier Pulse Width Modulation (PWM) for the control of the switching devices. The VSC also has some limitations. Voltage source converters have high harmonic content in their output voltages. High switching frequencies are required to remove harmonic content, which requires the bulky and expensive harmonic reduction filters [24].

3.2 Matlab/Simulink Model for Grid-Tied 7-level MMC

In this section, the simulated model of the 7-level grid-tied MMC is presented. The single-line diagram of the grid-tied 7-level MMC as shown in Fig. 3.1.

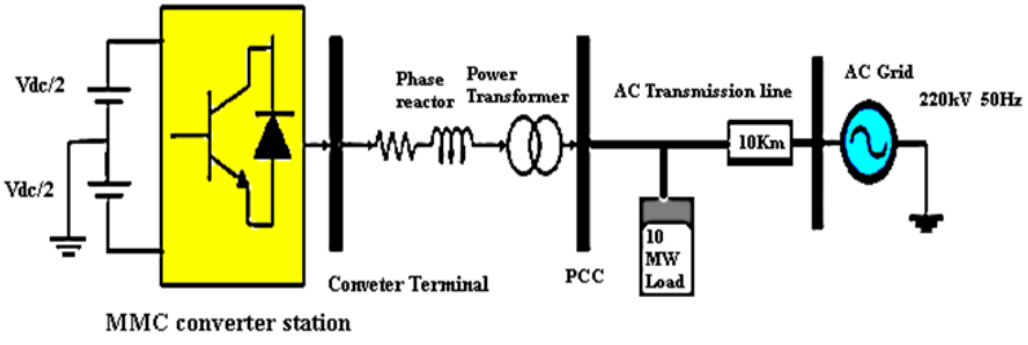

FIGURE 3.1: Single line diagram of grid tied 7-Level MMC

The model for the 7-level MMC was developed in the Matlab/Simulink environment. Fig. 3.2 presents a Matlab/Simulink model for the grid-tied 7-Level MMC. If the number of sub-modules connected in series in an arm of a phase leg is defined

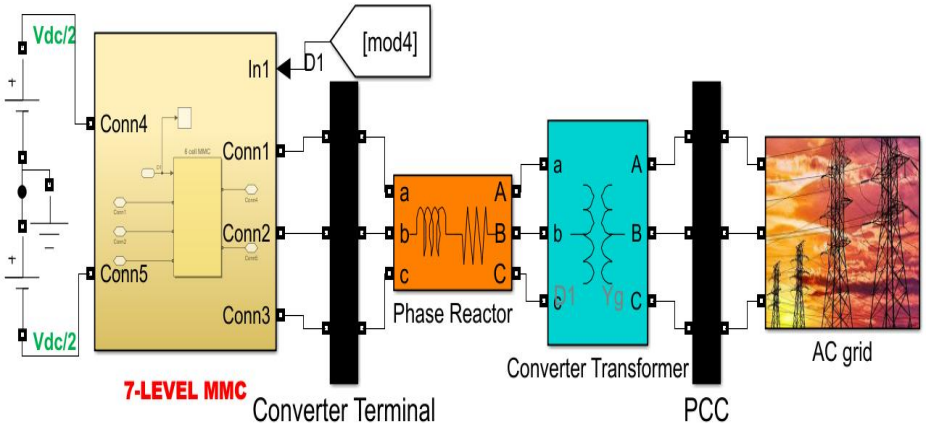

FIGURE 3.2: Matlab/Simulink model of grid tied 7-Level MMC

by N, then the output waveform has N+1 output voltage levels. There are 6 sub-modules connected in series in an arm of a phase leg in the above Matlab/Simulink model, so N=6. The output voltages have N+1(6+1) = 7 levels.

In this section, the different simulation blocks are discussed in detail.

The dc voltages denoted by V_{dc} = 100 kV are applied at the input of MMC.

The applied V_dc is divided into two halves, namely $\frac{V_{dc}}{2}$ = 50 kV divided by a reference point, with 0 V serving as a reference point throughout the simulation.

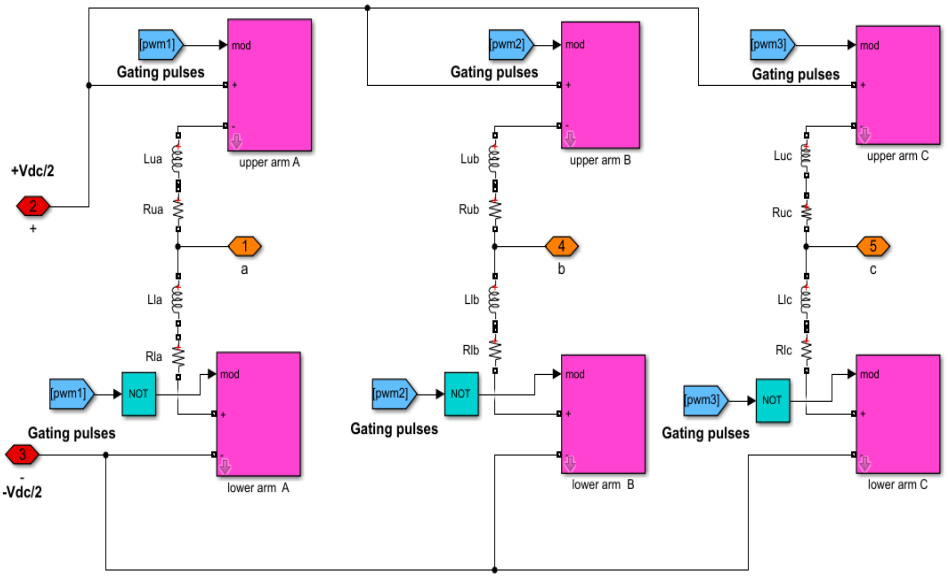

FIGURE 3.3: Simulation model of three phase 7-Level MMC

The Matlab/Simulink model of three-phase, 7-level MMC is shown in Fig. 3.3.

It is clear from the figure that the model is composed of three phase legs, with two arms in each phase leg, denoted by the upper arm and the lower arm, respectively.

If k=abc, then the upper arm inductance represented by L_{uk} and the lower arm inductance represented by L_{lk} are both of equal value, which is 1 mH.

The resistances offered by these arm reactance are denoted by R_{uk} for the upper arm and R_{lk} for the lower arm, and are also equal in value, which is 1 Ω.

In the simulation model shown in Fig. 3.3, each phase leg arm, denoted by the upper and lower arms, is made up of 6 cells, also known as sub-modules, that are connected in series shown in Fig. 3.4.

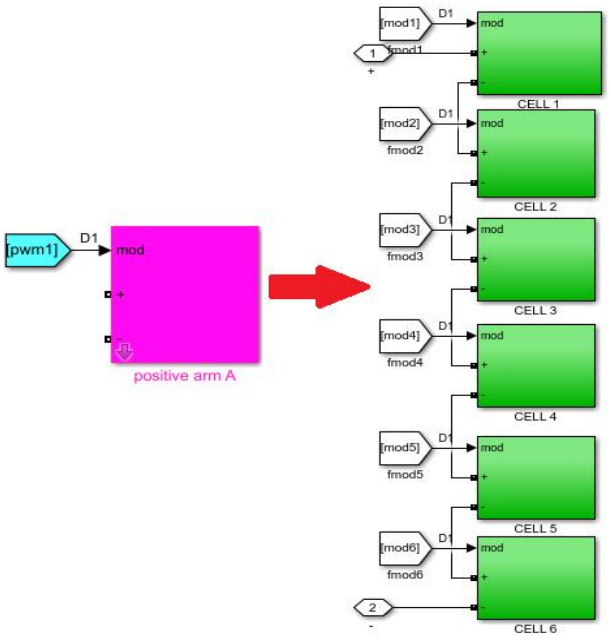

FIGURE 3.4: Internal structure of Phase leg arm, upper or lower arm used in 7-level MMC

In Fig. 3.4, the internal structure of a phase-leg arm, which is made up of six sub-modules connected in series.

The internal structure of each cell or sub-module is presented in Fig. 3.5. The sub-module structure is represented by a half-bridge topology in the simulation model.

It is composed of two IGBTs with an anti-parallel diode, and a capacitor is connected across both IGBTs.

To ensure that both IGBTs are not turned ON at the same time, a NOT gate is used to apply a complementary gating signal to the g terminal. A capacitor, C, with a value of 5 mF, is connected across the IGBTs.

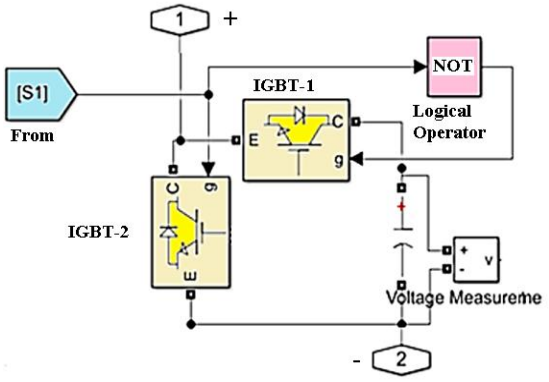

FIGURE 3.5: Simulation model of sub-module used in 7-level MMC

The voltage across this capacitor is:

$$V_c(t) = \frac{V_{dc}}{N} \tag{3.1}$$

V_{dc} represents the DC voltage applied to MMC input, and N represents the number of sub-modules connected in series in each phase leg arm. Six sub-modules are linked in series, so N=6.

$$V_c(t) = \frac{100000}{6} = 16666.66\ V \tag{3.2}$$

Simulation parameters of 7-level MMC are provided in Table 3.1.

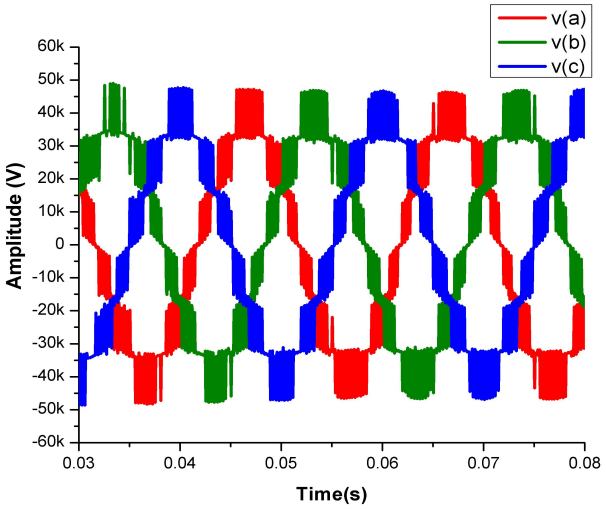

FIGURE 3.6: Matlab/Simulink simulation waveform of three phase 7-level MMC

TABLE 3.1: The simulation parameters of the 7-level MMC

Parameters	**Description**
Applied DC Voltage	100 kV
Converter AC side voltages	50 kV
Number of sub-module (N) in each arm	6
Level in output voltage(N+1)	7
$Arminductance L_{arm}$	1 mH
$Armequivalentresistance R_{arm}$	1 Ω
Sub module capacitance	5 mF
Voltage across each capacitor	16.66 kV
Fundamental frequency	50 Hz
Switching frequency	1.65 KHz

In Fig. 3.2, the phase reactor is used. Its function is to regulate the circulating current.

The phase reactor is used to minimize the high-frequency harmonics that are produced by the semiconductor switching devices, so it also works as a harmonic filter. The phase reactor block's selected inductance, L, is 2 mH, and the resistance provided by the phase reactance, R, is 0.08 Ω. In Fig. 3.2, the coupling

transformer is used between the converter station and the AC grid. Its function is to provide an interface between the converter station and the AC grid. It provides the AC grid voltages that are suitable for the converter station.

In this simulation model, the $Y_g\Delta$ three-phase transformer configuration is used. The Δ side of the coupling transformer is toward the converter station side and the Y_g side of the transformer is towards the AC grid. The Δ configuration can allow the circulation of a third harmonic circulating current within the transformer, and it blocks this circulating current from affecting the supply line voltages [72]. Because the Y configuration of the coupling transformer requires less insulation inside the transformer, the Y side is mostly used at the AC grid side [72].

3.3 Modeling of AC Grid

The simulation parameters used for the design of the AC grid are presented in Table 3.2.

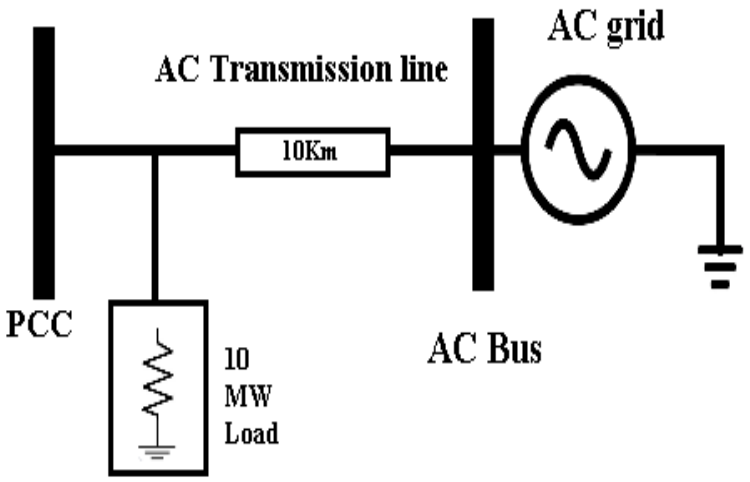

FIGURE 3.7: Single line diagram of AC grid

Fig. 3.3 presents the Matlab/Simulink model for the 7-Level MMC.

The AC side of the MMC converter is connected to the AC grid through coupling transformers. In this section, the modelling of a three-phase AC grid is discussed.

TABLE 3.2: The simulation parameters of AC Grid

Description	**Symbol**	**Values**
AC Grid Voltages	Vs	220 kV(r.m.s)
AC Grid Current	Is	2.673e+01 A (r.m.s)
Grid Frequency	f	50 Hz
Transmission Line	π	10 km
Load	L	10 MW

A simple diagram of the AC grid is shown in Fig. 3.7. For AC grid modeling in Matlab/Simulink, a three-phase symmetrical balanced voltage source is used. To have specifications like a practical grid, a three-phase load is connected to the AC grid using a Pi-section line of 10 km length through the grid side bus, and also this load interconnects with the Point of Common Coupling (PCC). PCC is the point at which the output of the converter will be interconnected to the AC grid.

3.3.1 Modeling of the AC Grid in Matlab/Simulink

In Matlab/Simulink, the modeling of the AC grid is performed using the model that was presented in Fig. 3.7.

In this model shown in Fig. 3.8 the 3-phase balanced voltage source is used, having a nominal voltage of 220 kV with a nominal frequency of 50 Hz.

In Fig. 3.8, a balanced three-phase voltage source is used, and a 10 MW three-phase active load is connected to the three-phase AC source via a 10 km Pi-section transmission line through the grid side bus.

The grid side bus is used to interconnect the three-phase grid and the transmission line and is also used as a measurement port to measure the grid voltage and current.

The Fig. 3.9 and the Fig. 3.10 present the 3-phase voltage and current waveform results, respectively. These waveforms are obtained from the simulation of an AC grid model that was performed using Matlab/Simulink.

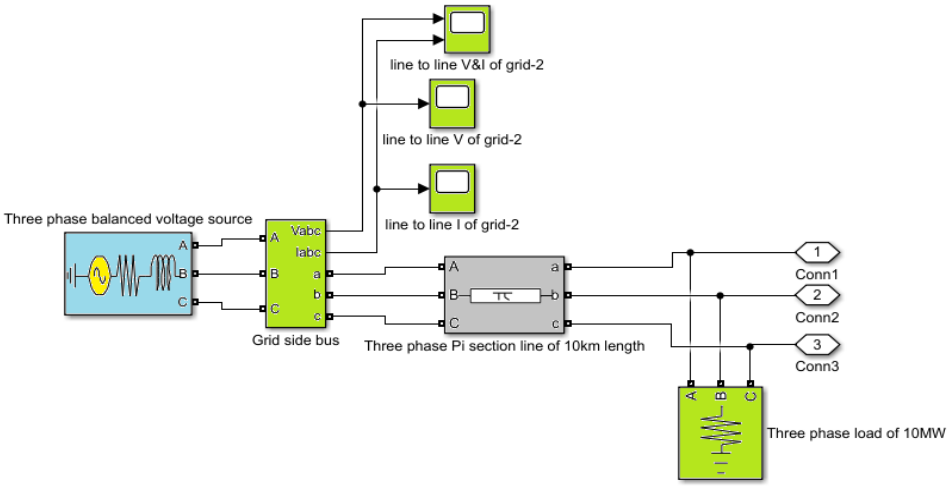

FIGURE 3.8: Matlab/Simulink simulation model of AC grid

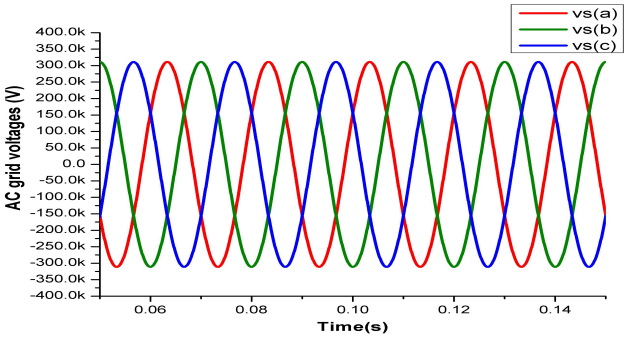

FIGURE 3.9: AC grid voltages waveform used in Matlab/Simulink model

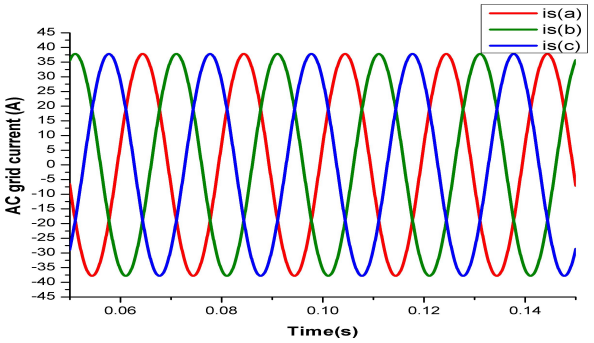

FIGURE 3.10: The current waveform of the AC grid

3.4 Matlab/Simulink Model for MMC Control

This section discusses the software based simulation model that is designed to control the grid tied MMC. The MMC output terminal voltage is controlled by

the inner current control loop of the converter, and the method that is used for the development of the Simulink-based model of MMC control is elaborated in the following sections.

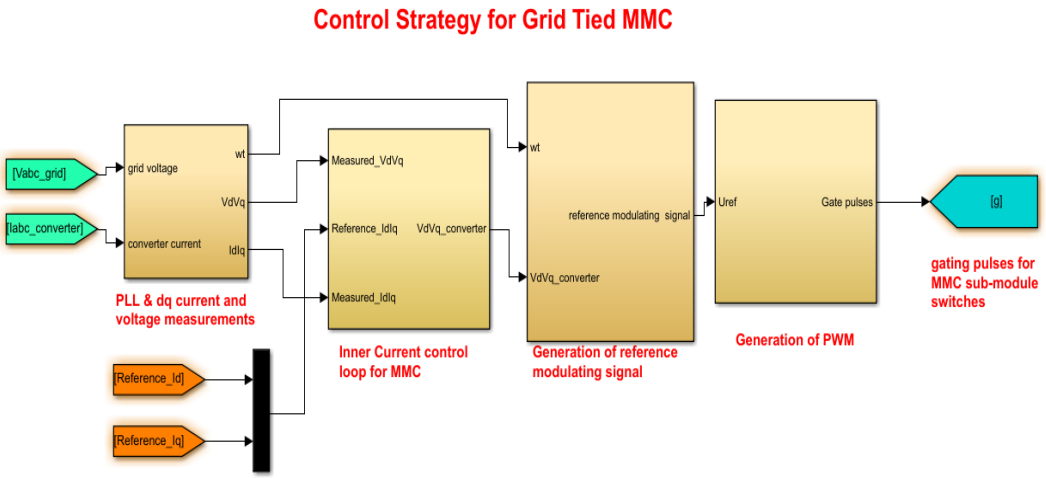

FIGURE 3.11: Matlab/Simulink model for the control strategy for grid tied MMC

Fig. 3.11 shows that the three-phase grid voltages and three-phase converter currents are applied at the input of the PLL and measurement block.

The PLL and measurement block provide the ωt, which is the synchronization angle, and it provides the DQ transformed grid voltage and converter current.

The measured DQ frame grid voltages and converter currents are applied at the input of the inner current control loop, also called the current regulator, and along with these measured DQ values, their references are applied at the input of the current control loop.

The current control loop block outputs the converter output terminal voltages in a DQ frame. The reference modulating signal block receives the converter's DQ frame output terminal voltages as well as the synchronisation grid angle ωt. This block generates the reference modulating signal, which is in the ABC reference frame. This reference modulating signal is then applied to the PWM generator block.

The PWM generator block compares the reference modulating signal with the high frequency triangular carrier signal and produces the gating signals for switching of

sub-module IGBTs in each arm of the MMC. The explanation of each block shown in Fig. 3.11 with its detailed simulation model is presented in the next sections.

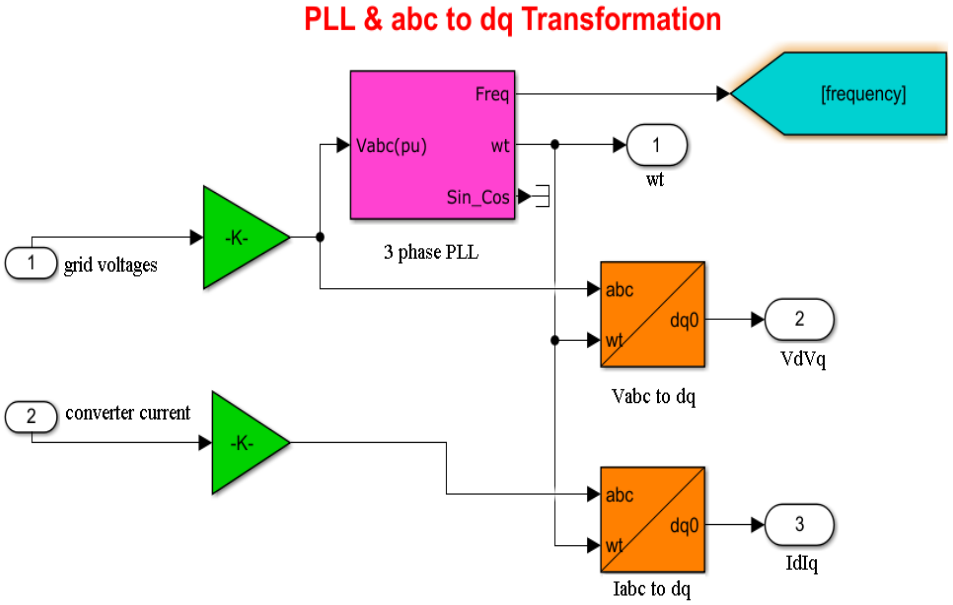

FIGURE 3.12: PLL(Phase Locked Loop) and dq transformation

The phase angle by which the PLL synchronizes the grid space phasor and DQ rotating reference frame and frequency that is tracked by the PLL is shown in Fig. 3.13.

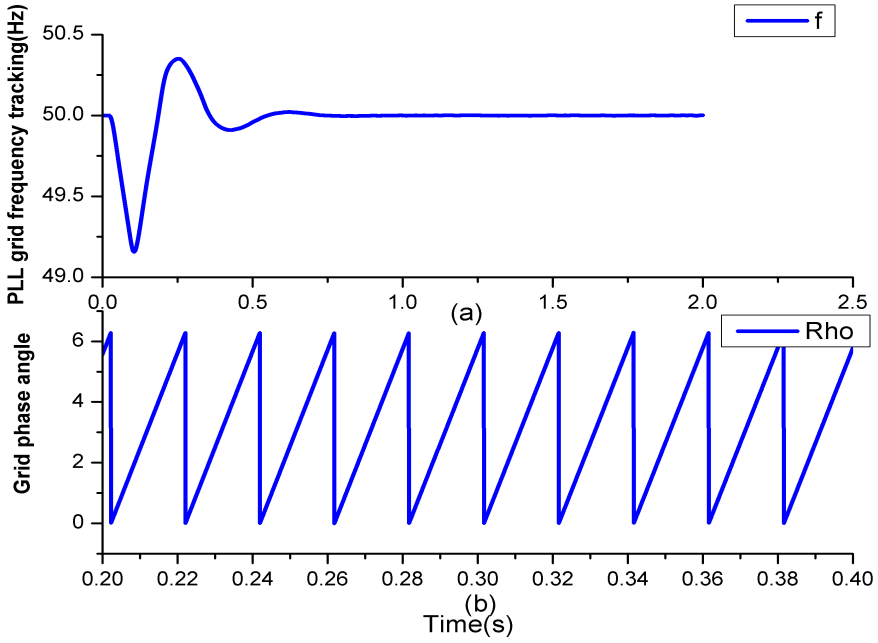

FIGURE 3.13: (a) grid frequency tracking by PLL (b) Grid phase angle

With the implementation of PLL, the grid and MMC converter are synchronized with each other, as the grid voltage and converter current of phase A are in phase with each other, as shown in Fig. 3.14.

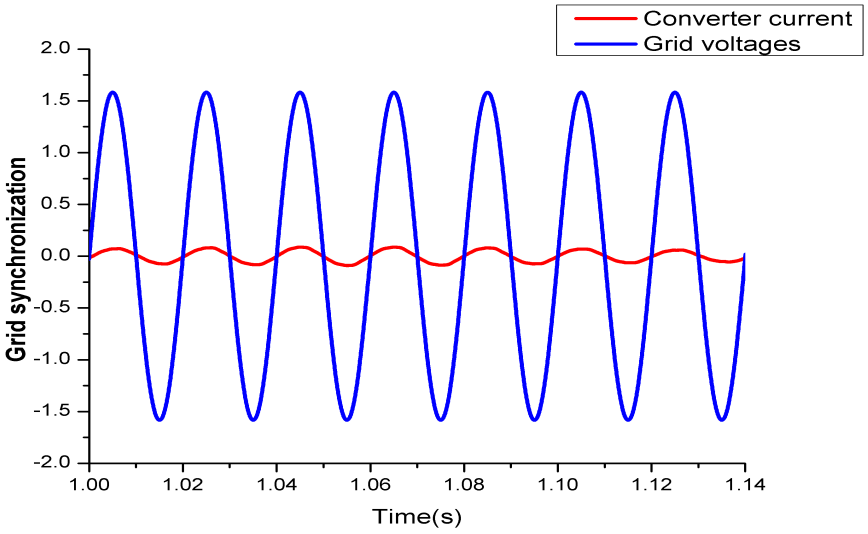

FIGURE 3.14: Grid voltages and converter currents synchronization

The structure of the inner current control loop block, which controls the active and reactive power independently, is presented in Fig. 3.15. In the inner current control loop block, two PI controllers are used. One PI controller is used for the d-axis current, and the second PI controller is used for the q-axis current.

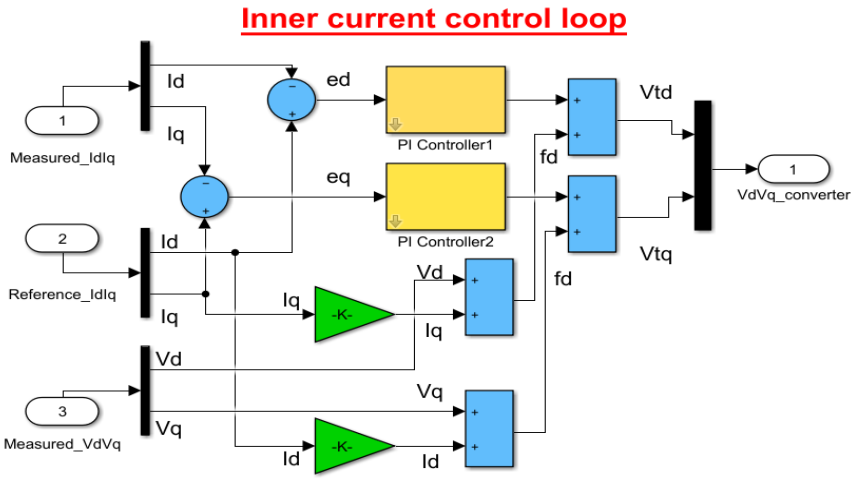

FIGURE 3.15: The inner current control loop for MMC in dq frame

Fig. 3.16, shows the simulation model for the generation of reference active and reactive power, and it also generates the reference DQ current signals.

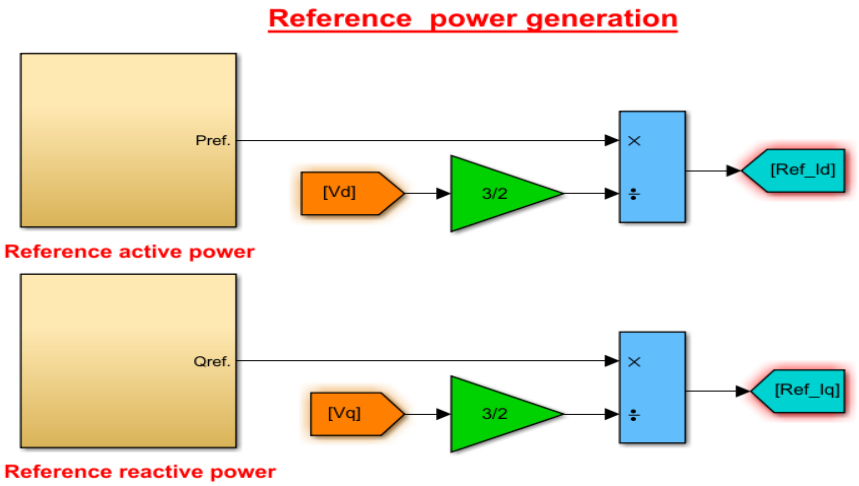

FIGURE 3.16: Reference active and reactive power generation simulation model

As we discussed in earlier sections, when we make changes in reference values of active and reactive currents, those correspond to changes in reference active and reactive powers.

As a consequence, we can control the active and reactive power independently by controlling the d-axis and q-axis current components. This control methodology is called direct power control at PCC.

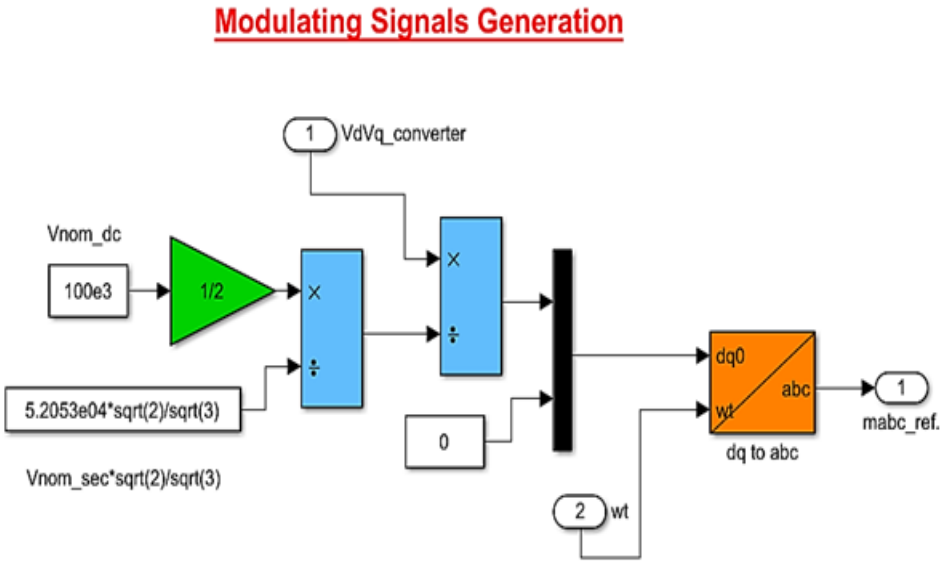

FIGURE 3.17: Reference modulating signal generation simulation model

The Fig. 3.17, shows the reference modulation signal generation block. In this simulation model, first of all, nominal DC voltages denoted by Vdc are divided by

a factor of 1/2, so they become Vdc/2. This means that half of the nominal DC voltages are divided by the nominal secondary voltages. This process makes VDC normalized.

After this, the converter output terminal voltages are denoted by V_{td} and V_{tq} divided by these normalized half-dc voltages denoted by Vdc/2, and as a result, we obtain the reference modulation signals denoted by m_d and m_q.

These are in the DQ reference frame.

These DQ rotating reference frame modulation signals are transformed into three-phase ABC reference frame modulation signals denoted by $m_{abc}(t)$ by using the DQ to ABC transformation block from the Simscape Simulink library.

These three-phase reference modulation signals are placed at 120 degrees from each other.

These three-phase reference modulation signals are applied to the PWM block for the generation of gating pulses for semiconductor switching devices of MMC sub-modules.

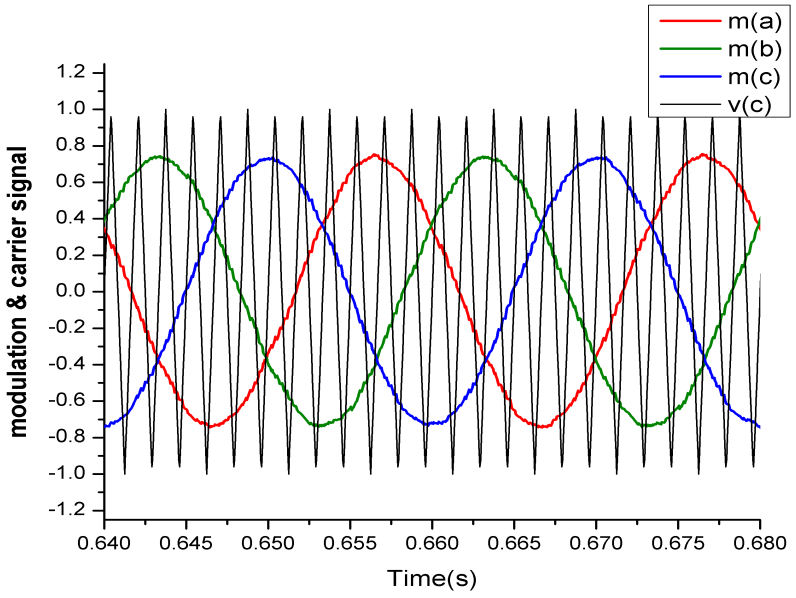

FIGURE 3.18: Three phase reference modulation signal with carrier signal for 7-level MMC

Fig. 3.18 depicts the three-phase reference modulation signal used for seven-level MMC, denoted by $m_abc(t)$ with a fundamental frequency of 50 Hz and an amplitude ranging from 1 to -1.

This reference modulation signal is compared with a carrier waveform having a frequency of 1650Hz and whose amplitude varies between 1 and -1. When the reference modulation signal is compared with the carrier signal, then gating pulses are generated for the switching of sub-module IGBTs for each phase leg of MMC.

The gating or switching pulses for 7-level MMC are generated by the PWM generator block from the Simulink library.

The PWM generator block generates the gating pulses using a phase shifted carrier pulse width modulation pattern in which 6 half bridge sub-modules are switched at the frequency of 1650 Hz. The phase shift carrier PWM block is shown in Fig. 3.19

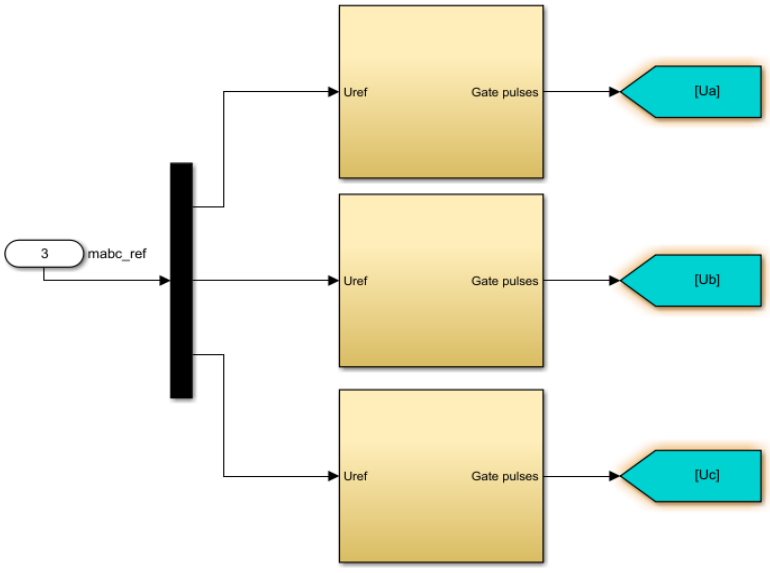

FIGURE 3.19: Phase shift carrier PWM generation model for 7-level MMC

The phase shift carrier PWM technique is also known as multi-carrier sinusoidal PWM. In this modulation technique, a single sine wave modulation signal is compared with multiple triangular carrier waveforms for the generation of gating pulses for the semiconductor switches for one arm of a phase leg. In this thesis, the simulation model is composed of a 7-level MMC.

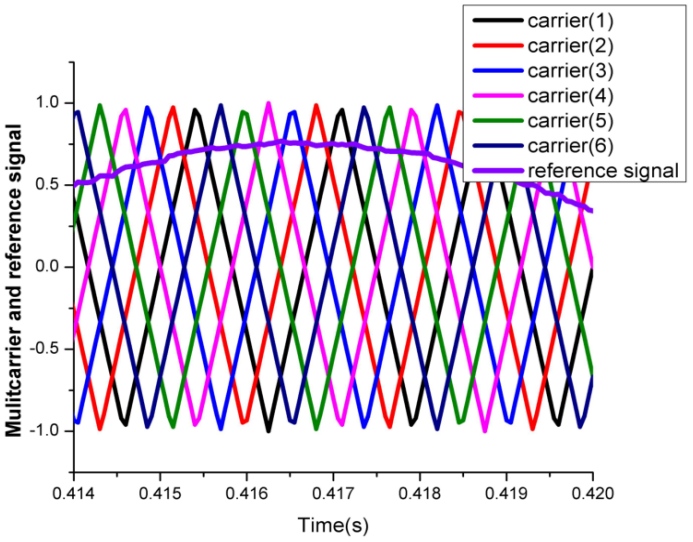

FIGURE 3.20: Phase shift carrier PWM with reference modulation signal for 7-level MMC

In our case, 7-level MMC is used, so the number of sub-modules in 7-level MMC is N, and N=6, implying that six sub-modules are used in an arm of a phase leg of MMC, resulting in six triangular carrier waveforms in the modulation technique shown in Fig. 3.20.

For 7-level MMC, the PWM generator block uses six phase-shifted carrier waveforms that have a phase difference of 60 degrees according to the given equation.

$$\phi = \frac{360 degree}{N} \tag{3.3}$$

The modulation signal's amplitude varies between 1 and -1 with a frequency of 50 Hz, and the amplitude of the carrier signal varies between 1 and -1 with a frequency of 1650 Hz.

The carrier waveform with reference modulation signal for phase A of 7-level MMC is shown in Fig. 3.20.

The parameters which are used for the generation of gating signals using phase shifted carrier PWM are presented in Table 3.3.

TABLE 3.3: The parameters for generation of gating signals using PSC-PWM

Description	**Symbol**	**Value**
Number of sub-modules	N	6
Number of carrier	N	6
Phase displacement in carrier	ϕ	60 deg.
Modulation frequency	f	50 Hz
Amplitude modulation index	m	0.85
Carrier frequency	f_c	1650 Hz
Frequency modulation index	m_f	33
Sampling time	T_s	$6.06e-6$ s

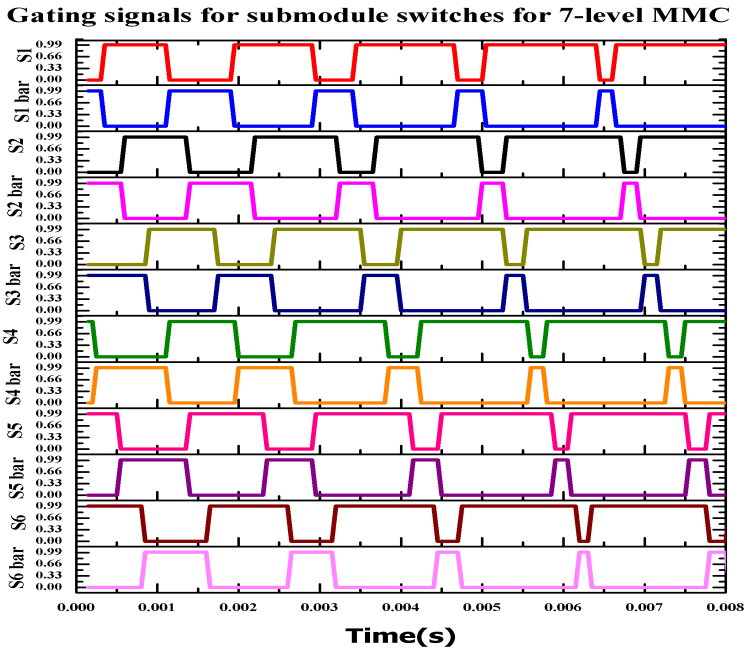

FIGURE 3.21: Gating signals of an arm of a phase leg for 7-level MMC

The MMC is composed of a series of connected sub-modules in an arm of a phase leg. Each sub-module consists of two IGBTs. These are operated in a complementary manner, so each sub-module requires two gating signals which are opposite to each other.

As we know, a single arm of a 7-level MMC is composed of six series-connected

sub-modules, and in each sub-module, there are two IGBTs, so they require twelve gating pulses for an arm of a phase leg.

These twelve gating pulses for one arm are inverted and used for the switching of IGBTs of the second arm of the same phase leg or bridge.

Chapter 4

Simulations and Results

4.1 Introduction

The simulation results for the DC fault analysis in the multi-terminal MMC based HVDC power transmission systems are presented in this chapter.

The Matlab/Simulink environment has been used to perform these simulations.This research utilised 7-level MMC converter stations to develop three terminal MMC-HVDC power transmission systems using series, star, and ring topologies.

DC faults are generated at the sending end converter station, the receiving end converter station side, and on the transmission line, including pole to pole and pole to ground faults.

We generate these faults and then examine how they affect the currents and voltages on the AC and DC sides.

First of all, fault analysis is performed in the three-terminal series MTDC power transmission system.

We obtain the simulation findings by generating a pole to pole fault at the sending end converter side and a pole to ground fault at the transmission line.

After that, a star and ring topology three terminal MTDC power transmission system fault analysis is carried out.

4.2 DC Fault Analysis in Three Terminal Series MTDC Power Transmission System

This thesis is based on a comprehensive study on DC fault analysis in multi-terminal MMC HVDC power transmission systems.

For the DC fault analysis, first of all, a Matlab/Simulink model of the three terminal series MTDC has been developed. It is composed of three 7-level MMC converter stations.

A single line diagram of the series MTDC is shown in Fig. 4.1. Fig. 4.2 presents the Matlab/Simulink model of the series MTDC. model of series MTDC.

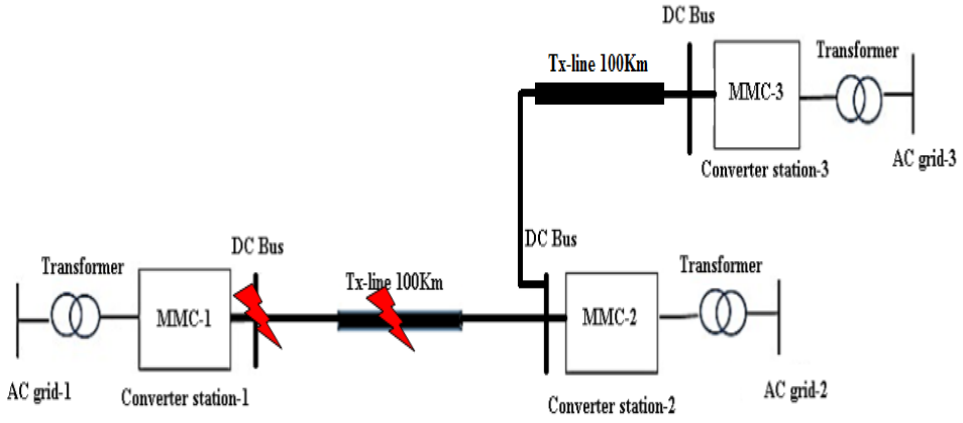

FIGURE 4.1: Single line diagram of series MTDC

The simulation parameters that are used for the development of three terminal series MTDC power transmission system are presented in Table 4.1.

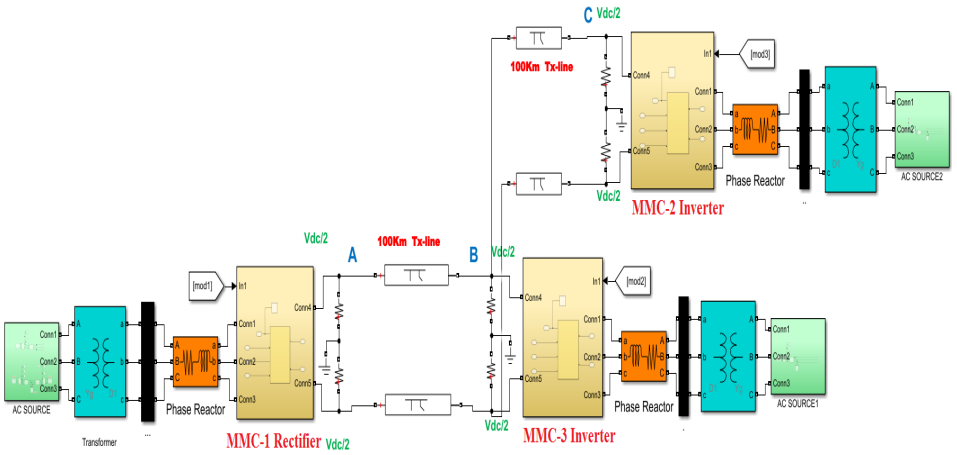

FIGURE 4.2: Matlab/Simulink model of series MTDC

According to Fig. 4.2, three 7-level MMC converter stations are used in series MTDC and are individually connected with 220 kV and 50 Hz AC grids on the AC side via phase reactors and coupling transformers. These converter stations are connected on the DC side by a 200 km transmission line of the pi-section type.

The DC bus voltage is $Vdc = 100$ kV. On the dc side of MMC converter stations, the Vdc is divided into two halves, that is , $\frac{V_{dc}}{2} = 50$ kV split by a reference point at 0 V, which serves as a reference point for the entire simulation.

As a rectifier, the MMC Converter Station-1 transforms AC into DC. The sending end converter station is another name for converter station 1. The receiving end converter stations, also known as MMC converter stations 2 and 3, act as inverters to convert DC into AC.

In Fig. 4.2 the phase reactor is used between each MMC converter station and the coupling transformer. Its function is to regulate the circulating current. The phase reactor is also used to minimize the high frequency harmonics that are produced by the semiconductor switching devices, so it also works as a harmonic filter. The phase reactor block's selected inductance, L, is 2 mH, and the resistance provided by the phase reactance is 0.08 Ω.

In Fig. 4.2 the coupling transformers are used in between each MMC converter

TABLE 4.1: The simulation parameters for three terminal Series MTDC

Parameters	**Description**
MMC-1(7-level)	Working as Rectifier
MMC-2(7-level)	Working as inverter
MMC-3(7-level)	Working as inverter
DC Bus Voltage	100 kV
Converter AC side voltages	50 kV
Number of sub-module (N) in each arm	6
Level in converter AC output voltage (N+1)	7
Arm inductance L_{arm}	1 mH
Arm equivalent resistance R_{arm}	1 Ω
Sub module capacitance	5 mF
Voltage across each capacitor	16.66 kV
Fundamental frequency	50 Hz
Switching frequency	1.65 kHz
Transmission line length	100 km
Transformer Nominal voltages V_{sec}: V_{pri}	52 kV : 220 kV
Transmission line type	Pi Section
Number of pi section between two converters	2
Resistance of transmission cable	0.01273 Ω/km
Inductance of transmission cable	0.9337e-3 H/km
Capacitance of transmission cable	12.74e-9 F/km
Inductance of phase reactor	2 mH
Equivalent resistance of phase reactor	0.08 Ω
Clamping Resistor	1 MΩ
AC grid -1,grid-2 and grid-3 voltages	220 kV

station and AC grid. Its function is to provide an interface between the converter stations and the AC grid and step down the AC grid voltages that are suitable for the converter station.

In this simulation model, the $Y_g\Delta$ three-phase transformer configuration is used.

The Δ side of the coupling transformer is towards the converter station side and the Y_g side of the transformer is towards the AC grid. The Δ configuration can allow the circulation of third harmonic circulating current flows within the transformer, and it blocks this circulating current from affecting the supply line voltages [72].

Because the Y configuration of the coupling transformer requires less insulation inside the transformer, it is mostly used on the AC grid side [72].

4.2.1 Pole to Pole Short circuit Fault in Series MTDC

The most severe fault on the DC side is the pole to pole fault. According to [72], the pole to pole fault is a permanent fault caused by insulation damage.

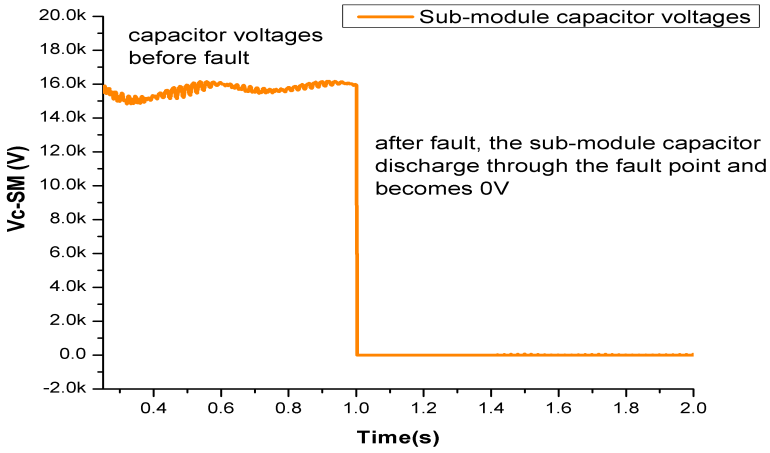

FIGURE 4.3: Sub-module capacitor voltage drops to 0 V after pole to pole fault at MMC-1 side

The simulated waveforms that are acquired during the pole to pole fault are shown in the following figures in the case where the short circuit fault occurs at the DC side terminal of the sending end converter station between the positive pole and the negative pole.

Due to a pole to pole fault in the MMC HVDC power transmission system, which

causes a rapid discharge of the sub-module capacitors on each side of the converter stations. The voltages of the sub-module capacitors are shown in Fig. 4.3.

The voltage of the sub-module capacitor was 16 kV prior to the pole to pole fault. The sub-module capacitor voltages rapidly decrease to zero after fault.

Power transmission between the two converter stations terminated as a result of a pole to pole fault.

Pole to pole voltages were 100 kV, positive pole voltages were 50 kV, and negative pole voltages were -50 kV prior to the fault.

The pole to pole, positive pole, and negative pole voltages decrease to 0 V as a result of a pole to pole short circuit fault at point A, as shown in Fig. 4.4.

Due to the pole to pole short circuit fault, the positive pole current and negative

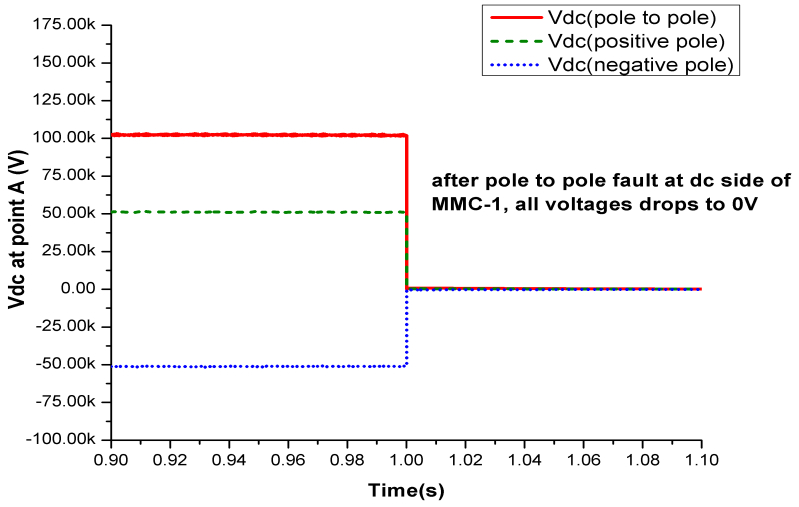

FIGURE 4.4: Pole to pole, positive pole and negative pole voltages drop to 0 V when pole to pole fault occurs at point A in Fig. 4.2, at MMC-1 DC side

pole currents increases drastically as shown in Fig. 4.5.

In Fig. 4.5, various current waveforms are shown. Positive pole current and negative pole current both increase quickly as a result of a pole to pole short circuit

fault that happens at the sending end converter station's output and is denoted as point A in Fig. 4.2.

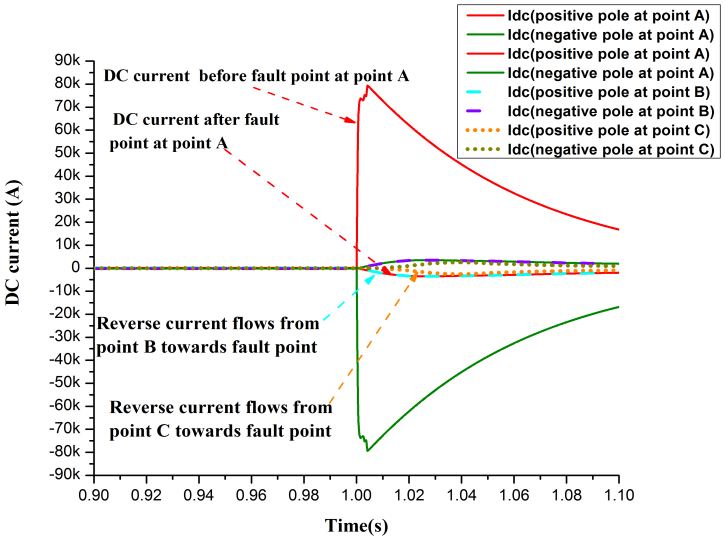

FIGURE 4.5: DC currents increases drastically after pole to pole fault at point A, that was shown in Fig. 4.2

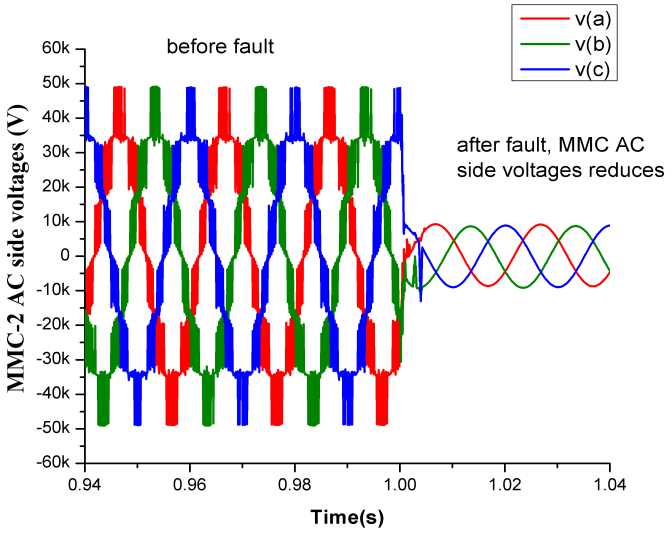

FIGURE 4.6: Due to pole to pole fault at point A, shown in Fig. 4.2, MMC-2 AC side voltages are reduced

The currents from nearby locations, like from point B and point C, flow towards the fault point. This means reverse current flows towards the fault point.

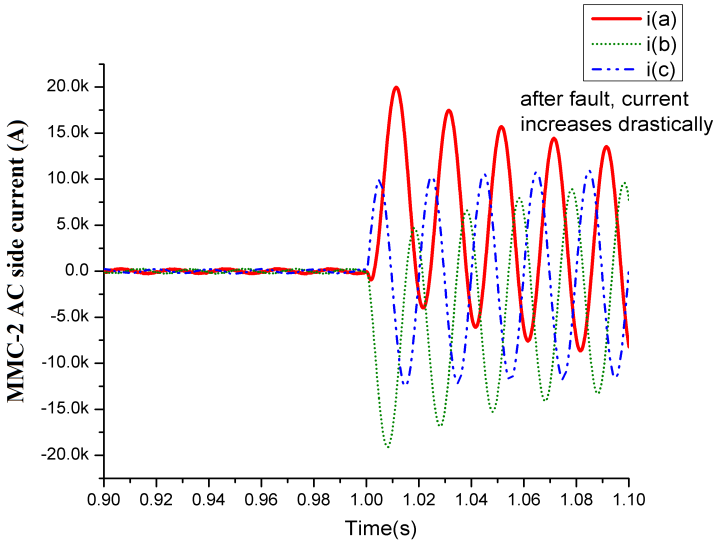

FIGURE 4.7: Due to pole to pole fault at point A, shown in Fig. 4.2, MMC-2 AC side current increases

Fig. 4.6 shows that the three phase AC voltages at the MMC-2 outlet reduce during a pole to pole fault. Due to a pole to pole fault, the MMC-2 AC side current rises rapidly to a three phase short-circuit current as shown in Fig. 4.7.

4.2.2 Pole to Ground Short Circuit Fault in Series MTDC

Cable breakage and connection to the ground terminal or cable insulation damage and connection to the ground due to an external force are the causes of pole to ground faults.

When a pole is connected to the ground, a large short circuit current flows. Two 1 MΩ clamping resistors were placed between the positive and negative poles of the DC transmission line to reduce the amplitude of short circuit current.

That provide the potential reference point for the DC transmission line and clamp the DC voltages [70].

In Fig. 4.2, the bipolar transmission mode is used for power transmission.

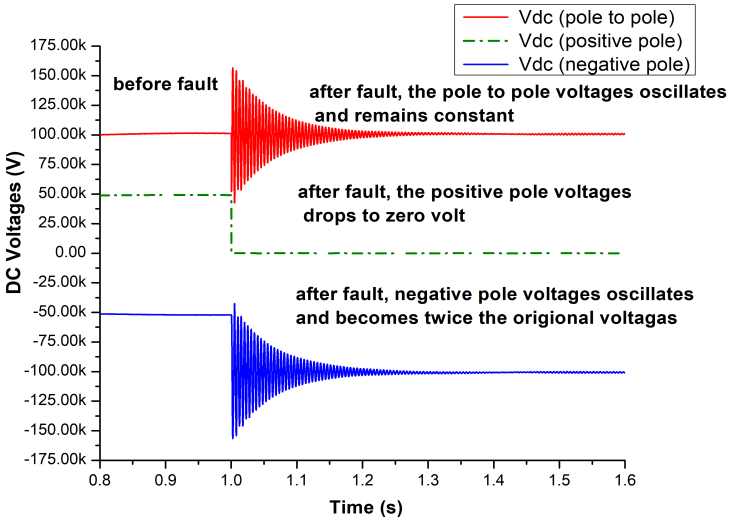

FIGURE 4.8: Due to positive pole to ground fault at transmission line, pole to pole voltages oscillates and remains constant, positive pole voltage drop to 0 V and negative pole voltages oscillates and becomes twice

When the positive pole of the transmission line is shorted to the ground, then the clamping resistor of the positive pole is shorted to the ground.

When this happens, the DC side will transform from the bipolar power transmission mode to a uni-polar transmission mode.

The positive pole voltage drops to 0 V when a pole to ground fault occurs, as shown in Fig. 4.8. The DC side pole to pole voltages will be supported by the negative pole clamp resistor.

As a result, the transmission line's capacitance and inductance cause the negative pole voltages to oscillate and increase to twice what they were before the fault. The voltage between the poles fluctuates but is constant.

Fig. 4.9 and Fig. 4.10 show the DC current waveforms at point A and at point B shown in Fig. 4.2, when a pole to ground short-circuit fault occurs.

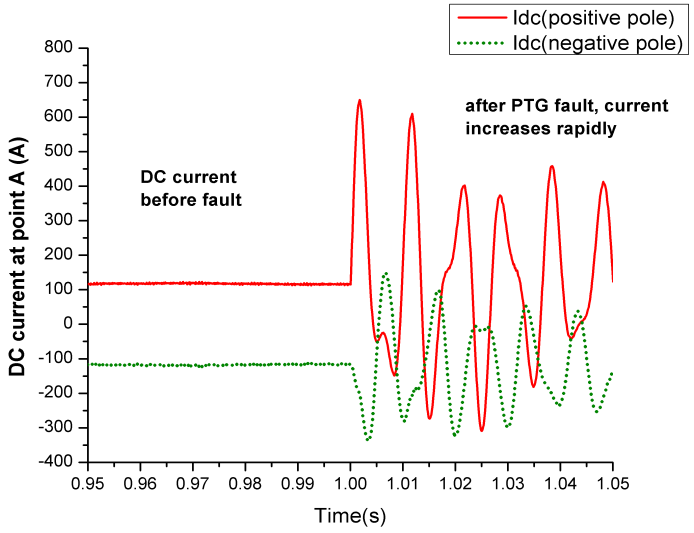

FIGURE 4.9: DC current at point A shown in Fig. 4.2 increases and flows towards the fault point, during positive pole to ground short circuit fault at transmission line

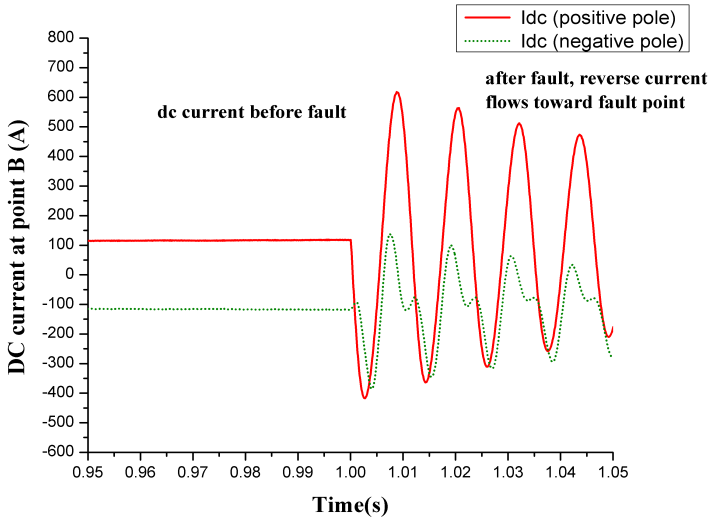

FIGURE 4.10: DC current at point B shown in Fig. 4.2, reverse current flows toward the fault point during positive pole to ground short circuit fault at transmission line

Transmission line inductance and capacitance cause certain oscillations in positive and negative DC currents during a pole to ground fault. From both point A and point B, the current flows towards the fault point.

It is clear from Fig. 4.9 and Fig. 4.10 that from point A, the current flows in a forward direction, and from point B, the current flows in a reverse direction toward the fault point.

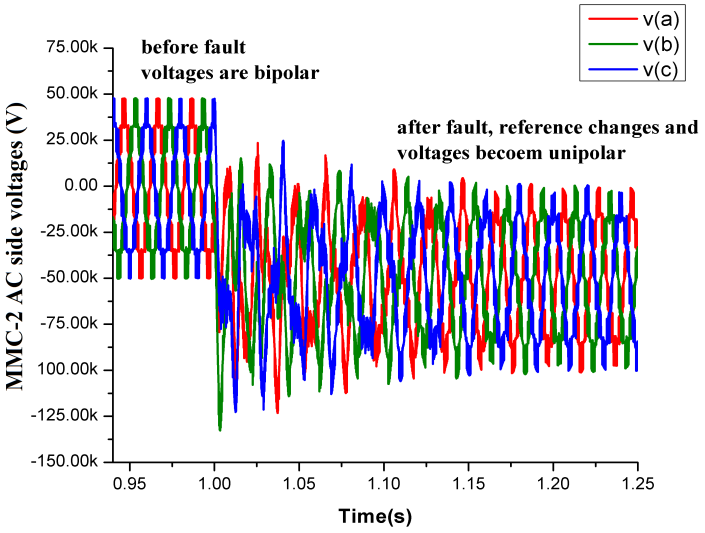

FIGURE 4.11: MMC-2 AC side voltages drops to single pole operational voltages during positive pole to ground short circuit fault at transmission line

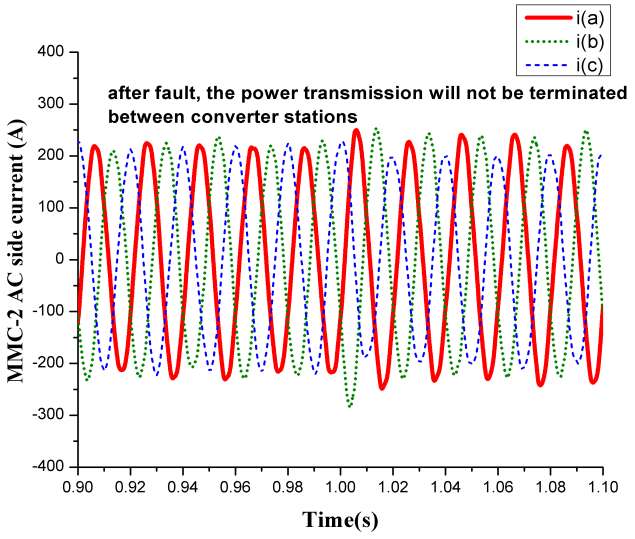

FIGURE 4.12: MMC-2 AC side current is unaffected by pole to ground short circuit fault at transmission line,its means the power transmission will not be terminated

The MMC-2 AC side voltages drop to single pole operational voltages, as shown in Fig. 4.11.

Which means its voltage value becomes -100 kV because the positive pole voltages abruptly change to 0 V shortly after the pole to ground fault. Fig. 4.12 shows the MMC-2 AC side current.

The AC side current is unaffected by a pole to ground fault. It means when a pole to ground fault occurs, the power transmission will not be terminated.
The summary of all pre fault and post fault conditions is presented in Table 4.4.

4.3 DC Fault Analysis in Three-Terminal Star MTDC Power Transmission System

In Fig. 4.13, a single line diagram of a three-terminal MMC-HVDC power transmission system is shown.

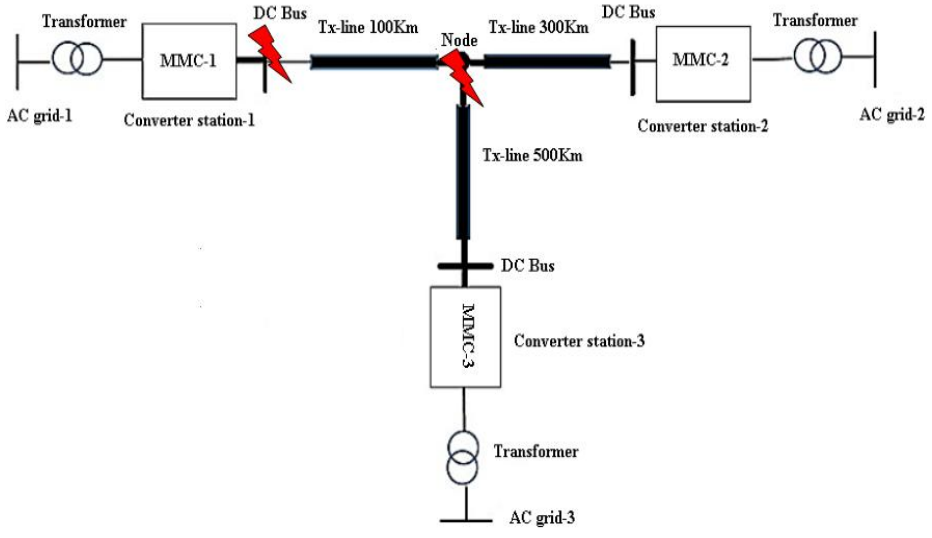

FIGURE 4.13: Single line diagram of three terminal star MTDC

The simulation parameters that are used for the development of three terminal star MTDC power transmission system are presented in Table 4.2.

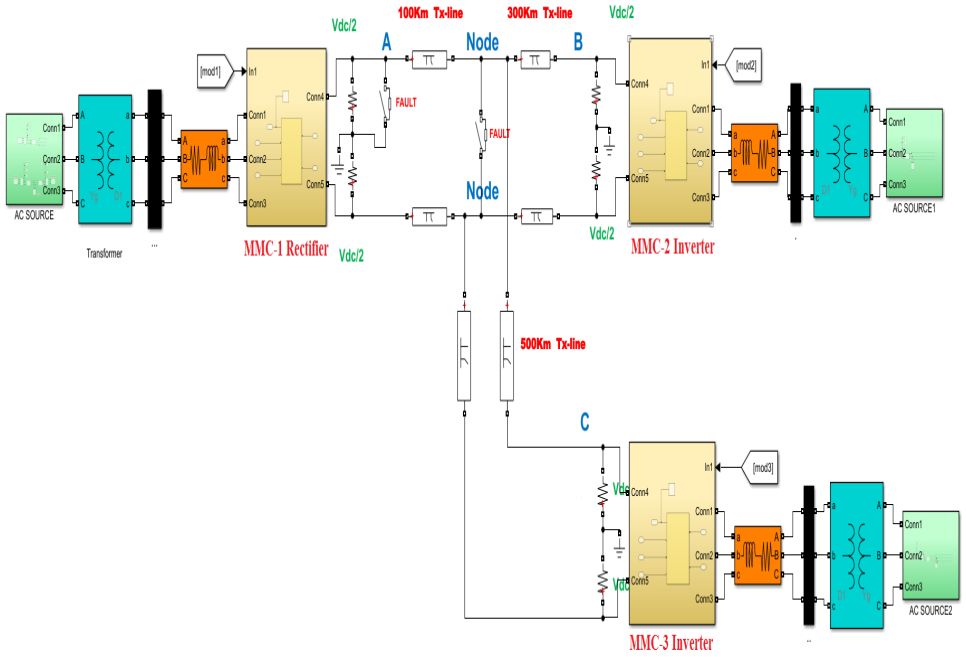

FIGURE 4.14: Matlab/Simulink model of star MTDC

A Matlab/Simulink model for the star MTDC is shown in Fig. 4.14. According to the MTDC's balancing principle, the total current delivered by the sending end converter station and the total current drawn by the receiving end converter station should be equal.

Three 7-level MMC converter stations, each individually connected to the 220 kV AC grid through a coupling transformer and phase reactor, make up the three-terminal star MTDC power transmission system.
For the star topology, taping is carried out for connecting the receiving end converter stations.

One of these three converter stations, also known as a sending end converter station, functions as a rectifier. The remaining two converter stations, also known as receiving end converter stations, function as inverters.

At a common node, MMC-1, MMC-2, and MMC-3 are connected by a 500 km pi-type DC transmission line, a 100 km pi-type DC transmission line, and a 300 km pi-type DC transmission line, respectively.

TABLE 4.2: The simulation parameters for three terminal Star MTDC

Parameters	**Description**
MMC-1(7-level)	Working as Rectifier
MMC-2(7-level)	Working as inverter
MMC-3(7-level)	Working as inverter
DC Bus Voltage	100 kV
Converter AC side voltages	50 kV
Number of sub-module (N) in each arm	6
Level in converter AC output voltage (N+1)	7
Arm inductance L_{arm}	1 mH
Arm equivalent resistance R_{arm}	1 Ω
Sub module capacitance	5 mF
Voltage across each capacitor	16.66 kV
Fundamental frequency	50 Hz
Switching frequency	1.65 kHz
Transmission line length	100 km-500 km
Transformer Nominal voltages V_{sec}: V_{pri}	52 kV : 220 kV
Transmission line type	Pi Section
Number of pi section between two converters	2
Resistance of transmission cable	0.01273 Ω/km
Inductance of transmission cable	0.9337e-3 H/km
Capacitance of transmission cable	12.74e-9 F/km
Inductance of phase reactor	2 mH
Equivalent resistance of phase reactor	0.08 Ω
Clamping Resistor	1 MΩ
AC grid -1,grid-2 and grid-3 voltages	220 kV

4.3.1 Pole to Pole Short Circuit Fault in Star MTDC

When a pole to pole short circuit fault occurs at point A, as shown in Fig. 4.14 at the sending end converter station's output terminal, the following simulation results are obtained: Pole to pole voltages were 100 kV, positive pole voltages were

50 kV, and negative pole voltages were -50 kV prior to the fault.

Pole to pole voltages, positive pole voltages, and negative pole voltages all quickly drop to 0 V when a pole to pole fault occurs at point A because of the short circuit shown in Fig. 4.15.

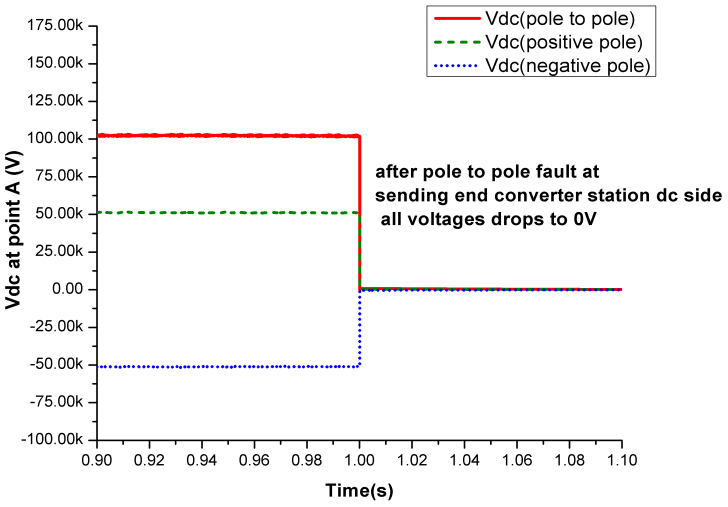

FIGURE 4.15: Pole to pole, positive pole and negative pole voltages drop to 0 V when pole to pole fault occurs at point A in Fig. 4.14, at MMC-1 DC side in star MTDC

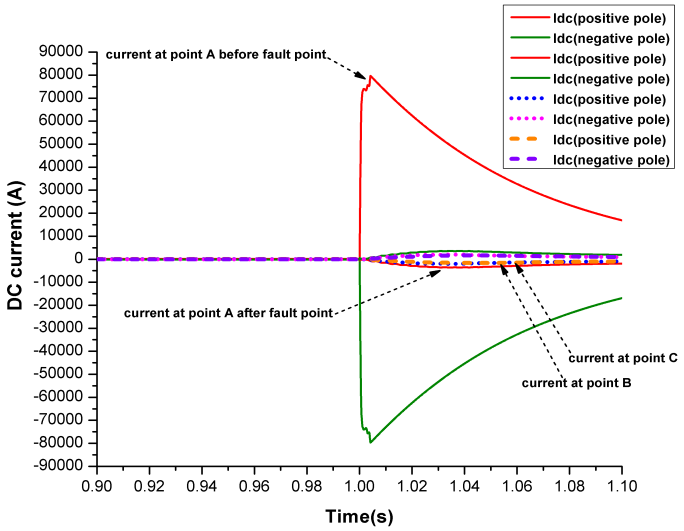

FIGURE 4.16: Due to pole to pole fault at point A in Fig. 4.14, positive pole and negative pole DC currents increases in star MTDC

The three terminal MMC-HVDC's current is shown in Fig. 4.16.

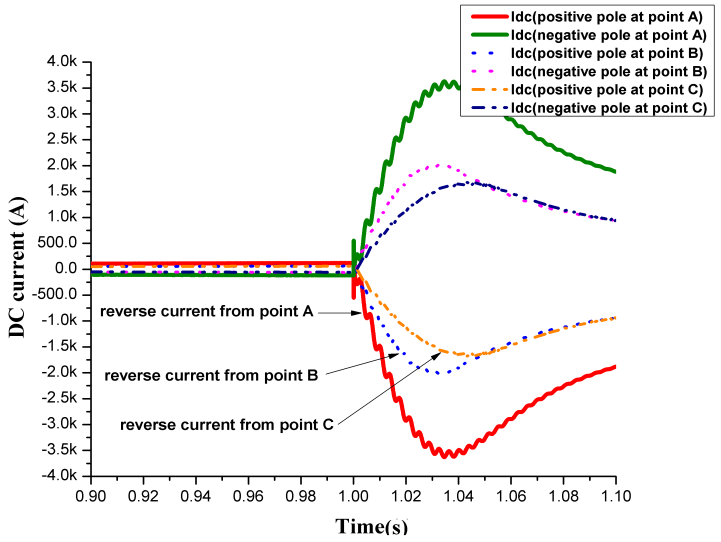

FIGURE 4.17: Reverse current flows from point A, B and from point C towards the fault point as shown in Fig. 4.14 due to pole to pole fault

The figure clearly shows that the current dramatically increases when a pole to pole fault, as in Fig. 4.14, occurs at point A.

Reverse current flows in the direction of the fault point after the fault at point A.

It should be noted that from points B and C, the reverse current flows towards the fault point.

These points are marked near the two inverter stations. In Fig. 4.17, these reverse currents are presented separately for better understanding.

The sending end converter station's total current output and the receiving end converter station's total current draw are equal, according to the balance principle.

Therefore, it is evident that the reverse current that flows from point A toward the fault point, as illustrated in Fig. 4.14, is the sum of the currents that flow from points B and C toward the fault point.

The AC side voltages of the MMC-2 are shown in Fig. 4.18.

A pole to pole fault resulted in a decrease in the voltages on the MMC-2 AC side. The MMC-2 AC side current is shown in Fig. 4.19, and the pole to pole short circuit causes a dramatic increase in the current.

All of these simulations demonstrate that power transmission will be terminated when a pole to pole fault occurs at the sending end converter station side.

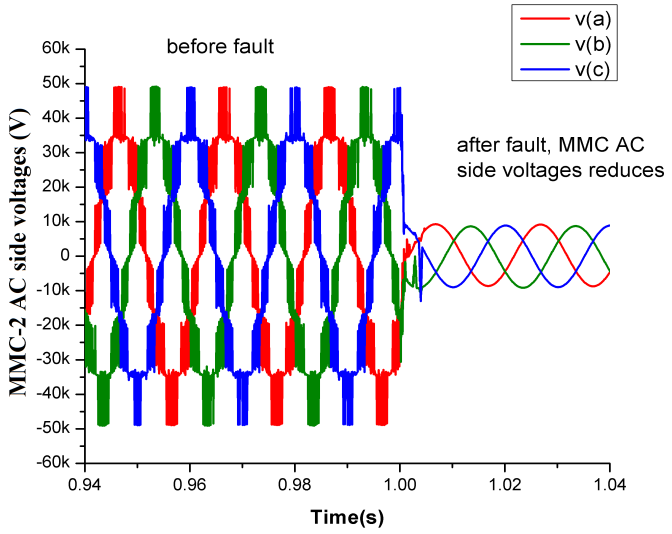

FIGURE 4.18: MMC-2 AC side voltages reduces during pole to pole fault at point A, shown in Fig. 4.14

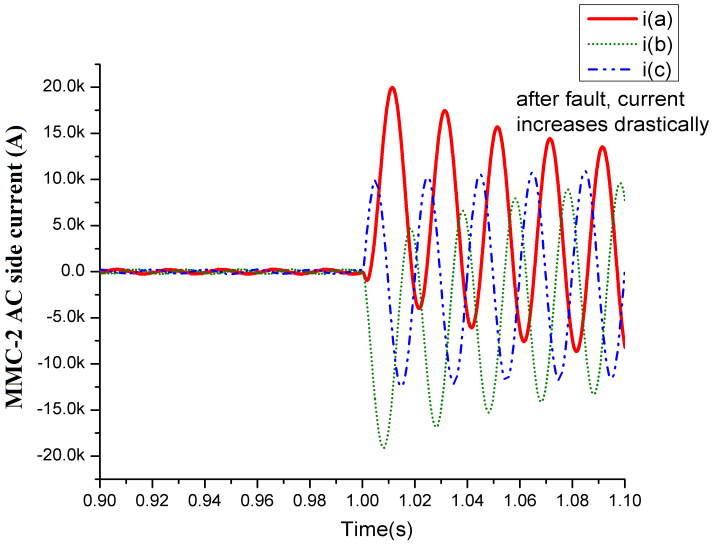

FIGURE 4.19: MMC-2 AC side current increases during pole to pole fault at point A, shown in Fig. 4.14

4.3.2 Pole to Pole Fault at Node Terminal in Star MTDC

When a pole to pole fault occurs at a node, the following simulation outcomes are obtained:

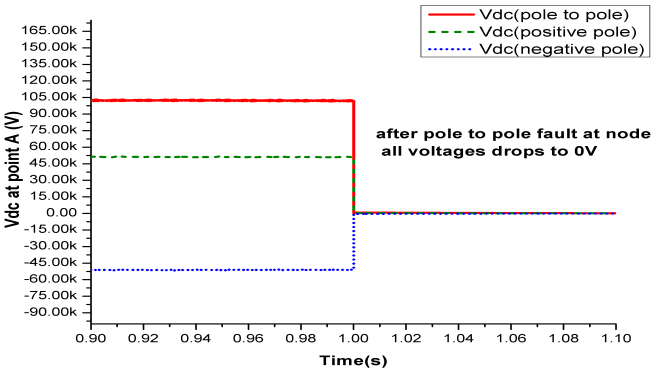

(a)

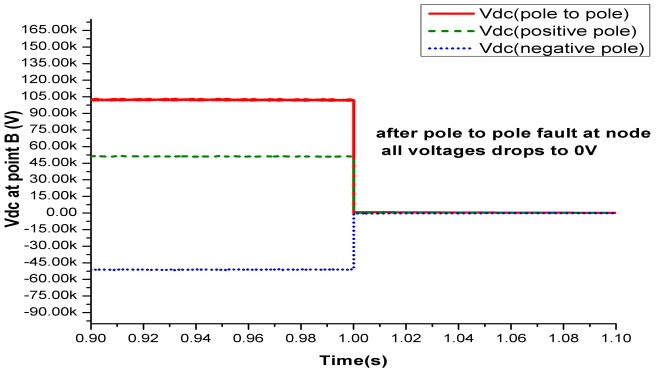

(b)

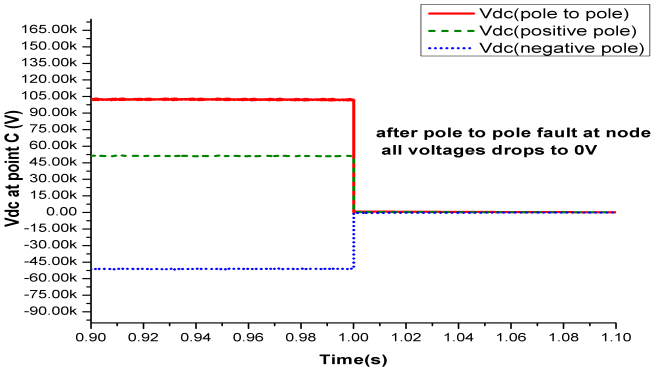

(c)

FIGURE 4.20: Pole to pole, positive pole and negative pole voltages drops to 0 V, due to pole to pole fault at node in star MTDC

According to Fig. 4.20, all converter stations are lost when a pole to pole fault occurs at a node because all converter stations are connected to the same node, which causes the pole to pole, positive pole, and negative pole voltages to drop to 0 V.

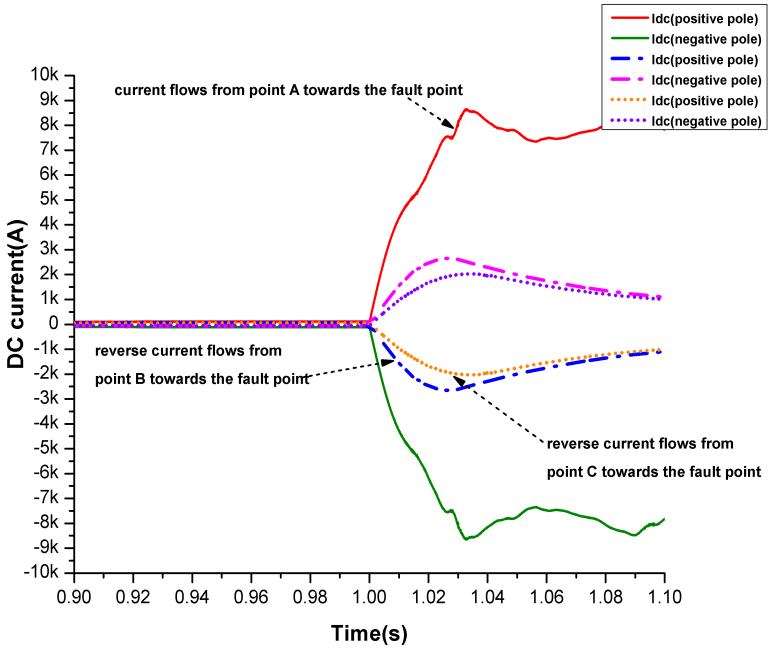

FIGURE 4.21: DC currents at point A,B and at point C shown in Fig. 4.14, from point A the current flows towards the fault point and form point B and C, reverse current flows, during pole to pole fault at node

The DC currents during a pole to pole fault at the node terminal are shown in Fig. 4.21.

It is evident from Fig. 4.21, that when a fault develops at a node, the current at points A, B, and C dramatically increases and flows in the direction of the fault.

The current flows in a forward direction from point A towards the node fault point and in a reverse direction from points B and C towards the fault point. Since each converter station is positioned at a different distance from the node terminal, point A's fault current has a larger amplitude than converter stations-2 and converter stations-3. As the converter station-3 is located 500 km apart from the other two converter stations, its fault current is lower, as shown in Fig. 4.21.

Before the fault, the MMC-2 and MMC-3 AC outlet voltage was ± 50 kV.

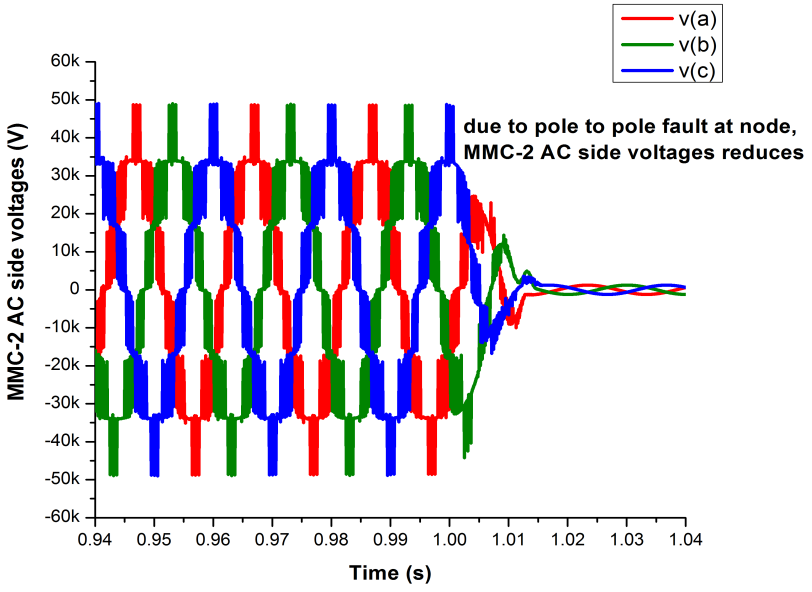

(a)

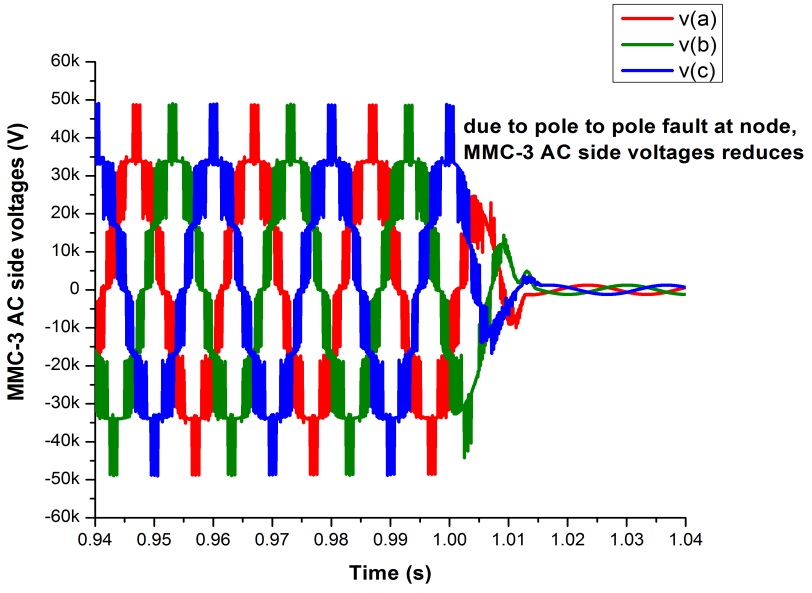

(b)

FIGURE 4.22: (a) MMC-2 (b) MMC-3 AC side voltages reduces , during pole to pole fault at node

When a fault occurs at the node, then MMC-2 and MMC-3 AC side voltages are reduced due to a short circuit at the node, as presented in Fig. 4.22. In Fig. 4.23, MMC-2, and MMC-3 AC side currents are shown in case of pole to pole fault at

the node terminal.

Due to the fault, the MMC AC side current increases drastically.

It means the power transmission will be terminated due to the fault at the node, and we will lose all converter stations when the fault occurs at the node terminal.

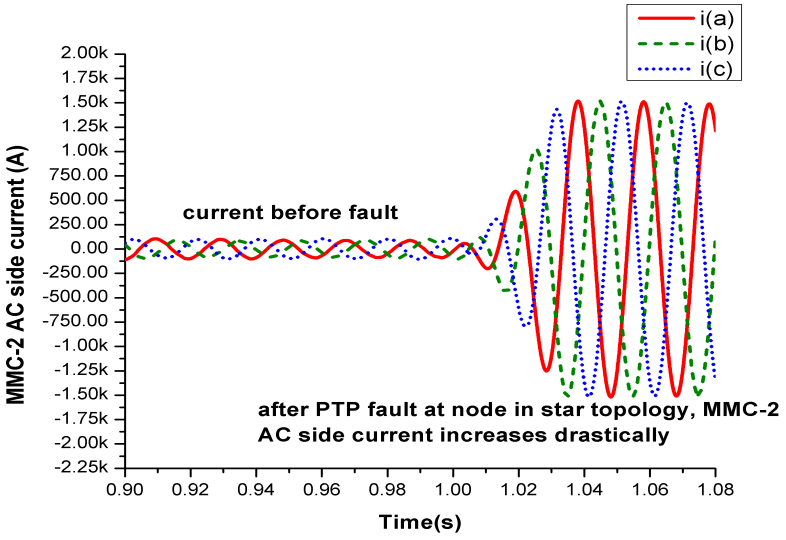

(a)

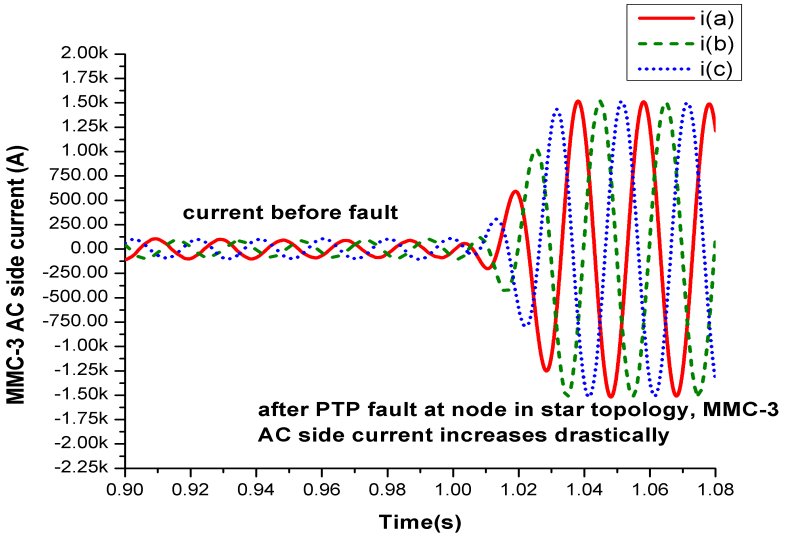

(b)

FIGURE 4.23: (a) MMC-2 (b) MMC-3 AC side currents increases when pole to pole fault occurs at the node

The summary of all pre fault and post fault conditions is presented in Table 4.5.

4.4 DC Fault Analysis in Three Terminal Ring MTDC Power Transmission System

This section analyzes the DC faults in the ring MTDC power transmission system. Fig. 4.24 shows the single line diagram of ring MTDC.

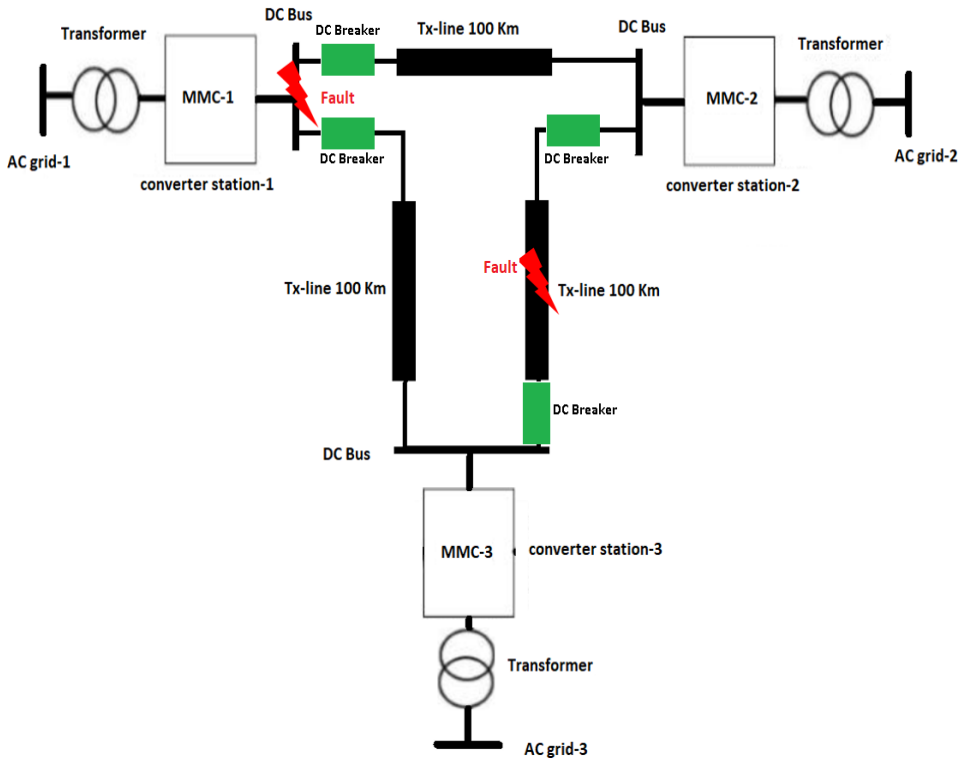

FIGURE 4.24: Single line diagram of Ring MTDC power transmission system

Simulation parameters that are used for the development of three terminal Ring MTDC power transmission system are presented in Table 4.3.

In Fig. 4.24, a Matlab/Simulink model for ring MTDC is shown. In ring topology, all converter stations are connected with DC links or HVDC transmission lines, forming a ring.

The ring topology is operated in two modes; these are the open loop and closed loop modes. The ring topology is operated in closed loop mode during normal operation in case of no fault in the power transmission system.

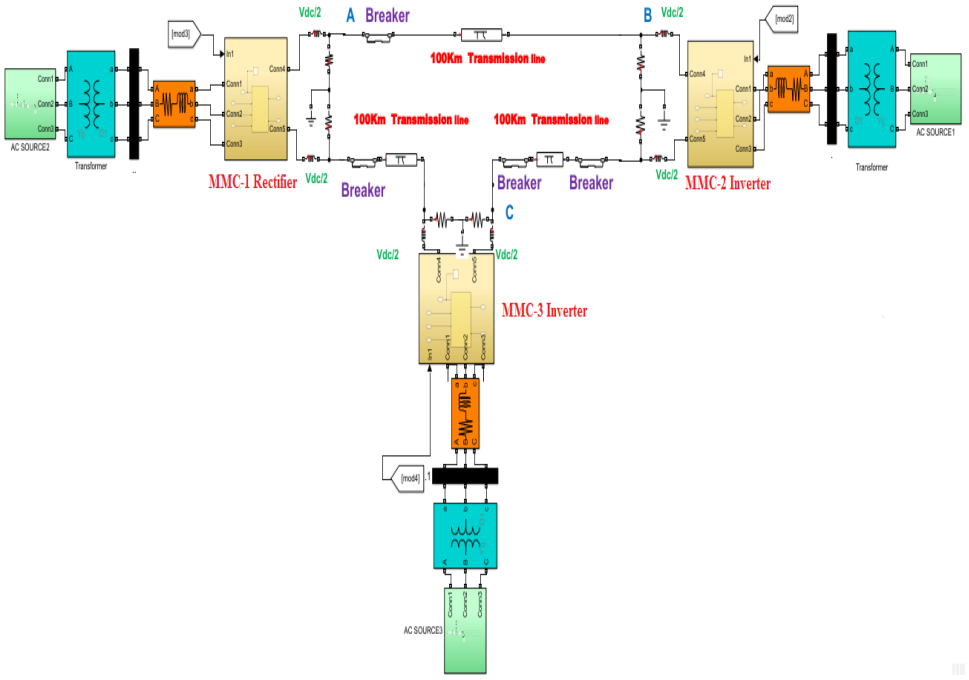

FIGURE 4.25: Matlab/Simulink model of Ring MTDC

The simulation parameters that are used for the development of three terminal Ring MTDC power transmission system are presented in Table 4.3.

Ring topology requires the DC breakers and the fast fault detection and communication systems for their operation for fault coordination and protection between converters.

If a transmission line is interrupted due to some fault or fault comes in any converter station, the respected DC breakers situated on each side of the faulty transmission line or converter stations suddenly open up and decouple the respective faulty transmission line or faulty converter station.

The rest of the system is now operating in an open-loop mode. Also, make sure that you are not losing the output of the remaining converter stations.

TABLE 4.3: The simulation parameters for three terminal Ring MTDC

Parameters	**Description**
MMC-1(7-level)	Working as Rectifier
MMC-2(7-level)	Working as inverter
MMC-3(7-level)	Working as inverter
DC Bus Voltage	100 kV
Converter AC side voltages	50 kV
Number of sub-module (N) in each arm	6
Level in converter AC output voltage (N+1)	7
Arm inductance L_{arm}	1 mH
Arm equivalent resistance R_{arm}	1 Ω
Sub module capacitance	5 mF
Voltage across each capacitor	16.66 kV
Fundamental frequency	50 Hz
Switching frequency	1.65 kHz
Transmission line length	100 km
Transformer Nominal voltages V_{sec}: V_{pri}	52 kV : 220 kV
Transmission line type	Pi Section
Number of pi section between converters	3
Resistance of transmission cable	0.01273 Ω/km
Inductance of transmission cable	0.9337e-3 H/km
Capacitance of transmission cable	12.74e-9 F/km
Inductance of phase reactor	2 mH
Equivalent resistance of phase reactor	0.08 Ω
Clamping Resistor	1 MΩ
AC grid -1,grid-2 and grid-3 voltages	220 kV

4.4.1 Pole to Pole Fault in Ring MTDC

In case of pole to pole fault occurrence at the output of converter station 1, the following simulation results are obtained: Fig. 4.26, shows that when a pole to

pole fault occurs at the output terminal of converter station-1, pole to pole voltages, positive pole, and negative pole voltages all drop to 0 V due to short circuit.

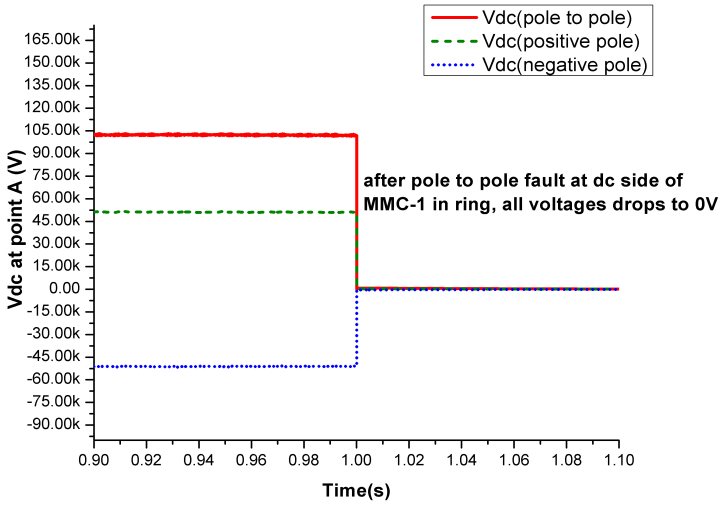

FIGURE 4.26: Pole to pole, positive pole and negative pole voltages drop to 0 V when pole to pole fault occurs at point A in Fig. 4.25, at MMC-1 dc side in ring MTDC

Due to pole to pole fault, the DC breakers situated at the output of converter station-1 open up suddenly and decouple the converter station-1.

After the decoupling of converter station-1, the rest of the system is now operating in open loop mode as mentioned above, and make sure that you are not losing the output of the remaining converter stations as shown in Fig. 4.27.

Fig. 4.28, shows the case of fault occurrence at the output terminal of converter station-1, the DC current rises drastically because of a short circuit.

Due to a pole to pole short circuit fault on the DC side of converter station 1, there is no effect on the MMC-2 and MMC-3 AC side voltages because when a fault occurs on the DC side of the converter station 1, the DC breaker located on the DC side opens up suddenly and decouples the converter station-1.

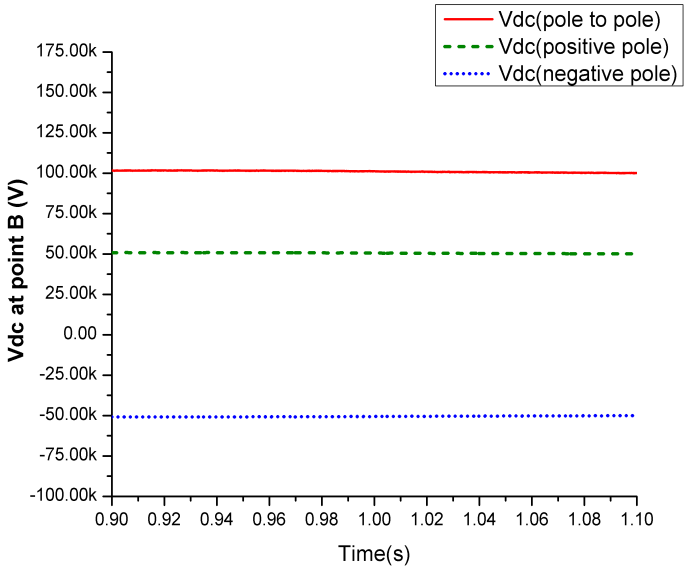

(a)

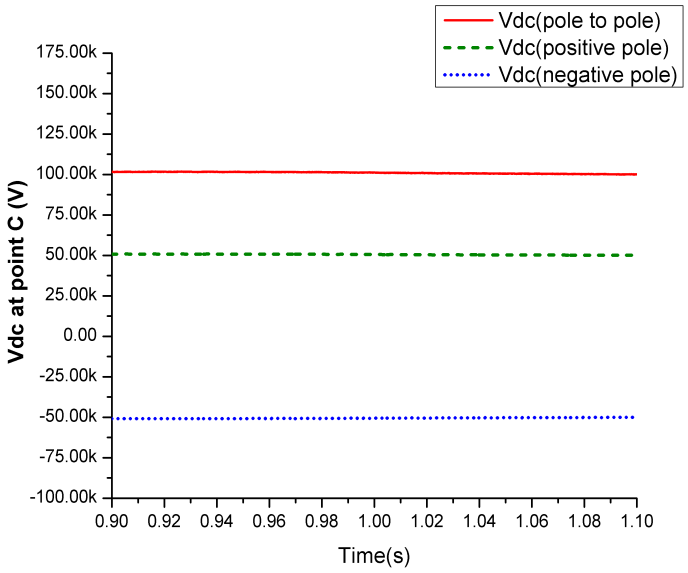

(b)

FIGURE 4.27: (a) Vdc at point B (b) Vdc at point C in Fig. 4.25, pole to pole, positive pole and negative pole voltages remains unchanged during pole to pole fault on MMC-1 dc side in ring MTDC

During this fault, make sure that the remaining converter stations do not suffer during the pole to pole fault and that they are kept in working condition.

The MMC-2 AC side voltages are shown in Fig. 4.29. The AC side voltages of MMC-3 also remain the same as the MMC-2 AC voltages.

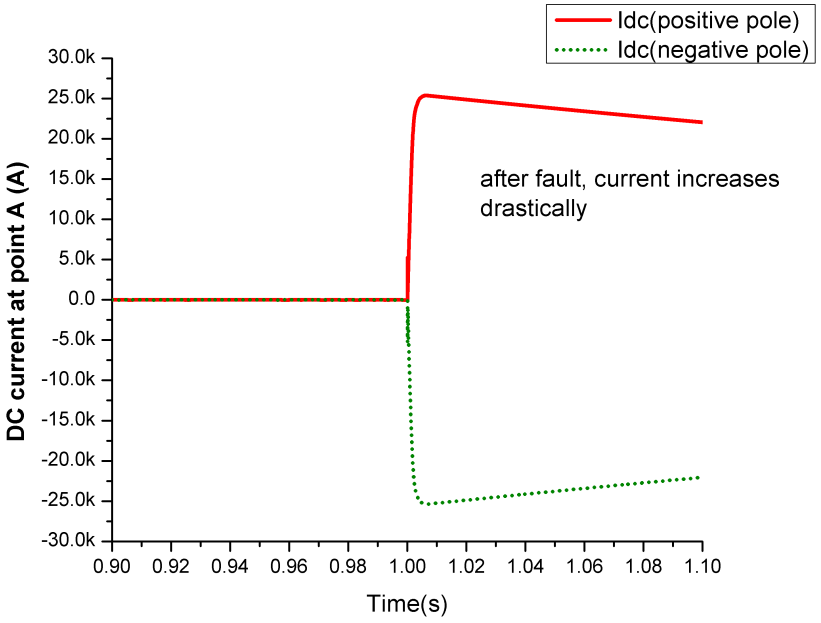

FIGURE 4.28: DC current at point A as marked on Fig. 4.25 increases, during pole to pole fault at the DC side terminal of converter station-1 in Ring MTDC

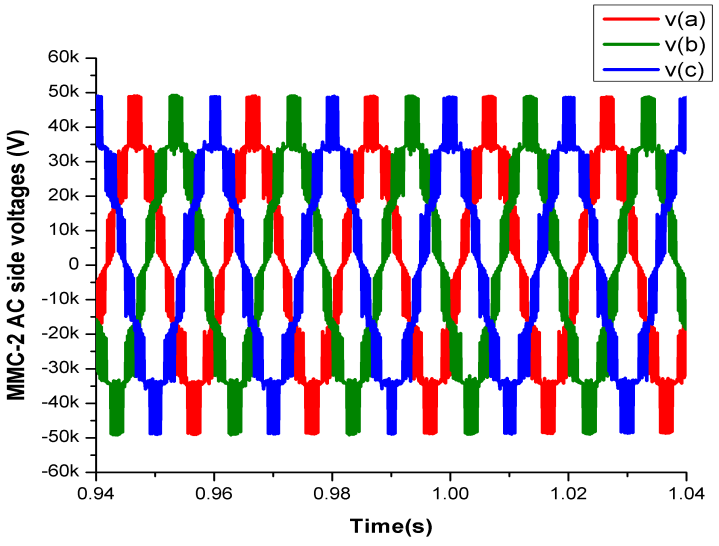

FIGURE 4.29: MMC-2 AC side voltages remains unchanged during pole to pole fault at MMC-1 dc side in ring MTDC

Fig. 4.30, shows the MMC-2, AC side current. The MMC-3 AC side current also remains the same as the MMC-2 current.

According to Fig. 4.30, when pole to pole fault comes on the DC side of converter station-1, the converter station-1 quickly decouples after a pole to pole fault.

The remaining converter stations will be in working condition due to this protection coordination.

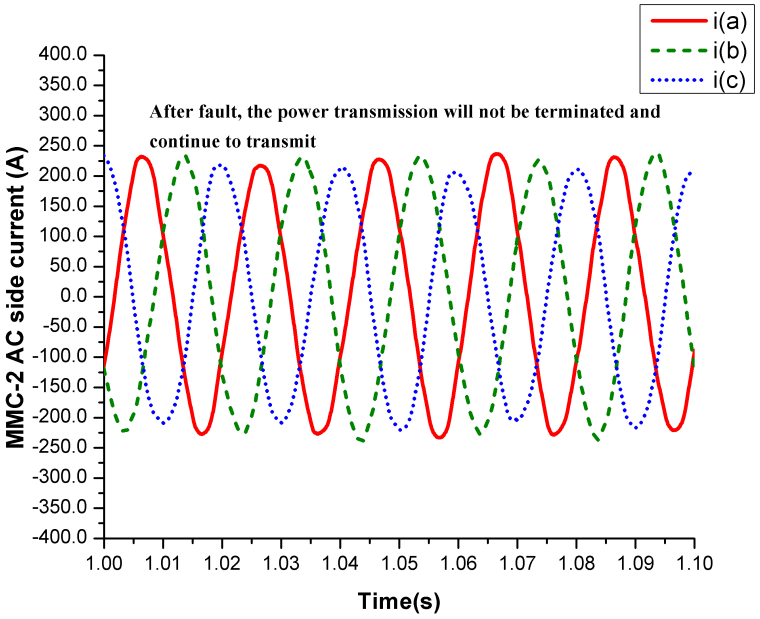

FIGURE 4.30: MMC-2 AC side current remains unchanged during pole to pole fault at MMC-1 dc side in ring MTDC

So these are the simulations that come out during the pole to pole fault at the DC side of converter station-1.

Now in the next section, we will discuss the fault on the transmission line in a ring topology.

4.4.2 Pole to Ground Fault on a Transmission Line in Ring MTDC

The following simulation results are obtained when a pole to ground fault occurs at the transmission line:

In Fig. 4.31, the Vdc at points A, B, and C is shown in case of fault occurs on the transmission line, these point are marked on Fig. 4.25. The DC breaker situated

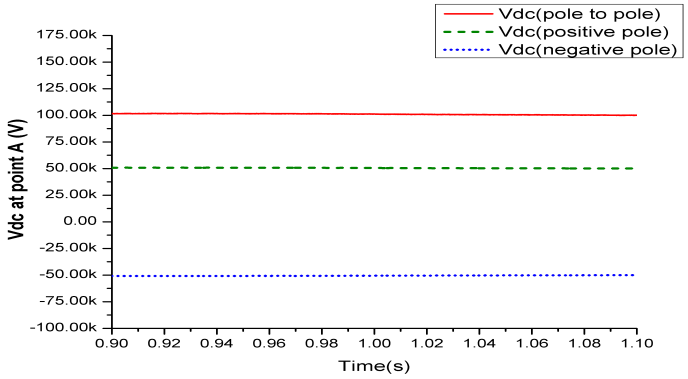

(a)

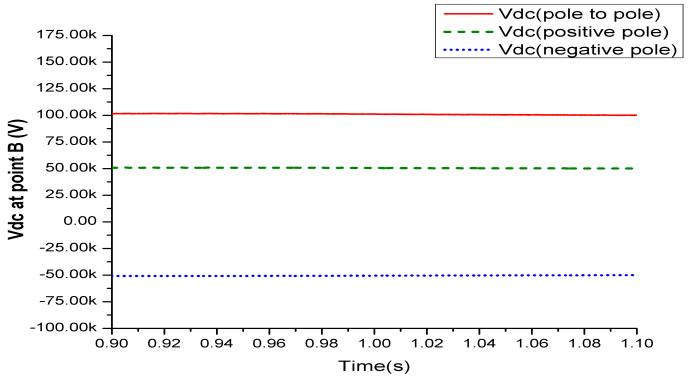

(b)

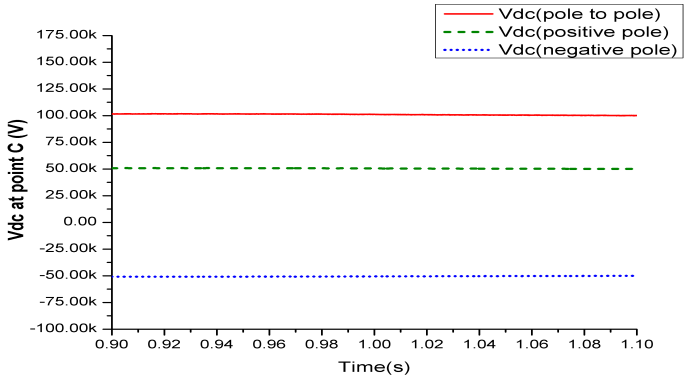

(c)

FIGURE 4.31: (a) Vdc at point A(b) Vdc at point B (c) Vdc at point C during pole to pole fault at transmission line in ring MTDC marked on Fig. 4.25

on each side of the respective transmission line suddenly opens up and decouples the faulty transmission line. Hence, the MTDC is now operating in open loop mode without losing any converter station output. Fig. 4.32 shows the MMC-2, AC side voltages and Fig. 4.33 shows the MMC-2, AC side current. The summary

of all pre fault and post fault conditions is presented in Table 4.6.

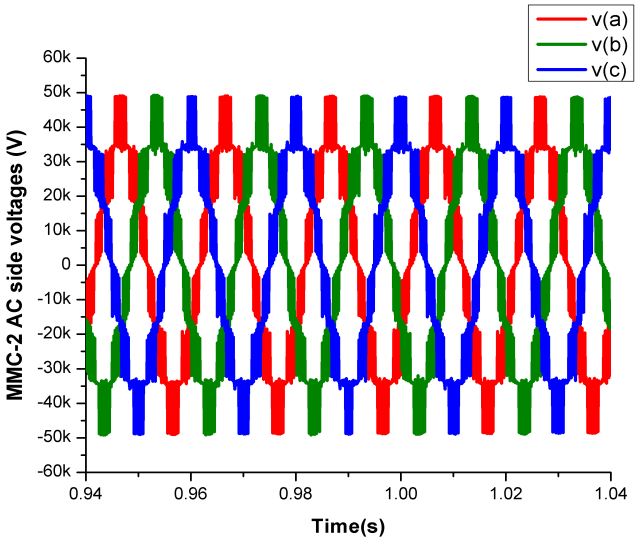

FIGURE 4.32: MMC-2 AC side voltages during pole to pole fault at transmission line in ring MTDC

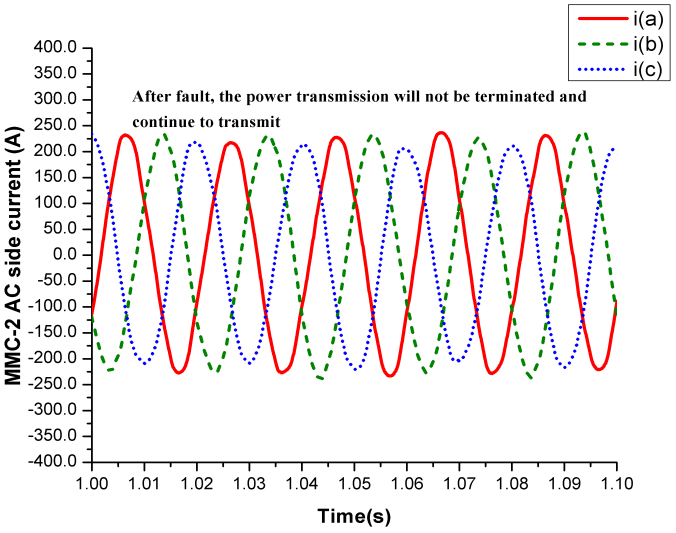

FIGURE 4.33: MMC-2 AC side current during pole to pole fault at transmission line in ring MTDC

4.5 Summary of Simulation Results

The study of DC faults for Series MTDC topology is summarized in table 4.4. The pre fault and post fault values for AC and DC side currents and voltages are listed

in this table. Before the fault or during normal operation, the DC side pole to pole voltage was 100 kV. The voltage on the positive pole was 50 kV, and the voltage on the negative pole was -50 kV. The MMC-2 and MMC-3 AC side voltages were ±50 kV. The pole to pole, positive pole, and negative pole voltages all drop to 0 V when a pole to pole fault occurs on the DC side of MMC-1. This is because a pole to pole fault causes the capacitors in the MMC sub-module to discharge through the fault point, causing their voltages to drop to 0 V. A blocking state will occur in MMC as a result of under voltages or over currents. The pole to pole fault causes an increase in the DC side current. Sub-module capacitor discharge and AC side current injection through anti-parallel diodes are the main causes of the rise in DC current, respectively. These diodes are connected across each sub-module. The MMC will function as an uncontrolled rectifier at this stage. The fault current is supported by the injection of AC source current. MMC-2 and MMC-3 AC side voltages decrease because the DC side voltages abruptly drop to 0 V due to a pole to pole fault. A pole to pole fault will stop the power from being transmitted. When a pole to ground fault occurs at the transmission line, the positive pole voltages drop to 0 V. The negative pole voltage oscillates due to the transmission line capacitance and inductance. The negative pole supports the pole to pole voltages after the pole to ground fault and its voltages become twice. When a fault occurs, there are some oscillations in the pole to pole voltages, but the voltages remain constant. The DC side current fluctuates and rises as a result of a pole to ground fault. A pole to ground fault causes the positive pole voltages on the DC side to abruptly drop to 0 V, changing the reference of the AC side voltages. Because the negative pole sustains the pole to pole voltages, the AC side current is unaffected and the power transmission will not be interrupted.

The study of DC faults for Star MTDC topology is summarized in table 4.5. The pre fault and post fault values for AC and DC side currents and voltages are listed in this table. Before the fault or during normal operation, the DC side pole to pole voltage was 100 kV. The voltage on the positive pole was 50 kV, and the voltage on the negative pole was -50 kV. The MMC-2 and MMC-3 AC side voltages were ±50 kV. The pole to pole, positive pole, and negative pole voltages all drop to 0 V

when a pole to pole fault occurs on the DC side of MMC-1. Due to the pole to pole fault, the AC side current that is injected through the free-wheeling anti-parallel diodes causes an increase in the DC side current. Points B and C, which are indicated in Fig. 4.14, are the points from which the reverse current flows in the direction of the fault point. The pole to pole fault causes a drop in voltage and an increase in current on the AC side of the MMC-2 and MMC-3. The transmission of power will be interrupted because of a pole to pole fault. We lose all connected converter stations when the node experiences a pole to pole fault. The pole to pole voltages, positive and negative pole voltages, drop to 0 V. The pole to pole fault at the node causes an increase in the DC side current. The current flows from point A, denoted in Fig. 4.14, in the direction of the fault point. Reverse current flows in the direction of the node fault point from points B and C. Pole to pole fault causes the AC side voltages of MMC-2 and MMC-3 to decrease and the AC side current to rise.

The study of DC faults for Ring MTDC topology is summarized in table 4.6. The pre fault and post fault values for AC and DC side currents and voltages are listed in this table. The ring topology is operated in two modes: closed loop and open loop. It is operating in closed loop mode without any fault. It will be operating in open loop mode when a fault occur. Ring topology requires the deployment of DC breakers, quick fault detection, and communication systems for protection and coordination between converter stations. The DC breakers installed at each side of MMC-1 open abruptly to disconnect the faulty converter station when a fault develops on the DC side of MMC-1. The rest of the system is now operating in open loop mode after the decoupling of MMC-1. The DC breakers installed at the transmission line's ends abruptly open up and bypass the faulty transmission line when a fault occurs.

Table 4.4: Series MTDC Topology

	Vdc				Idc		AC Outlet Voltages		AC Outlet Current	
Pre fault values	**Vdc at point A**	**Pole to pole voltages** 100 (kV)	**Positive pole voltages** +50 (kV)	**Negative pole voltages** -50 (kV)	**Idc at point A**	111.4 A (Mean)	**MMC-1 AC outlet voltages**	+50 kV (Max) -50 kV (Min) 25 kV (RMS)	**MMC-1 AC outlet current**	314 A(Max) -319 A (Min) 163 A (RMS)
	Vdc at point B	**Pole to pole voltages** 100 (kV)	**Positive pole voltages** +50 (kV)	**Negative pole voltages** -50 (kV)	**Idc at point B**	111.1 A (Mean)	**MMC-2 AC outlet voltages**	+50 kV (Max) -50 kV (Min) 25 kV (RMS)	**MMC-2 AC outlet current**	160 A (Max) -160 A (Min) 68 A (RMS)
	Vdc at point C	**Pole to pole voltages** 100 (kV)	**Positive pole voltages** +50 (kV)	**Negative pole voltages** -50 (kV)	**Idc at point C**	52 A (Mean)	**MMC-3 AC outlet voltages**	+50 kV (Max) -50 kV (Min) 25 kV (RMS)	**MMC-3 AC outlet current**	160 A(Max) -160 A(Min) 68 A(RMS)
PTP Fault at MMC-1 output	**Vdc at point A**	**Pole to pole voltages** 161 V	**Positive pole voltages** 80 V	**Negative pole voltages** -80 V	**Idc at point A**	80 KA	**MMC-1 AC outlet voltages**	+9.103 kV (Max) -8.9 kV (Min) 6.357 kV (RMS)	**MMC-1 AC outlet current**	18.54 KA (Max) -18.42 KA (Min) 13.972 KA (RMS)
	Vdc at point B	**Pole to pole voltages** 2.7 kV	**Positive pole voltages** 1.37 kV	**Negative pole voltages** -1.37 kV	**Idc at point B**	-5.182 KA	**MMC-2 AC outlet voltages**	+3.165 kV (Max) -3.037 kV (Min) 1.122 kV (RMS)	**MMC-2AC outlet current**	1.552 KA (Max) -1.556 KA (Min) 1.076 KA (RMS)
	Vdc at point C	**Pole to pole voltages** 3.7 kV	**Positive pole voltages** 1.86 kV	**Negative pole voltages** -1.86 kV	**Idc at point C**	-3.919 KA	**MMC-3 AC outlet voltages**	+3.555 kV (Max) -3.513 kV (Min) 1.202 kV (RMS)	**MMC-3 AC outlet current**	1.552 KA (Max) -1.570 KA (Min) 1.093 KA (RMS)
PTG Fault at Tx-line	**Vdc at point A**	**Pole to pole voltages** 100 (kV)	**Positive pole voltages** osc. & become 0 V	**Negative pole voltages** oscillate and becomes twice	**Idc at point A**	650Amp.	**MMC-1 AC outlet voltages**	-1.663 kV (Max) -100 kV (Min) 57.21 kV (RMS)	**MMC-1 AC outlet current**	316 A (Max) -310 A (Min) 163 A (RMS)
	Vdc at point B	**Pole to pole voltages** 100 (kV)	**Positive pole voltages** osc. & become 0V	**Negative pole voltages** oscillate and becomes twice	**Idc at point B**	-156 A	**MMC-2 AC outlet voltages**	-1.94 kV (Max) -100 kV (Min) 57.59 kV (RMS)	**MMC-2 AC outlet current**	160A(Max) -161A (Min) 67A (RMS)
	Vdc at point C	**Pole to pole voltages** 100 (kV)	**Positive pole voltages** osc. & become 0 V	**Negative pole voltages** oscillate and becomes twice	**Idc at point C**	-39 A	**MMC-3 AC outlet voltages**	-1.690 kV (Max) -100 kV (Min) 57.09 kV (RMS)	**MMC-3 AC outlet current**	160A(Max) -161 A (Min) 66 A (RMS)

Table 4.5: Star MTDC Topology

		Vdc			Idc		AC Outlet Voltages		AC Outlet Current	
Pre-fault values	**Vdc at point A**	**Pole to pole voltages** 100 (kV)	**Positive pole voltages** +50 (kV)	**Negative pole voltages** -50 (kV)	**Idc at point A**	113 A (Mean)	**MMC-1 AC outlet voltages**	+50 kV (Max) -50 kV (Min) 25 kV (RMS)	**MMC-1 AC outlet current**	320 A (Max) -310 A (Min) 164 A (RMS)
	Vdc at point B	**Pole to pole voltages** 100 (kV)	**Positive pole voltages** +50 (kV)	**Negative pole voltages** -50 (kV)	**Idc at point B**	56.5 A (Mean)	**MMC-2 AC outlet voltages**	+50 kV (Max) -50 kV (Min) 25 kV (RMS)	**MMC-2 AC outlet current**	160 A (Max) -160 A (Min) 62 A (RMS)
	Vdc at point C	**Pole to pole voltages** 100 (kV)	**Positive pole voltages** +50 (kV)	**Negative pole voltages** -50 (kV)	**Idc at point C**	56.5 A (Mean)	**MMC-3 AC outlet voltages**	+50 kV (Max) -50 kV (Min) 25 kV (RMS)	**MMC-3 AC outlet current**	160 A (Max) -160 A (Min) 62 A (RMS)
PTP Fault at MMC-1 output	**Vdc at point A**	**Pole to pole voltages** 164 V	**Positive pole voltages** 82.67 V	**Negative pole voltages** -82.01 V	**Idc at point A**	80 kA	**MMC-1 AC outlet voltages**	+9.014 kV (Max) -8.935 kV (Min) 6.383 kV (RMS)	**MMC-1 AC outlet current**	20.01 KA (Max) -20.01 KA (Min) 15.072 KA (RMS)
	Vdc at point B	**Pole to pole voltages** 5.5 kV	**Positive pole voltages** 2.721 kV	**Negative pole voltages** -2.720 kV	**Idc at point B**	-2.6 kA	**MMC-2 AC outlet voltages**	+5.231 kV (Max) -5.236 kV (Min) 1.899 kV (RMS)	**MMC-2AC outlet current**	1.564 KA (Max) -1.579 KA (Min) 1.069 KA (RMS)
	Vdc at point C	**Pole to pole voltages** 5.5 kV	**Positive pole voltages** 2.724 kV	**Negative pole voltages** -2.723 kV	**Idc at point C**	-2.6 kA	**MMC-3 AC outlet voltages**	+5.231 kV (Max) -5.238 kV (Min) 1.890 kV (RMS)	**MMC-3 AC outlet current**	1.552 KA (Max) -1.570 KA (Min) 1.066 KA (RMS)
PTP Fault at Node	**Vdc at point A**	**Pole to pole voltages** 16.84 (kV)	**Positive pole voltages** 8.419 (kV)	**Negative pole voltages** -8.419 (kV)	**Idc at point A**	9.25 kA	**MMC-1 AC outlet voltages**	+37.03 kV (Max) -39.88 kV (Min) 13.64 kV (RMS)	**MMC-1 AC outlet current**	17.3 KA (Max) -17 KA (Min) 8.741 KA (RMS)
	Vdc at point B	**Pole to pole voltages** 2.708 (kV)	**Positive pole voltages** 1.354 (kV)	**Negative pole voltages** -1.354 (kV)	**Idc at point B**	-4.746 kA	**MMC-2 AC outlet voltages**	+3.070 kV (Max) -3.404 kV (Min) 1.178 kV (RMS)	**MMC-2 AC outlet current**	1.55 KA (Max) -1.55 KA (Min) 1.070 KA (RMS)
	Vdc at point C	**Pole to pole voltages** 2.637 (kV)	**Positive pole voltages** 1.319 (kV)	**Negative pole voltages** -1.319 (kV)	**Idc at point C**	-4.746 KA	**MMC-3 AC outlet voltages**	+3.070 kV (Max) -3.404 kV (Min) 1.178 kV (RMS)	**MMC-3 AC outlet current**	1.55 KA (Max) -1.55 KA (Min) 1.071 KA (RMS)

TABLE 4.6: Ring MTDC Topology

		Vdc			Idc		AC Outlet Voltages		AC Outlet Current	
Close loop mode	**Vdc at point A**	**Pole to pole voltages** 100 (kV)	**Positive pole voltages** +50 (kV)	**Negative pole voltages** -50 (kV)	**Idc at point A**	92.91 A (Mean)	**MMC-1 AC outlet voltages**	+50 kV (Max) -50 kV (Min) 25 kV (RMS)	**MMC-1 AC outlet current**	320 A (Max) -310 A (Min) 164 A (RMS)
Pre-fault values	**Vdc at point B**	**Pole to pole voltages** 100 (kV)	**Positive pole voltages** +50 (kV)	**Negative pole voltages** -50 (kV)	**Idc at point B**	92.91 A (Mean)	**MMC-2 AC outlet voltages**	+50 kV (Max) -50 kV (Min) 25 kV (RMS)	**MMC-2 AC outlet current**	160 A (Max) -160 A (Min) 62 A (RMS)
	Vdc at point C	**Pole to pole voltages** 100 (kV)	**Positive pole voltages** +50 (kV)	**Negative pole voltages** -50 (kV)	**Idc at point C**	92.91 A (Mean)	**MMC-3 AC outlet voltages**	+50 kV (Max) -50 kV (Min) 25 kV (RMS)	**MMC-3 AC outlet current**	160 Amp.(Max) -160 Amp.(Min) 62 Amp.(RMS)
Open loop mode PTP Fault at MMC-1 output	**Vdc at point A**	**Pole to pole voltages** 157.3 V	**Positive pole voltages** 73.5 V	**Negative pole voltages** -73.1 V	**Idc at point A**	77.52 KA	**MMC-1 AC outlet voltages**	+6.103 kV (Max) -4.9 kV (Min) 3.357 kV (RMS)	**MMC-1 AC outlet current**	9.34 KA (Max) -9.31 KA (Min) 5.452 KA (RMS)
	Vdc at point B	**Pole to pole voltages** 100 (kV)	**Positive pole voltages** +50 (kV)	**Negative pole voltages** -50 (kV)	**Idc at point B**	Ring break open circuit	**MMC-2 AC outlet voltages**	+50 kV (Max) -50 kV (Min) 25 kV (RMS)	**MMC-2AC outlet current**	160 A (Max) -160 A (Min) 62 A (RMS)
	Vdc at point C	**Pole to pole voltages** 100 (kV)	**Positive pole voltages** +50 (kV)	**Negative pole voltages** -50 (kV)	**Idc at point C**	Ring break open circuit	**MMC-3 AC outlet voltages**	+50 kV (Max) -50 kV (Min) 25 kV (RMS)	**MMC-3 AC outlet current**	160 A (Max) -160 A (Min) 62 A (RMS)
Open loop mode	**Vdc at point A**	**Pole to pole voltages** 100 (kV)	**Positive pole voltages** +50 (kV)	**Negative pole voltages** -50 (kV)	**Idc at point A**	Ring break open circuit	**MMC-1 AC outlet voltages**	+50 kV (Max) -50 kV (Min) 25 kV (RMS)	**MMC-1 AC outlet current**	320 A (Max) -310 A (Min) 164 A (RMS)
PTG Fault at Tx-line	**Vdc at point B**	**Pole to pole voltages** 100 (kV)	**Positive pole voltages** +50 (kV)	**Negative pole voltages** -50 (kV)	**Idc at point B**	Ring break open circuit	**MMC-2 AC outlet voltages**	+50 kV (Max) -50 kV (Min) 25 kV (RMS)	**MMC-2 AC outlet current**	160 A (Max) -160 A (Min) 62 A (RMS)
	Vdc at point C	**Pole to pole voltages** 100 (kV)	**Positive pole voltages** +50 (kV)	**Negative pole voltages** -50 (kV)	**Idc at point C**	Ring break open circuit	**MMC-3 AC outlet voltages**	+50 kV (Max) -50 kV (Min) 25 kV (RMS)	**MMC-3 AC outlet current**	160 A (Max) -160 A (Min) 62 A (RMS)

Chapter 5

Conclusion and the Future's Work

This chapter concluded the proposed study and discussed the expansion of this research work for future aspects.

5.1 Conclusion

In this research thesis, DC faults are studied and simulated and their characteristics are analyzed, including pole to pole and pole to ground DC faults. DC fault analysis is performed for MMC based MTDC power transmission systems, including three-terminal series, star, and ring topologies.

From the simulations of pole to pole fault, it is concluded that pole to pole fault is the most severe fault on the DC side. When the positive and negative poles are short circuited to each other, the capacitor voltage of all sub-modules drops to 0 V. The bridge arm currents, the positive and negative pole DC currents increase. The pole to pole voltages, positive pole, and negative pole voltages drop to 0 V due to the short circuit. At the point where the fault occurs, there is a drastic increase in current at the beginning of the fault. It is also analyzed that when

fault occurs at a point, the reverse current flows towards the fault point from the nearby locations. Due to the pole to pole fault, the AC side voltages of MMC decrease, and the AC side current increases. Due to a pole to pole fault, the power transmission will be terminated.

When a pole to ground fault occurs, in the case of a positive pole to ground fault, the positive pole voltages oscillate and drop to 0 V suddenly, while the negative pole voltages oscillate and become twice the negative pole voltages.

There are slight oscillations in pole to pole voltages during a pole to ground fault. The positive pole and negative pole DC currents rise and oscillate. The AC side voltages of the MMC converter are reduced to single pole operating voltages because of the sudden change of positive pole voltages to 0 V.

In series MTDC, if a fault occurs in the transmission line, then we lose the converter stations that are connected to the transmission line. It is also concluded that in the MTDC star topology, if a fault occurs at a node terminal, then we lose all connected converter stations. The DC side voltages of all converter stations drop to zero volts due to short circuit at the node. The DC current at all converter station increases drastically. The AC side voltages of all converter stations reduce and the AC side current increases rapidly when a fault occurs. Due to a fault at the node terminal, the power transmission will be terminated. In a ring topology, there are two modes of operation; one is the closed loop mode and the second is the open loop mode. In normal operation without fault, the ring topology is operated in close loop mode. When fault comes in a converter station or when a fault arises in a transmission line, the ring topology is operated in an open loop mode. In a ring topology, it is necessary to decouple the faulty converter station or a faulty transmission line quickly in such a way that the DC output voltages of the remaining converter stations will not be affected by that fault. They will continue to work.

It is also concluded that when the converter stations are placed at a faraway

from the fault point, the effect of the fault is less on those converter stations as compared to the effect of the fault on the converter stations that are placed near to the fault point. Recently, the super grid is in its growing stage and because the super grid is composed of a large number of converter stations, the probability of fault occurrence is severe. As a result, the conclusions drawn from this research thesis are beneficial for both the researchers conducting research on multi-terminal HVDC power transmission systems and the power industry.

5.2 Future Work

In this research work, the fault analysis is performed on the multi-terminal HVDC power transmission systems on the DC side. We investigate the pole to pole and pole to ground faults on the DC transmission line that connects the MMC converters on the DC side and their impact on overall system performance.

For future work, it is proposed that in addition to the DC fault analysis in the MMC based MTDC power transmission systems, the fault analysis on the AC side, including the single phase to ground fault, the 2 phase to ground fault, and the 3 phase to ground fault that occur on the AC side of the MMC converter station, can be performed and their effect on overall system performance analyzed.

In the future, it is also hoped to develop an MTDC power transmission system in which, when a fault occurs at a converter station, it is quickly bypassed or replaced with another operational converter station, and the fault is quickly removed to increase system reliability.

Bibliography

[1] M. N.Ji, Y.Gao and G.Li, "The ac-dc hybrid transmission system calculation based on continuation power flow," *IEEE Transactions*, vol. 9, pp. 1–7, 2009.

[2] G.Ccorimanya, "Operation of hvdc grids in parallel with ac grids," vol. 3. IEEE, 2010, pp. 48–53.

[3] Ismunandar, "Control of multi-terminal vsc-hvdc for offshore wind power integration," *Proceedings of the IEEE*, vol. 69, no. 6, pp. 303–307, 2010.

[4] A.Stan, "Control of vsc-based hvdc transmission system for offshore wind power plants," *IEEE Transactions on Power Electronics*, vol. 12, no. 1, pp. 116–123, 2010.

[5] R. Marquardt, "Modular multilevel converter topologies with dc short circuit current limitation," in *In proceeding of 8th International Conference on Power Electronics-ECCA Asia,Jeju,Korea.* IEEE, 2011, pp. 1425–1431.

[6] Lesnicar and A.Marquardt, "An innovative modular multilevel converter topology suitable for a wide power range," in *In proceedings of the power Tech Conference, Bologna, Italy.* IEEE, 2003, pp. 23–26.

[7] Dodds and B. Railing, "Hvdc vsc (hvdc light) transmission operating experiences," *IEEE transactions on Power Electronics*, vol. 97, pp. 346–352, 2010.

[8] M. Bahrman and B.K, "The abcs of hvdc transmission technologies," *Power and Energy Magazine, IEEE*, vol. 5, no. 2, pp. 32–44, 2007.

[9] Siemens, "High voltage direct current-proven technology for power exchange," *Siemens publication*, vol. 15, no. 3, pp. 2–17, 2005.

[10] Sood, "Hvdc and facts controllers applications of static converters in power systems," *Proceedings of the IEEE*, vol. 60, no. 24, pp. 2992–2994, 2004.

[11] Meier, "Novel voltage source converter based hvdc transmission system for off shore wind farms," *Licentiate Thesis*, vol. 10, no. 10, pp. 455–457, 2005.

[12] Arrillaga, "High voltage direct current transmission," *Proceedings of the IEEE*, vol. 17, no. 4, pp. 594–609, 1998.

[13] Adapa, "High-wire act: Hvdc technology: The state of the art," *Proceedings of the IEEE*, vol. 10, no. 6, pp. 18–29, 2012.

[14] A.Siemens, "High voltage direct current transmission-proven technology for power exchange," *Tech.Rep*, vol. 55, no. 7, pp. 1237–1238, 2011.

[15] K.Meah and S.Ula, "Comparative evaluation of hvdc and hvac transmission systems," *in Power Engineering Society General Meeting*, vol. 90, no. 6, pp. 1–5, 2007.

[16] Cuiqing, "Vsc-hvdc for industrial power systems," vol. 1. IEEE, 2007, pp. 57–60.

[17] Breuer and G.D.Hauth, "Hvdc increasing popularity," *Proceedings of the IEEE*, vol. 7, no. 02, pp. 18–21, 1988.

[18] Glinkowski, "Guest editorial special section on hvdc systems and technologies," in *Power Delivery, IEEE Transactions*, vol. 29. IEEE, 2014, pp. 307–309.

[19] de Moraes and J.Salatko, "Power coming 12 600 megawatts at itaipu island new approaches were needed to solve problems of 'bigness in the world's largest power plant yet conceived," *Spectrum, IEEE*, vol. 20, no. 8, pp. 46–52, 1983.

[20] N. Flourentzou and V.G.Demetriades, "Vsc-based hvdc power transmission systems: An overview," *IEEE Transactions on Power Electronics*, vol. 24, no. 3, pp. 542–602, 2009.

[21] M. M. K. P. Vittal, "Dc fault protection in multi-terminal vsc-based hvdc transmission systems with current limiting reactors," *Journal of Electrical Engineering and Technology*, vol. 17, pp. 84–92, 2018.

[22] O.Gomis and J.Liang, "Topologies of multi-terminal hvdc vsc transmission for large offshore wind farms," *Electric Power Systems Research*, vol. 81, pp. 271–281, 2011.

[23] N. U. Mohan and T. Robbin, "Electronics: Converters, applications and design," *Int.J.Electr.Power Energy Syst.*, vol. 10, no. 6, pp. 9–12, 1995.

[24] F. Rodrigo and D.Ramirez, "Modular multilevel converters: Control and applications," *IEEE Transactions on Energies*, vol. 10, no. 11, p. 1709, 2017.

[25] S.Cole and R.Belmans, "Transmission of bulk power," *IEEE Industrial Electronics Magazine*, vol. 3, no. 3, pp. 1442–1447, 2009.

[26] B. A.Dekka and R. Fuentes, "Evolution of topologies, modeling, control schemes, and applications of modular multilevel converters," *IEEE Journal of Emerging and Selected Topics in Power Electronics*, vol. 5, no. 4, pp. 1631–1656, 2017.

[27] I. O.E.Oni and K. Mbangula, "A review of lcc-hvdc and vsc-hvdc technologies and applications," *in Environment and Electrical Engineering (EEEIC),*, vol. 46, no. 10, pp. 1–7, 2016.

[28] BAndersen, "Vsc transmission tutorial," *in Proc. CIGRE Study Committee Meeting*, vol. 83, no. 1, pp. 96–99, 2005.

[29] C. Chunyi.Guo and Zhao, "Supply of an entirely passive ac network through a double-in feed hvdc system," *Power Electronics, IEEE Transactions*, vol. 25, pp. 2835–2841, 2010.

[30] O. A. D.M.Larruskain, I.Zamora, "Vsc-hvdc configurations for converting ac distribution lines into dc lines based on multi parameter mobility model," *International Journal of Electrical Power and Energy Systems,*, vol. 54, no. 7, pp. 589–597, 2014.

[31] J. Liang and T. Jing, "Operation and control of multi terminal hvdc transmission for offshore wind farms," *IEEE Transactions*, vol. 26, pp. 2595–2604, 2011.

[32] B. Prieto Arau and F.D.unyent, "Methodology for droop control dynamic analysis of multi terminal vsc-hvdc grids for offshore wind farms," *IEEE Transactions*, vol. 26, no. 4, pp. 2476–2485, 2011.

[33] Baradar, "Modeling of multi terminal hvdc systems in power flow and optimal power flow formulations," vol. 21. IEEE, 2013, pp. 5–6.

[34] L. X. L. Y. Sasse and Christian, "Grid integration of large dfig-based wind farms using vsc transmission," *Power Systems, IEEE Transactions*, vol. 22, no. 3, pp. 976–984, 2007.

[35] T.Joseph and J.Liang, "Dynamic control of mvdc link embedded in distribution network: Case study on angle dc," *in 1st IEEE Conference on Energy Internet and Energy System Integration, Beijing, China*, vol. 12, no. 4, pp. 56–57, 2017.

[36] LuW and Ooi, "Dc over voltage control during loss of converter in multiterminal voltage sourced converter based hvdc," in *Transactions on Power Delivery*, vol. 679. IEEE, 2003, pp. 915–920.

[37] J.Rodriguez and F.Z.Peng, "Multilevel inverters: a survey of topologies, controls, and applications," *IEEE Transactions on industrial electronics*, vol. 49, no. 4, pp. 724–738, 2002.

[38] L. K.Sharifabadi and H.Nee, "Design, control, and application of modular multilevel converters for hvdc transmission systems," *Industrial Electronics, IEEE Transactions*, vol. 21, no. 5, pp. 7–8, 2002.

[39] B. Du and A. Dekka, "Modular multilevel converters: Analysis, control, and applications," in *IEEE Press Series on Power Engineering*, vol. 711. IEEE, 2018, pp. 104–108.

[40] M.A.Perez.S.Bernet.J.Rodriguez.S.Kouro and R.Lizana, "Circuit topologies modeling,control schemes and applications of modular multilevel converters," *Power Electronics,IEEE Transactions*, vol. 41, no. 5, pp. 77–80, 2015.

[41] A. Lharnefors and S.Norrga, "Dynamic analysis of modular multilevel converters." IEEE, 2013, pp. 676–678.

[42] S.-M. Montilla Djesus, M and D.Arnaltes, "Optimal reactive power allocation in an offshore wind farm with lcc-hvdc link connection," *Renew. Energy 2012*, vol. 40, pp. 157–166, 2012.

[43] D. Larruskain and I.Abarrategui, "Vsc-hvdc configuration for converting ac distribution lines in to dc lines," *Int.J.Electr.Power Energy Syst.*, vol. 54, pp. 589–597, 2014.

[44] A. Penalba and Egea-Alvarez, "Optimum voltage control for loss minimization in hvdc multi-terminal transmission system for large offshore wind farm," vol. 89. IEEE, 2012, pp. 54–63.

[45] G. Sousa and M.L.Heldwein, "Three phase unidirectional modular multilevel converter," *Power Electronics and Applications*, vol. 60, pp. 1–10, 2013.

[46] G.B.Diaz, "Modular multilevel converter control for hvdc operation: Optimal shaping of the circulating current signal for internal energy regulation," in *PhD dissertation.* IEEE, 2015, pp. 75–78.

[47] B.J.Pawar and V.J.Gond, "Modular multilevel converters: A review on topologies, modulation, modeling and control schemes," *Electronics, Communication and Aerospace Technology (ICECA)*, p. 431, 2017.

[48] S. T.M.Iversen and T.Undeland, "Multilevel converters for on shore wind generator system," in *Power Electronics and Applications.* IEEE, 2013, pp. 1–10.

[49] a. R. S.Allebrod, R.Hamerski, "New transformer less, scale able modular multilevel converters for hvdc-transmission," *Power Electronics Specialists Conference*, vol. 16, no. 2, pp. 174–179, 2008.

[50] R.Marquardt, "Modular multilevel converter: A universal concept for hvdc networks and extended dc-bus-applications." IEEE, 2010, pp. 502–507.

[51] Yazdani and R.Iravani, "Voltage-sourced converters in power systems modeling, control, and applications)," *Energy Proceeding*, vol. 9, pp. 28–30, 2010.

[52] Y. Zhang, "Modular multi-level converter based multi-terminal hvdc system for offshore wind power transmission)," *Power Engineering Conference*, vol. 8, pp. 22–24, 2017.

[53] G.M.Tina and G.Celsa, "A matlab/simulink model of a grid connected single-phase inverter," *Power Engineering Conference*, pp. 1–6, 2015.

[54] T.Kalitjuka, "Control of voltage source converters for power system applications," *Transactions of the American Institute of Electrical Engineers*, pp. 16–18, 2011.

[55] L.Angquist and L.Lindberg, "Inner phase angle control of voltage source converter in high power applications," *IEEE Power Electronics Specialists Conference*, pp. 293–297, 1991.

[56] a. E. h. L.Xu, V.G.Agelidis, "Development considerations of dsp controlled pwm vsc-based statcom," *IEEE Proceedings: Electric Power Application*, pp. 449–455, 2001.

[57] A.R.Bergen, "Power system analysis and control," *Power Electronics and Applications*, pp. 49–51, 1986.

[58] M. kowski and L.Malesani, "Current-control techniques for three phase voltage-source pwm converters," *IEEE Transactions on Industrial Electronics*, pp. 691–703, 1998.

[59] M. S. Ifarad, "Multilevel converters for medium/high-power applications," *Power Electronics Conference*, vol. 20, pp. 184–1960, 2019.

[60] D. Hertem and M.Ghandhari, "Multi-terminal vsc hvdc for the european super grid: Obstacles," *IEEE transactions on Power Electronics*, pp. 3156–3163, 2010.

[61] S. won Kim and A. Yokohama, "Economic benefits comparison between point-to-point and multi-terminal vsc hvdc systems with large-scale wind farms," *IEEE transactions on electrical and electronics engineering*, vol. 7, pp. 150–159, 2018.

[62] Y. X.Yu and Q.Jiang, "Statcom operation scheme of the cdsm-mmc during a pole to pole dc fault," *IEEE Trans.Power Del*, vol. 31, pp. 1150–1159, 2016.

[63] E. U.Lamm and P.Danfors, "Some aspects of tapping hvdc transmission systems," *Direct Current*, vol. 8, no. 5, pp. 124–129, 1963.

[64] J.Reeve, "Multi terminal hvdc power systems," in *IEEE transactions on power apparatus and system*, vol. 99. IEEE, 1980, pp. 729–737.

[65] H. N.Ahmed, S.Norrga and A.Haider, "Hvdc super grids with modular multilevel converters - the power transmission backbone of the future," in *International Multi-Conference on Systems*. IEEE, 2012, pp. 1–7.

[66] S.Lundberg and N. Zargari, "Wind farm configuration and energy efficiency studies-series dc versus ac layouts," *IEEE Transactions on Sustainable Energy*, vol. 2, pp. 57–59, 2006.

[67] M.Popat and N. Zargari, "Coordinated control of cascaded current-source converter based off shore wind farm," *IEEE Transactions on Sustainable Energy*, vol. 3, pp. 557–565, 2012.

[68] L. T. Lu YanChun and Liang, "Research on the fault characteristics of dc side based on mmc-hvdc," *Electronics Letters*, vol. 40, no. 1, pp. 81–83, 2018.

[69] Y. J.J.Jung, S.Cui and S.K.Sul, "A cell capacitor energy balancing control of mmc-hvdc under the ac grid faults," *International Conference on Power Electronics and EC CE Asia*, pp. 1–8, 2015.

[70] C. T. PanVullo and J. chul, "Calculation of passing voltage of mmc-hvdc transmission line under dc fault," *Power construction*, vol. 35, no. 3, pp. 18–23, 2014.

[71] L. Tang and B. Teck, "Managing zero sequence in voltage source converter," *IEEE Industry Application Conference 37TH Annual Meeting*, pp. 795–802, 2002.

[72] Q. Hongxia and S. Gang, "Study on the coordination of the fault control between the poles of the flexible dc distribution network and the parameters of the main equipment," *Power system protection and control*, vol. 44, no. 21, pp. 150–156, 2016.

[73] Bin.jiang and Yanfeng.Gong, "Fault current analysis of mmc based hvdc system under pole to pole fault condition," *International Conference on Renewable Power Generation (RPG 2015)*, pp. 156–166, 2015.

[74] J. S.Y.Fan and E.M.Bian, "Research on dc faults of multi-terminal direct current system," *Energy and Power Engineering*, vol. 9, no. 1, pp. 756–764, 2017.

[75] Yang.Gao and Masoud.Bazargan, "Fault current analysis of mmc based hvdc system under pole to pole fault condition," *2nd IET Renewable Power Generation Conference (RPG 2013)*, pp. 1234–1240, 2013.

[76] R. sapkota and S. Kolluri, "Mmc based mtdc sub sea power transmission system with integration of offshore renewable energy," *Proceedings of the IEEE*, vol. 46, no. 2, pp. 321–325, 2017.

[77] X. Yao and L. Herrera, "Modulation and control of mmc mtdc," *Proceedings of the IEEE*, vol. 51, no. 3, pp. 245–248, 2014.

[78] D. schmitt and Y. Wang, "Dc side fault current management in extended mtdc grids," *Proceedings of the IEEE*, vol. 57, no. 6, pp. 125–130, 2012.